The Design of a Hydrofoil System for Sailing Catamarans

by

HOWARD LOVEDAY

Thesis presented in partial fulfilment of the requirements for the degree

Masters in Mechanical Engineering

at University of Stellenbosch

SUPERVISORS:

Prof. T.W. von Backström – University of Stellenbosch

Dr. G. Migeotte – CAE Marine (Ltd)

April, 2006

Declaration

I, the undersigned hereby declare that the work contained in this thesis is my own original work and has not previously, in its entirety or in part, been submitted at any University for a degree.

_____

Signature of Candidate

Signed on the _____ day of _____2006

Abstract

The *main objective* of this thesis was to design a hydrofoil system without a trim and ride height control system and investigate the change in resistance of a representative hull across a typical speed range as a result of the addition of the hydrofoil system, while retaining adequate stability.

The *secondary objectives* were as follows: Find a representative hull of sailing catamarans produced in South Africa, and to establish an appropriate speed range for that hull across which it is to be tested. Test and explain the drag characteristics of this hull. Find a suitable configuration of lifting foils for this hull that would not require any form of trim or ride height control to maintain stability throughout the speed range. Test and compare the resistance characteristics with and without the assistance of lifting foils. Test and explain the effects of leeway and heel on the total hydrodynamic resistance both with and without lifting foils.

A representative hull (RH1), based on a statistical analysis of sailing catamarans produced in South Africa and an existing hull design of suitable size, was designed. A speed range was then established (0 – 25 knots) based on the statistics of the original (existing) design. A scaled model (of RH1) of practical and suitable dimensions was designed and manufactured, and its characteristics determined through towing tank testing.

A hydrofoil system was then designed and during testing, was adjusted until a stable configuration was found. This resulted in a canard type configuration, with the front foil at the bow and the main foil between the daggerboards. Although a stable configuration was achieved, it was noted that any significant perturbation in the trim of the boat would result in instability and some form of trim control is recommended.

The main objective was achieved. The experimental results concluded that a canard configuration was found to be stable for the RH1 (foil positioning already mentioned) and the addition of the hydrofoils provided a significant improvement only above a displacement Froude number of 2, which for our full scale prototype, is equivalent to approximately 14.2 knots.

This is in agreement with the results of several other research projects that investigated hydrofoil supported catamarans with semi-displacement type demi-hulls. Below displacement Froude number of 2, a significant increase in total hydrodynamic resistance was observed.

Since the speed of sailing craft is dependent on wind speed, there will often be conditions of relatively low boat speed (below displacement Froude number of 2). So it was recommended that a prototype design would have a retractable hydrofoil system which could be engaged in suitable conditions (sufficient boat speed).

The effects of leeway and heel on the total hydrodynamic resistance were determined experimentally, but it was found that these trends were affected by the resulting changes in wave interference resistance. Since wave interference depended strongly on the hull shape, it was therefore concluded that no universal trends can be determined regarding the effects of heel and leeway on the total hydrodynamic resistance. These effects were determined for RH1 and it was shown that these effects are drastically altered by the addition of the lifting foils.

Opsomming

Die *hoofdoelwit* van hierdie tesis is om 'n hidrovleuel-ondersteunde seilkatamaraan sonder ’n heihoek- en hoogtebeheerstelsel te ontwerp en die verandering in weerstand van ‘n verteenwoordigende romp oor ’n tipiese snelheidsbereik as gevolg van die byvoeging van die hidroveuelstelsel te ondersoek, terwyl stabiliteit behou word.

Die sekondêre doelwitte was soos volg: Vind ‘n verteenwoordigende seilkatamaraanromp wat in Suid Afrika vervaardig word en vind ‘n toepaslike snelheidsbereik vir hierdie romp waardeur dit getoets kan word. Toets en verduidelik die weerstandkarakteristieke van hierdie romp. Vind ‘n gepaste konfigurasie van hidrovleuels vir hierdie romp wat nie enige vorm van hei- of ryhoogtebeheer benodig nie om stabiliteit in die snelheidsbereik te verseker. Toets en vergelyk die weerstandkarakteristieke met en sonder die toevoeging van hidrovleuels. Toets en verduidelik die effek van gierhoek en oorhelling op die totale hidrodinamiese weerstand met en sonder hidrovleuels.

'n Verteenwoordigende romp (“RH1”), gebaseer op 'n statistiese ontleding van Suid-Afrikaansvervaardigde seilkatamaraans, en 'n bestaande rompontwerp van geskikte grootte is ontwerp. 'n Snelheidsbereik is daarna vasgestel (0-25 knope) op die basis van die oorspronklike (bestaande) ontwerp se statistiek. 'n Skaalmodel met praktiese en toepaslike afmetings is ontwerp en vervaardig

Daarna is 'n hidrovleuelstelsel ontwerp en gedurende toetswerk is dit aangepas totdat ’n stabiele hidrovleuelstruktuur gevind is. Die gevolg was ’n canard-tipe konfigurasie, met die voorste vleuel by die boeg en die hoofvleuel tussen die kielvleuels. Alhoewel ‘n stabiele konfigurasie gevind is, word bevind dat enige beduidende versteuring in die heihoek van die boot onstabiliteite veroorsaak en ‘n sekere vorm van heibeheer word voorgestel.

Die *hoofdoelwit* is bereik. Die eksperimentele resultate dui daarop dat ’n canard hidrovleuelopstelling stabiel is vir die ‘RH1’ romp en die byvoeging van die hidrovleuels het 'n aansienlike verbetering by 'n Froude-verplasingsyfer bo 2 teweeggebring, wat vir die volskaal-prototipe gelykstaande is aan ongeveer 14.2 knope

Dit stem ooreen met die resultate van verskeie ander navorsingsprojekte wat hidrovleuel-ondersteunde katamaraans met deelse-verplasingstipe halfrompe ondersoek het. By 'n Froude-verplasingsyfer onder 2 was daar 'n opmerklike toename in totale hidrodinamiese weerstand.

Aangesien die snelheid van seilvaartuie van windspoed afhang, sal bootsnelheid dikwels relatief laag wees (Froude-verplasingsyfer onder 2). Daarom word aanbeveel dat 'n prototipe ontwerp 'n optrekbare hidrovleuelstelsel het wat in paslike toestande in werking gestel kan word. (genoegsame bootspoed).

Die uitwerking van gierhoek en oorhelling op die totale hidrodinamiese weerstand is eksperimenteel bepaal, maar daar is gevind dat hierdie tendense beïnvloed is deur die voortspruitende veranderinge in golf-interaksie weerstand. Golfweerstand hang grootliks af van die rompvorm. Gevolglik is afgelei dat geen algemene tendens gevind kan word met betrekking tot die uitwerking van oorhelling en gierhoek op die totale hidrodinamise weerstand nie. Hierdie effekte is vir 'RH1' gevind, en daar is getoon dat hierdie uitwerkings drasties verander met die byvoeging van die hidrovleuelstelsel.

Acknowledgements

First and foremost, I would like to thank God for opening up the required doors so as to provide me with the opportunity to study that which I formerly thought impossible. For that I am eternally grateful.

I'd like to thank my parents for all their support on a financial and advisory capacity both in my academic and sporting efforts. Their solid grounding and unwavering support has equipped me for all of my challenges and enabled me to reach my goals.

I'd like to thank my supervisors and their respective organisations. Firstly, Professor T.W. von Backström, of The Department of Mechanical Engineering of the University of Stellenbosch, for his guidance and organisation of financial support – without both I would not have been able to conduct this research. His critical analysis and vast experience in postgraduate research aided me greatly. I would also like to thank the National Research Foundation for the financial grants that they provided me with. Studying this degree would have been impossible without it. Next I would like to thank Dr. G. Migeotte. (CAE Marine) His wide knowledge of hydrofoil supported craft has been invaluable to me. Despite his busy schedule he was able to organise the administration for my project before I came to Stellenbosch and met with me on a regular basis where he provided direction and guidance to my project and explained many concepts. I would also like to thank CAE Marine for their financial support and company facilities made available to me, both of which assisted me greatly. In addition I would like to thank Professor V. Bertram for his input into the style, presentation and content of my thesis.

Next I would like to thank Mr. K. Thomas, Mr S Tannous and Mr L. Kababula for their assistance in the towing tank testing. Their time and patience were vital constituents to the success of my experimental testing.

"The way of a fool seems right to him, but a wise man listens to advice." – Proverbs 12:15

Nomenclature

Symbol	Explanation
Abbreviations	
AOA	**A**ngle **o**f **A**ttack
CE	**C**entre of **E**ffort on the sails.
CLR	**C**entre of **L**ateral **R**esistance
COB	**C**entre **o**f **B**uoyancy
COD	**C**entre **o**f **D**rag
COG	**C**entre **o**f **G**ravity
DWL	**D**esign **W**ater**l**ine
LWL	**W**ater**l**ine **L**ength
LOA	**L**ength (**O**vera**l**l)
LCG	**L**ongitudinal **C**entre of **G**ravity
STIX	**St**ability **Ind**e**x**
TCR	**T**ransverse **C**entre of **R**esistance
WSA	**W**etted **S**urface **A**rea
Greek	
α , α_T	Angle of attack
α_0	Zero lift angle of attack
ε	Resistance – displacement ratio for a hull
μ	Water viscosity
ϱ	Density
υ	Water kinematic viscosity
β	Angle of strut away from vertical with water surface.
Λ	Sweep angle
∇	Displacement **V**olume
Δ	Displacement weight = weight of boat.
σ	Cavitation number / Munk's interference factor
σ_i	Cavitation index
λ	Linear scale of model
ℓ_n	Span of front foil
ξ	Plan form factor
δ	Reserve buoyancy factor
Γ	Dihedral angle

General

(1+k)	Form factor / Correction for non-elliptic lift distribution.
a	Distance between vertical struts
A_z	Area (projected) no z = projected area of foil z = T (transom), x(max cross-sectional) *or* WL (waterplane)
AP	**A**ft **P**erpendicular
AR	**A**spect **R**atio
b	**B**eam of demi-hull
B / BOA	**B**eam of Boat (**O**vera**l**l)
B_F	Immersed span of **b**ow **f**oil
c	**C**hord length
c_z	**C**oefficient of resistance where subscripts are F, R and DP
C_B	**B**lock **c**oefficient
C_P	**P**rismatic **c**oefficient
C_{WL}	**W**ater p**l**ane area **C**oefficient
C_L	**C**oefficient of **L**ift
C_{L0}	**C**oefficient **lift** at 0^0 angle of attack
d	**D**epth of the transom below static waterline.
D	**D**rag force (foils)
E	**E**fficiency in terms of induced drag
Fr_x	**Fr**oude number where x = ∇ or L
F_{BL}	**B**uoyancy force on **L**eeward Hull
FBD	**B**eam **d**isplacement **f**actor
F_{BW}	**B**uoyancy force on **W**indward Hull
FDF	**D**own**f**looding **f**actor
FDL	**D**isplacement **l**ength **f**actor
FDS	**D**ynamic **s**tability **f**actor
FIR	**I**nversion **r**ecovery **f**actor
FKR	**K**nock down **r**ecovery **f**actor
F_{MF}	Lift **f**orce created by **M**ain **F**oil
F_{RFL}	Lift **f**orce created by **R**ear **F**oil on **L**eeward side
F_{RFW}	Lift **f**orce created by **R**ear **F**oil on **W**indward side
F_{LR}	**F**orce created by **L**ateral **R**esistance of the Hull and foils
F_{SS}	The **S**ideward component of the **f**orce on **S**ails
F_{MG}	The **f**orce created by **m**ass of boat (weight)
FP	**F**orward **P**erpendicular
FWM	**W**ind **m**oment **f**actor
g	Gravitational acceleration
h	Depth of foil below surface
i	Quarter chord depth.
k	Constant / factor related to its subscript
k_w	Coefficient related to wave resistance

K	Free surface constant
L	**L**ift force (foils)
L_{BS}	**B**ase **l**ength factor
L_H	**L**ength of wave **h**ollow behind front foil
L_K	Longitudinal separation between foils
N_j	Number of 90^0 junctions
N_S	Number of element piercing the surface.
q	Velocity pressure
Re	Reynolds number
s	Span of foil.
S	Separation between demihulls
S_w	Wetted surface area (Hull or foils)
t	Maximum thickness of foil cross-section
T	Draft
U	Free stream velocity
V	Velocity

Subscripts

D	**D**rag
DP	**P**rofile **D**rag (of foils)
e	**E**ffective
F,f	**F**rictional
i	**I**nduced
j	Interference
L	**L**ift
M, m	**M**odel
P,p	**P**rototype
R	**R**esidual
s	**S**pray
T	**T**otal
v	**V**iscous
w	**W**ave (generation) / wetted surface

Superscripts

*	Model scale

List of Figures and Tables

Chapter 1: Introduction

Chapter 2: Hull Hydrodynamics and Design

Chapter 3: Hydrofoil Theory and Design

Chapter 4: Computational Analysis

Chapter 5: Experimental Methodology and Setup

Chapter 6: Results

Contents

APPENDICES

Chapter 1

Introduction

1.1 Brief Introduction to Hydrofoils

Foils (hydrofoils) are important components of sailing craft. These are wing-like structures, located below the surface of the water, which are designed to have high lift to drag ratios (L/D). The hulls to which they are attached rely on both dynamic and static (buoyancy) forces to support them and their performance is usually defined in terms of the resistance-displacement ratio (ε) which is the inverse of L/D. The L/D ratio of well designed hydrofoils is much higher than 1/ ε of most hulls when both are travelling with sufficient boat speed for dynamic forces to dominate. As a result, at these speeds hydrofoil support is known to reduce total hydrodynamic resistance.

The same basic principles apply to airfoils and hydrofoils and so a lot of the terminology is shared. As a result, the force resulting from pressure distribution across the foil, directed perpendicular to the direction of flow and in the plane of the foil cross-section is called the lift force. This may result in some confusion when it comes to hydrofoils as the main axis (root to tip) may be directed vertically for some hydrofoils, resulting in the lift force acting in the sideward direction. The force in the direction of flow is termed the drag force.

Conventional sailing craft have predominantly vertical, symmetric foils while hydrofoil supported craft have predominantly horizontal asymmetric foils which raise the hulls out of the water. Symmetric foils will, at zero angle of attack, have similar pressure distributions on both sides when deeply submerged, and when acting at an angle of attack provide a lift force. They are therefore used to provide resistance to lateral movement (daggerboards, keels, centreboards, fins and skegs) and directional control (rudder) while minimizing drag when positioned vertically.

On the other hand, asymmetric hydrofoils provide a perpendicular (lift) force when at zero angle of attack and are designed to provide maximum lift with minimal drag for a range of angles. In order to differentiate a bit better the asymmetric foils are also called 'lifting foils'.[1]

Another aspect to mention about hydrofoils is that the lift they produce is reduced as they near the free surface (within about 1 chord length). This is known as free surface effects and the implication of this is a natural

[1] See Chapter 4.1 for a more in-depth explanation of lifting hydrofoils

stability, not only in terms of heave but also in pitch and roll. This will be discussed in more detail in section 3.3.1.

1.2 Catamarans and Sailing Catamarans

"From early European explorers' descriptions, the crew sailed with families, friends, lovers, singers and dancers in one joyous group from island to island - a marvellous way of life." – James Wharram [WB91]

The word catamaran is derived from the Tamil word *kattumarum* which is composed of the words 'to tie' and 'tree'. [Bir03] This comes from it's origins in the east as primitive canoes used for fishing. The concept is to use 2 demi-hulls fixed in parallel to provide a very stable (in roll) vessel while maintaining slender, low wetted surface area (WSA) and therefore low drag hulls. (See figure 1.1 below)

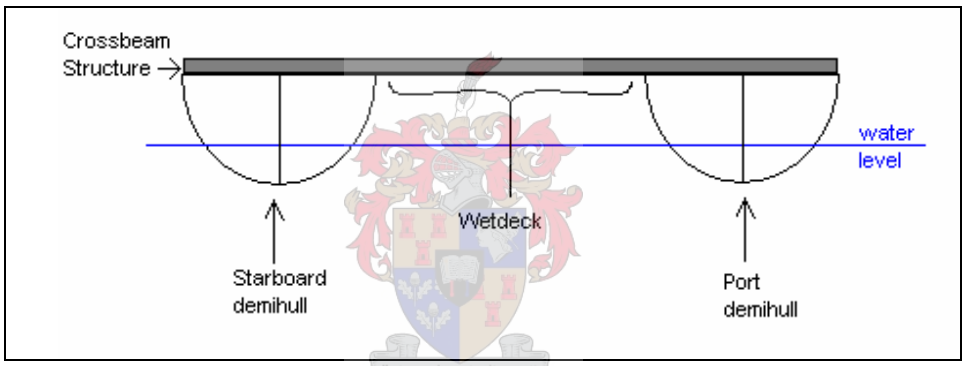

Figure 1.1 – Front view (looking from bow) of a simple catamaran

As shall be explained shortly, roll stability is very important for sailing vessels as they need to resist large heeling moments induced by the sideward component of the aerodynamic force on the sail. A catamaran is naturally stable due to its laterally placed buoyancy and is therefore superior in that regard to monohulls. The WSA of a monohull is less for a particular length and displacement than a catamaran of the same length and displacement. This can be demonstrated using a simply analogy of 2 half cylinders compared to one larger half cylinder of same total volume[2]. Modern sailing monohulls however, gain their heel stability from the introduction of a heavy keel. A catamaran on the other hand has no need for this heavy keel and will therefore displace far less and sit relatively higher than a monohull, thus countering this effect. From practical experience the reduction in wave drag due to reduced displacement and smaller angles of entry for a given sail area dominates over slight increase in viscous drag due to small increase in WSA (see Appendix B), making sailing catamarans faster that their monohull counterparts. As the catamaran heels, the WSA will decrease rapidly as the windward hull emerges (see Appendix G) therefore also reducing the viscous drag.

[2] A more accurate comparison of slender hull WSA is made in Appendix B, using the formulae taken from [DL01]

Another difference is that catamarans tend to be less manoeuvrable as the resistance on the demihulls is far from its centre of rotation and they also have high rotational (yaw) inertia.

In order to model a sailing boat accurately, an understanding of the forces acting on it must first be established. The sails act either as wings in the vertical plane or as 'bags' that absorb the momentum of the passing air. There is therefore often a sideward component to the thrust force acting on the sails. This is undesirable and is therefore countered by an equal hydrodynamic force resulting from the high lateral resistance (mostly on the daggerboards and rudders). The alignment of the hydrodynamic and aerodynamic forces is important in maintaining directional control of the boat and will be discussed in more depth in section 1.3.

One of the fundamental differences between sailing catamarans and power catamarans is the location of the thrust force. For sailing cats, the thrust force acting on the sails will act at their Centre of Effort (CE) and the method for determining this is laid out by Larsson et al. [LE02]. Since this position will be elevated above the hydrodynamic forces, the result is that the forward component of the thrust force results in a pitching moment (nose down) and the sideward component results in a heeling moment (to leeward). Since catamarans have slender hulls with little buoyancy near the bow, the pitching moment makes them susceptible to pitchpole. The aerodynamic side force causes the boat to drift sideways, resulting in a slight angle of attack of the boat with its direction of movement (leeway angle). This in turn causes a hydrodynamic side force on the foils (rudders and daggerboards) and hull which apposes the aerodynamic force.

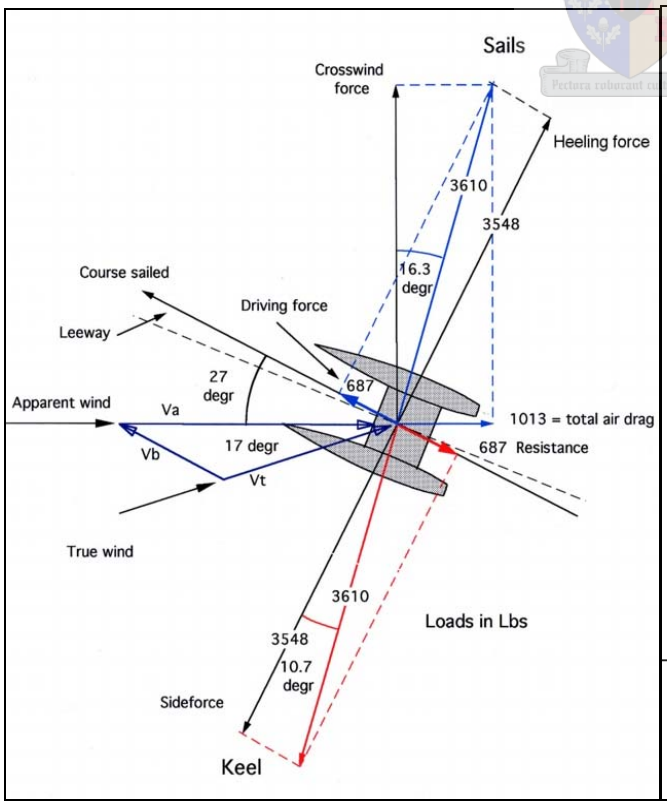

Fig 1.2 - Top view of the aerodynamic and hydrodynamic forces on a sailing catamaran (Taken from [Shut05(ii)])

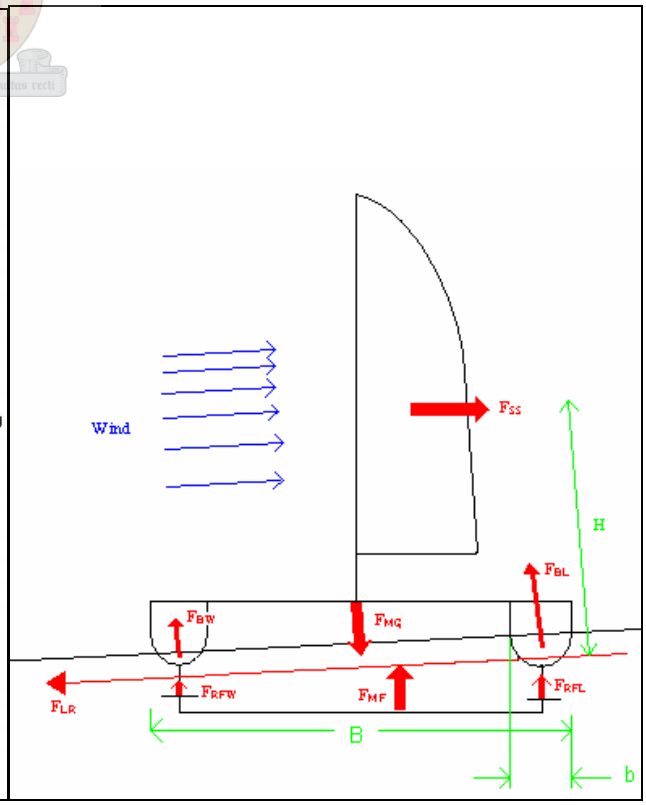

Fig 1.3 - Rear view of the aerodynamic and hydrodynamic forces on a hydrofoil supported sailing catamaran

The direction of the wind onto the sail is affected by the speed of the boat. A vector addition of the boat speed and true wind speed results in the apparent wind over the sails. In Figure 1.2, the concept of apparent wind and the aerodynamic and hydrodynamic forces are shown. In figure 1.3, the sideward components of the aerodynamic and hydrodynamic forces are shown to produce heel, which in turn creates a shift in centre of buoyancy towards the leeward hull, which creates a righting moment. The lifting foils are also included and their stabilising effect, due to surface effects is also illustrated. A more complete description of the balance of forces and moments may be found in Chapter 16 of [LE02] but the additional effects of the hydrofoils are not included in this.

1.3 The Balance of Sailing Boats

An important factor in a sailing boat design is balance, i.e. balancing the hydrodynamic and aerodynamic forces to ensure yaw stability of the boat. The following is explained by Larsson et al. [LE02] in more detail, however figure 1.4 a) and b) below show the case of how these forces are aligned (designed for low heel) and become unbalanced as a result of large heel angles. This imbalance is then compensated for with rudder angle and is experienced as weather helm. Varying the rudder angle reduces or increases the amount of side force (lift) generated on the rudder and therefore shifts the CLR forward or aft respectively, thus realigning the hydrodynamic and aerodynamic forces.

a) b)

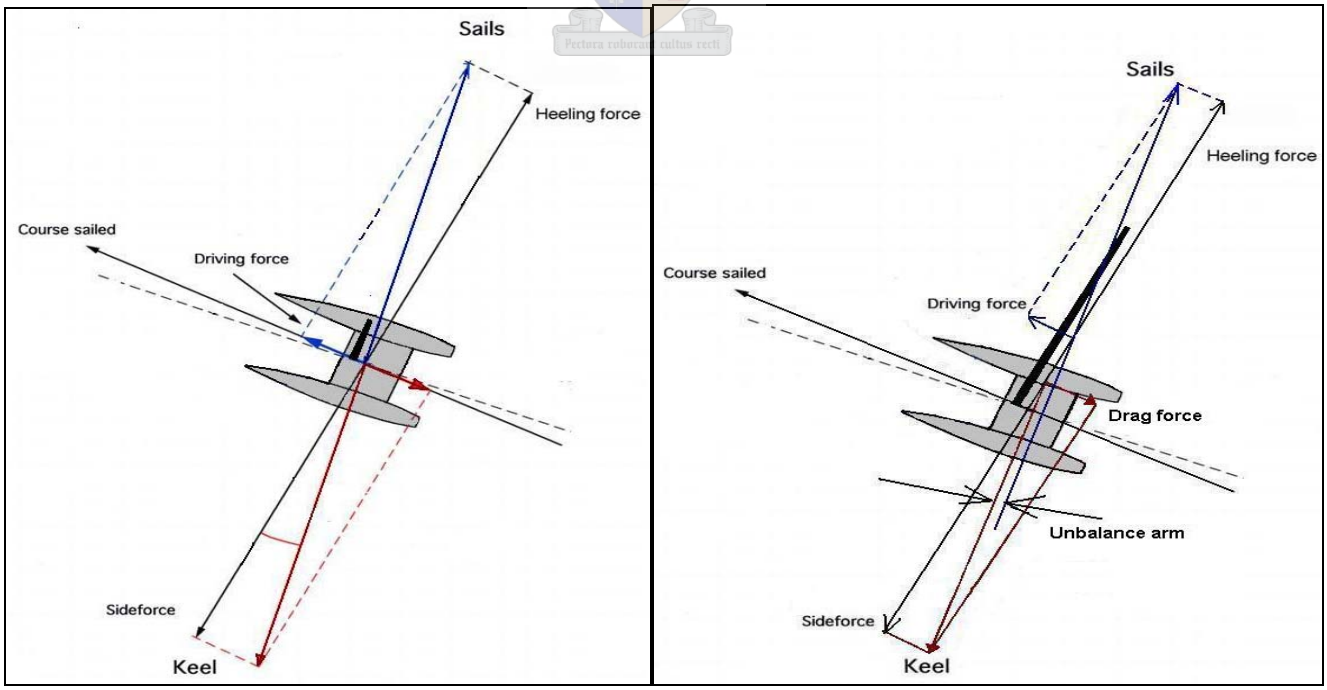

Figure 1.4- Cat at small (a) and large (b) heel angle (modified diagram from [Shut05(ii)])

In the case of monohulls, the COD moves sideways very slightly (as apposed to the large sideways movement of the CE) with heel and so the yawing moment created and the resulting weather helm will be significant

above say 15 degrees. For catamarans, the Centre of Drag (COD) moves further sideways (to leeward) with heel and therefore the range of heel angles for which catamarans don't experience significant weather helm is much larger than for monohulls. This has significant implications with regard to pointing ability and handling, but that lies beyond the scope of this study. It is important to note that as the boat heels, the force vector on the sails gains a vertical component and thus sinkage is increased with heel, while forward thrust is reduced.

1.4 Types of Hydrofoils & Configurations

1.4.1 Foil Arrangement

The use of a single lifting foil (unifoil) has been used with a certain amount of success in the past. For the case of a large amount of loading on the foils however, the boat becomes unstable (like a sea-saw) it is therefore advantageous in terms of pitch stability (especially for sailing craft), to support the boat with two or more foils. Since two foils provide the least amount of interference between foils and are the simplest, configurations of this sort are fairly common. The two foil configuration can be subdivided into three further categories, based on loading of the foils. (See figure 1.5)

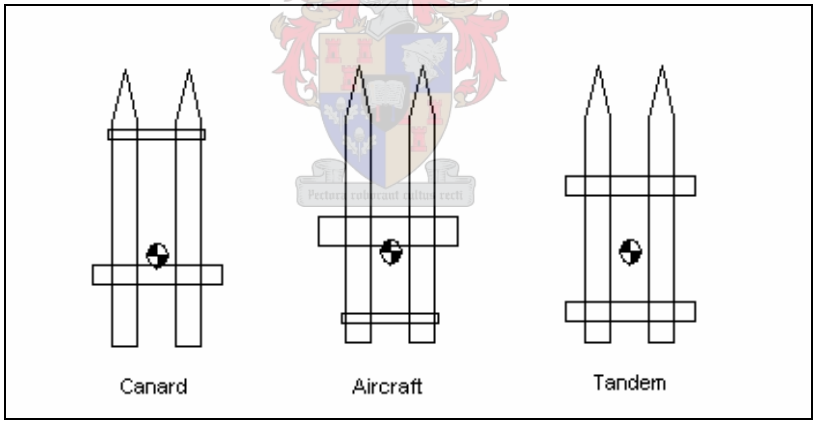

Figure 1.5 – The Canard, Aircraft (HYSUCAT type) and Tandem Configurations

- The Canard Configuration has a main foil just aft of the COG and thus provides most of the lift. A front or canard foil is situated near the bow and provides balance and pitch stability.
- The Aircraft Configuration is almost the opposite of the canard and the main foil is situated just in front of the COG with the rear foil providing the pitch stability.
- The Tandem Configuration has two foils which support the boat fairly evenly in terms of lift and distance from the COG.

1.4.2 Surface Piercing and Fully Submerged Foils

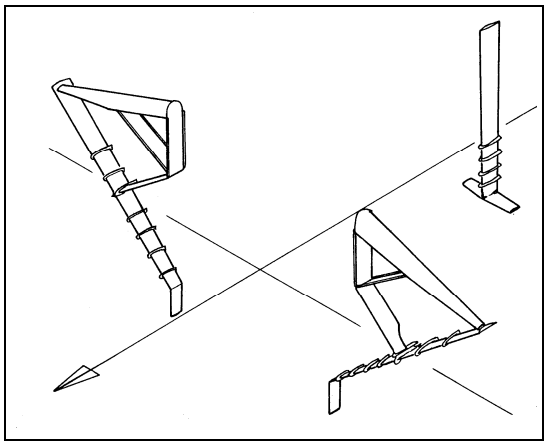

Figure 1.6 - Surface piercing foil configuration of *Mayfly* [Cha00]

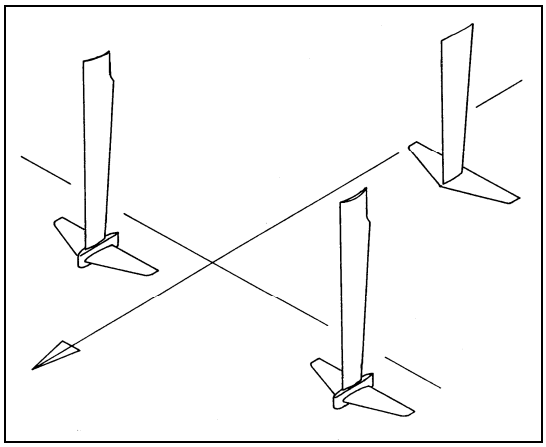

Figure 1.7 – Fully submerged, incidence controlled foil configuration. [Cha00]

Surface piercing foils are foils which have their root at the free surface and are characterised by a reduction in wetted area as the foil rises out of the water. This is achieved by angling the foils down when moving abeam towards the centreline along the horizontal plane and this angle is known as the dihedral angle. An added advantage is that due to this angle, the foil will provide additional natural heave, pitch and roll stability. This will be discussed in more detail in Chapter 3.3.3. Figure 1.6 is the foil configuration taken from 'Mayfly' where the main foil is a surface piercing foil and the rear foil is a standard T-foil on the rudder. (Refer to Appendix A, Figure A.3)

Fully submerged foils are almost exclusively found in a horizontal plane. Typically they are T-foil in nature but for large foils, multiple struts are used and their placement affects the aspect ratio (to be discussed in 3.3.4). Figure 1.7 shows an example of fully submerged T-foils.

1.5 Operating Regimes of Hydrofoil Assisted Craft

The operating regimes of hydrofoil assisted craft in general terms consist of three phases of operation, depending on displacement Froude numbers (Fn_∇). Migeotte [Mig01] provides a good explanation of the three phases of hydrofoil support – namely: Displacement, Transition and Planing. Figure 1.8 shows the kind of trends and boundaries of the three phases that are to be expected for a hydrofoil supported craft. The exact shape of the curves depends on the hull shape and the size of the foils i.e. relative amount of load that they carry.

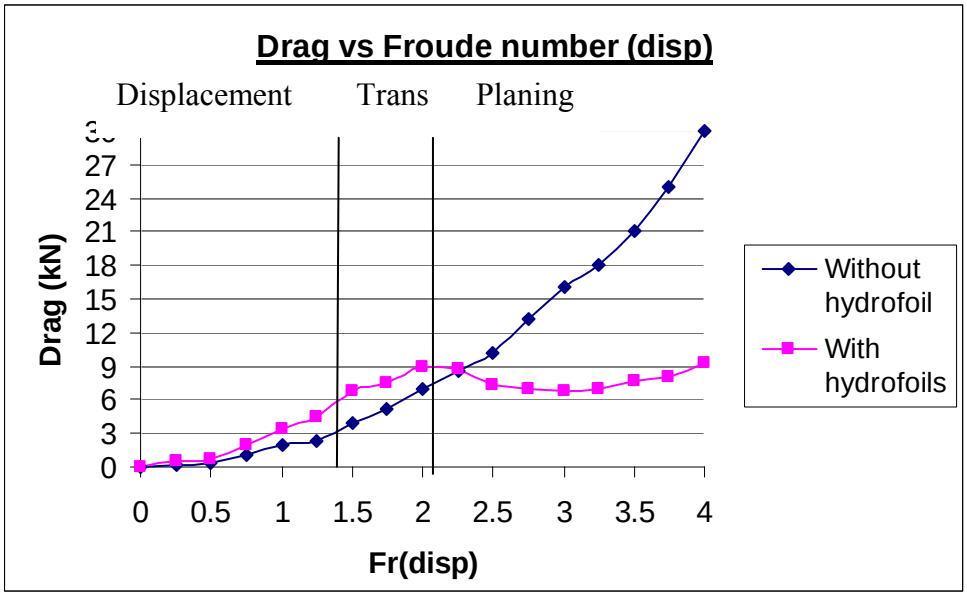

Figure 1.8 – Resistance trends to be expected on hydrofoil supported craft.
Trends were observed from results taken from [Mig01]

- The Displacement Phase is characterised by strong wave making patterns and very little rise. The foils provide very little lift as the velocity is insufficient to provide a strong lift force (see Chapter 3, equation 3.1) and since they are adding to the WSA, usually increase the total hydrodynamic resistance. Lift is mainly provided by the hull in the form of buoyancy. A main foil spanning the tunnel between the demihulls may also serve to reduce wave making resistance through wave cancellation of the foils and the demihulls. There is a displacement hump at around $Fr_{\nabla} = 1.5$ but this is normally only significant for heavily loaded hulls. This is not the case for sailing craft.

- The Transition Phase is characterised by a marked reduction in resistance as the foils begin to lift the hull clear of the water. The wave making is also reduced and at a particular Fn_{∇} the total hydrodynamic resistance drops to below what was experienced at lower Fn_{∇}. This is known as the transition hump speed. The characteristics of the curve are determined by the balance in dynamic forces (suction due to hull shape and hull foil interaction) and the lift of the foils. Aspects of hull shape are discussed in Chapter 2.3.

- The Planing Phase is when the boat is almost fully supported by foils and the remaining hull lift is primarily due to dynamic (planing) effects. The wave resistance is almost zero and the resistance begins to increase with increasing Fr_{∇} again because no more of the hull can be raised out of the water while the drag on the foils is increasing.

1.6 A Brief History of Hydrofoil Supported Sailing Catamarans

The concept of using hydrofoils to improve the performance of sailing craft has been around for many years. A good background into the development of the hydrofoil supported craft is given in the history section of the website for the hydrofoil supported trimaran L'Hydroptere [The95]. Another good reference for an historical review of the development of fast sailing yachts is an article entitled 'Greed for Speed' in Yachting World Magazine [YW02], where the development of the hydrofoil supported catamarans 'Mayfly' and 'Icarus' is described. Patents for hydrofoil supported sailing boats were found dating as far back as 1955 [Gil55], where a sailing catamaran dinghy was modified to operate with hydrofoils. (Refer to Appendix A, Fig A.1) In fact this 1955 configuration is an almost direct conversion from aircraft to sail craft, where the control system, seating position and trim and lift controls are identical.

Despite all of this development, it was noted that none of the companies listed on the internet that produce sailing catamarans in South Africa, employed any form of hydrofoil support system.

It was also noted that the bulk of hydrofoil assisted boats that are being tested at present are either tested at prototype level, without the assistance of rigorous towing tank tests (due to availability) or the test data was not made available. It would therefore be very useful to the South African Boat Building Industry for such an investigation to take place.

In Appendix A, figures A.1-5 gives some examples of the many hydrofoil assisted sailing catamarans found on the internet. Figures A.6-8 provides examples of other types of sailing craft that make use of hydrofoil support and Figure A.9 demonstrates an alternative use for a hydrofoil (as a paravane which improves the performance of the boat by countering the heeling moment rather than reducing the hydrodynamic resistance on the hull)

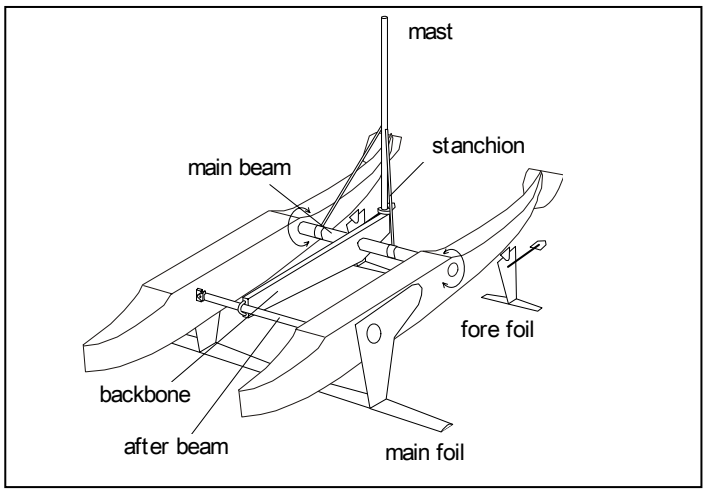

Figure 1.9 – Canard configuration of 'Twin Ducks' [KHK00]

The success of the examples given in Figures A.1-8, demonstrates that the principle of using hydrofoils to reduce the total hydrodynamic resistance can be applied to sailing boats and there are some important factors regarding these designs. All of the examples of hydrofoil supported craft had some form of trim and ride height control included in their design and had an aircraft type configuration, except the Miller Hydrofoil Sailboard (fig A.8) and the 'Twin Ducks' (fig A.5), which have canard configurations and the Miller Hydrofoil Sailboard relies on free surface effects to provide pitch and heave stability. Icarus, Mayfly and L'Hydroptere have surface piercing main foils – which provide additional heave and roll stability while the rest are fully submerged, although the 1955 patent has a slight dihedral angle on the main foil purely for roll stability.

From this we can deduce that the aircraft type and canard configurations, with surface piercing and fully submerged foils both with and without trim and ride height control, have all been used with a certain amount of success. The most popular combination seems to be an aircraft configuration with a surface piercing main foil and some form of trim and ride height control.

Figure 1.10 – Pictures of boats with aircraft type configuration,
surface piercing main foil, trim and ride height control.
Icarus (left) [Gro87] and L'Hydroptere (right) [The05]

Figure 1.11 – Pictures of Veal's Moth [Vea05])
Aircraft configuration, fully submerged foils and trim and ride height control

As can be seen in figure 1.11, the weight of the crew on a hydrofoil supported dinghy has a large influence on the COG. This allows for more freedom in terms of foil loading. Another thing to note about dinghies is that they have high sail area to displacement ratios and are therefore good candidates for lifting hydrofoils. For example, the boat that was ultimately used for this project was 37 foot catamaran and had a ratio approximately half of that of 'Mayfly'.

1.7 The Concept

Research into the HYSUCAT or Hydrofoil Supported Catamaran (motorised) has been conducted at the University of Stellenbosch for over 20 years [Uni06]. Based on the success of the research conducted on the HYSUCAT and other power boat craft, the concept of this research is to investigate the feasibility of using the HYSUCAT (aircraft type) configuration, which has no trim and ride height control, on a sailing catamaran that best represents those being produced in South Africa. The concept will be tested using towing tank tests of an appropriate model and verified computationally. Once the model has been tested with and without hydrofoil support, the practicality of the foil system can be assessed and any modifications made. Once a suitable hydrofoil support system has been established, the resistance characteristics of the boat with and without 'lifting' hydrofoils will be compared and the improvement (if any) commented on. During testing, no attempt will be made to test a control system (trim and ride height). It is hoped that this will not be necessary, given the correct configuration, but this may be proven otherwise.

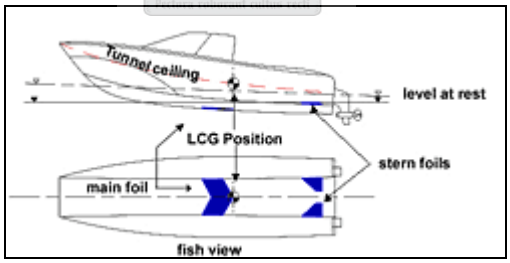

Figure 1.12 – Diagram of HYSUCAT [Cae06]

Given that a standard sailing catamaran has rudders near the stern and daggerboards are amidships, it would make sense to attach foils to these. If lifting foils are placed elsewhere they would require additional struts which in turn would upset the balance of the boat, thus requiring a redesign in terms of balance. Placing foils on the rudders and daggerboards would therefore allow for a simple 'add-on' hydrofoil design. The longitudinal centre of gravity (LCG) is intuitively expected to be not far aft of the main foil thus we would have an aircraft type configuration with most of the load on the main foil and as a result, poor pitch stability. Since pitch-pole is a problem for sailing catamarans, the stability of this configuration may not be suitable without the LCG relatively far aft or a trim control system.

The daggerboards provide an excellent platform for the attachment of a main foil spanning the tunnel and the rudders are suitable for rear T-foils. The idea is that the main foil being near the COG will provide most of the support while the rear foils provide the pitch stability. This configuration would not interfere significantly with the balance of the boat at low heel angles and the foils are placed in relative safety (against impact or entanglement) below the tunnel of the boat. Since the main foil will be no deeper than the daggerboards, if impact occurred with a sandbank or any submerged body, it is likely that it would have occurred in any case and the same can be said of the rear foils and their attachment to the rudders.

Since the span of the tunnel of sailing catamarans is usually quite large compared to power craft, a relatively high aspect ratio foil (very efficient – to be demonstrated in 3.2.1) could be placed between the daggerboards.

A problem with ending the main foil at the daggerboards is that there is a bending moment on the daggerboards which could be counter-balanced by extending the main foil beyond the daggerboards. (As in Appendix A, Figure A.1) The problem with that is that the main foil is no longer protected within the tunnel of the boat and despite the increase in aspect ratio, there will be more interference drag with the daggerboards due to twice as many 'corners'. (See Chapter 3.2.4)

1.8 Objectives of the Thesis

The *main objective* of this thesis: To design a hydrofoil system without a trim and ride height control system and investigate the change in resistance of a representative hull across a typical speed range as a result of the addition of the hydrofoil system, while retaining adequate stability.

The following *secondary objectives* were also identified so that the validity of the results is ensured and a greater understanding of the dynamic effect of adding the hydrofoils will have on the performance of the sailing catamaran.

1. To find a representative hull of sailing catamarans produced in South Africa, so that the results of this research could be applied to most sailing catamarans produced in South Africa and to establish an appropriate speed range for that hull across which it is to be tested.
2. To test and explain the resistance characteristics of this hull.
3. To find a suitable configuration of lifting foils for this hull that would not require any form of trim or ride height control to maintain stability throughout the speed range.
4. To test and compare the resistance characteristics of the representative hull with and without the assistance of lifting foils. This is to be tested concurrently with point 3 so that a configuration which

provides a reduction in total hydrodynamic resistance across a maximum portion of the speed range may be achieved while maintaining stability throughout that speed range.

5. To test and explain the effects of leeway and heel on the performance of the boat both with and without the assistance of lifting foils and draw conclusion as to how this would affect the overall performance of the boat. Since these aspects are significant in sailing boats, their effect on total hydrodynamic resistance will need to be considered and the effect of adding the hydrofoils on these aspects will also need to be considered.

1.9 South African Sailing Catamaran Representative

In order to establish the size of a suitable representative Sailing Catamaran produced in South Africa, a search was conducted over the internet so that a survey of most South African sailing catamaran building companies could be conducted. 23 Companies were found, producing 38 sizes of Catamarans. Figure 1.13 below shows the histogram of these sailing cats.

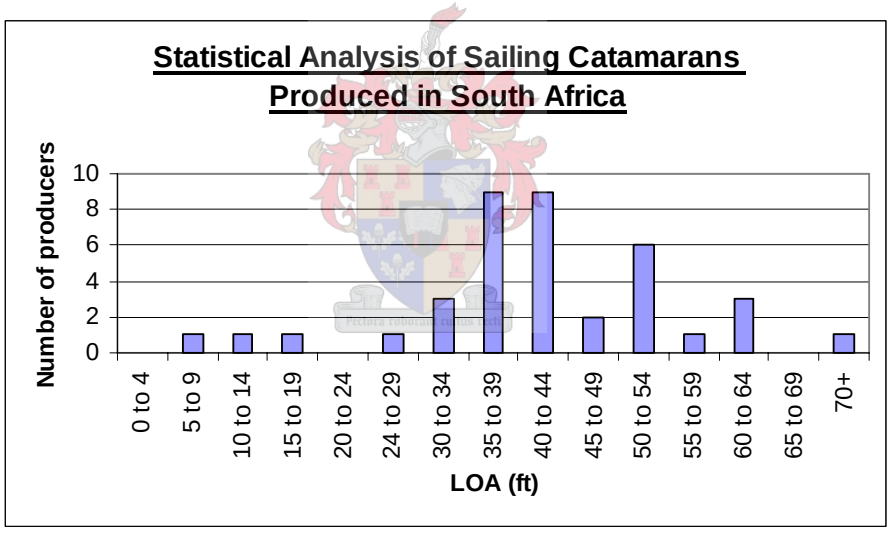

Fig.1.13 – Histogram of Sailing Cats produced in South Africa

From this it was decided that any sailing catamaran in the range of 35 to 44 foot Over-all Length (LOA) would be suitable. The dimensions of a hull produced in South Africa, which fits into this range, are provided in table 1.1 below. These dimensions were used as a representative sailing catamaran which formed the basis for investigations carried out in this project.

LOA (m)	11.2
BOA (m)	5.7
Δ (tons)	2.6
Boat speed range (knots)	0 – 25

Table 1.1 – Basic parameters for representative hull (See appendix C for more details)

Chapter 2

Hull Hydrodynamics and Design

2.1 Resistance Components on a Hull

Since the main objective of this project involves investigating the resistance of a hull and how it is affected by the introduction of hydrofoils, it is important to understand the components of this hydrodynamic resistance. Additional components will be added with the addition of the lifting foils and the interaction between the hulls and foils will also need to be accounted for. These will be discussed in chapter 3.

2.1.1 Viscous Resistance

The first and most obvious resistance component is the viscous resistance resulting from the hull skin friction and viscous pressure drag. Viscous resistance is dependent on Reynolds number and so for equivalent scaling of the model we would require Reynolds similarity.

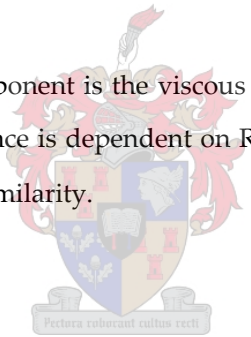

2.1.2 Form Resistance

Another component is the form resistance. This resistance component results from the shape of the hull as the fluid is forced to change direction (and speed as a result) in order to travel around the hull. This is modelled by simply adding a form factor (1+k) to the viscous resistance, which is roughly equivalent to the average increase in speed required to travel around the hull.

2.1.3 Wave Resistance

The next component is wave resistance. This resistance component results from the additional energy required to create the waves resulting from the hull travelling through the water. These waves may be divided into the following categories – diverging (from bow and stern) and transverse waves. For equivalent scaling, Froude similarity is required. Note: fluctuations in wave resistance are as a result of both interference of the bow and stern wave system (as discussed by Bertram [Ber02]) and the wave interference of the two demi-hulls to be discussed in Chapter 2.1.9)

2.1.4 Spray Resistance

This resistance component is a result of the energy required to produce the spray. It is however expected that since the given hull shape is semi-displacement and the speed range is not very high, this is not expected to be a very large component.

2.1.5 Interference Resistance due to foils

This is the added resistance due to interference of the boundary layers of the hull and foils where they join. This is discussed in section 3.2.4 where the low pressure above the foil creates a downward suction on the hull, which in turn cancels some of the lift generated by the foils. In terms of hull resistance, the reduced pressure and associated increase in flow in the gap between the hull and foils would result in an increase in viscous resistance. This may be factored by a change in the form factor on the hull due to foils. Since only a percentage of the hull is affected and at speeds where the effect is strong, the hull will be elevated from the water substantially, this is not expected to be large, but may account for errors in assuming minimal interference between hull and foils.

The wave interference of the foils and hull may be considered as acting on either the hydrofoils or the hull. It is a function of speed and positioning of foils. Migeotte [Mig97] indicates that these effects are both significant but no means of determining them theoretically or empirically are available.

2.1.6 Heel Resistance

This is simply the change in resistance (primarily wave and viscous) due to heel. An empirical equation describing the coefficient of resistance and its corresponding formula is found in Larsson et al. [LE02] however this is for a monohull, which behaves very differently to a catamaran. The main difference is that for a catamaran, the WSA is remarkably reduced with heel as the one hull emerges from the water, thus reducing the viscous resistance. It is however interesting to note that from the formula, the effect of heel resistance increases with the square of the Froude number. It must also be borne in mind that heel has other implications also as the force vector on the sail gains a vertical component with heel. Normally this is assumed to cancel with the upward component on rudders and daggerboards [LE02] but with the addition of lifting foils there is an increase in sideward component due to the heel angle and a righting moment due to the free surface effects.

2.1.7 Induced Resistance

Normally this resistance is associated with hydrofoils and is explained in more detail in chapter 3.2.1. If the hull is thin, it may be thought of as a symmetric hydrofoil of low aspect ratio, operating in the vertical plane. If there is an angle of attack or leeway angle on the hull, there will be a resulting side force and induced resistance. Since the effective aspect ratio and area of the hull are relatively small, the daggerboards and rudders will offer most of the resistance to leeway, and induced resistance on the hull is expected to be very small.

2.1.8 Resistance due to Submerged Transom

Transom sterns have several advantages, the most important being that the wetted area (and hence viscous resistance) is less than that of a hull with a streamlined stern while still producing an equivalent wave pattern. [DD97]

When the transom of the hull is submerged at low speeds, the flow does not separate cleanly off the transom and therefore produces a large stern wave due to the sudden change in flow direction. At higher speeds, the velocity pressure of the flow under the transom is sufficient for separation resulting in 'smooth' flow off the stern and reduced resistance (see figure 2.1 below). This means that the LCG may be placed further aft for high speeds, but the transom must be preferably in line with the water level for low speeds.

Doctors et al. [Doc98] quantified the speed at which flow off the submerged transom becomes 'cleanly separated' in terms of a Froude number based on depth of the transom below the static waterline (d). This critical Froude number is defined as follows…

$$\mathrm{Fr\_crit} = \frac{V}{\sqrt{gd}} = 4.14 \qquad (2.2)$$

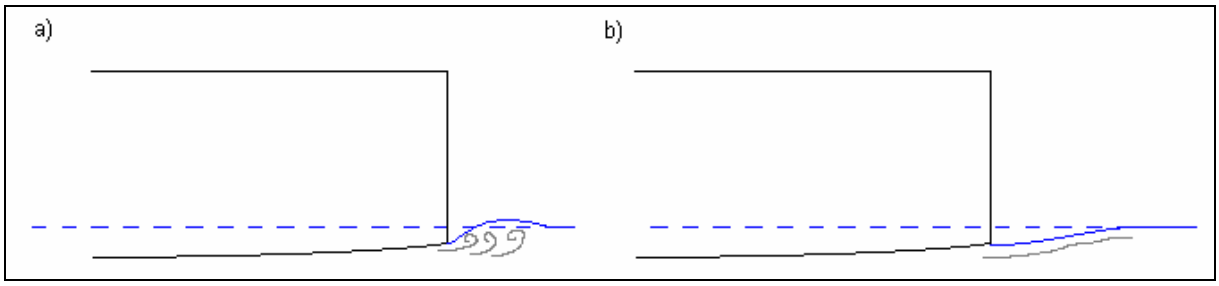

Figure 2.1 – Transom stern at below (a) and above (b) critical Froude number

2.1.9 Resistance due to Interference between Demihulls

- *Induced resistance on hulls due to asymmetric flow around demi-hulls*

This results from the flow over the two demihulls affecting one another. This effect is a function of Froude number and separation distance. As described by Couser et al. [CWM97] the flow about the demi-hulls centrelines is not symmetric resulting in a relative angle of attack and in turn a side force and induced drag force resulting on each hull (lift and induced drag as described above). The side forces on either hull cancel one another out. However, the induced drag on both demi-hulls acts in the same direction and therefore they add. It is logical to assume (as demonstrated by [CWM97]) that the greater the separation distance and the lower the speed, the less of an effect this has. It was also noted that even for smaller separation distances and narrow hulls (high effective aspect ratio) the resulting induced drag coefficient is much smaller than the drag coefficient for the demi-hulls alone and may therefore be ignored. This is again supported by [CMAP97] who states that the side force on the demihulls decreases rapidly with increasing separation while the drag remains relatively constant. This implies induced drag is not significant. The generation of side force is however significant and may be required for structural calculations. It was also noted that this side force is almost always outwards however for small separations the venturi effect may dominate over the impinging bow wave effect and cause suction between the hulls.

- *Wave and viscous interference between demi-hulls*

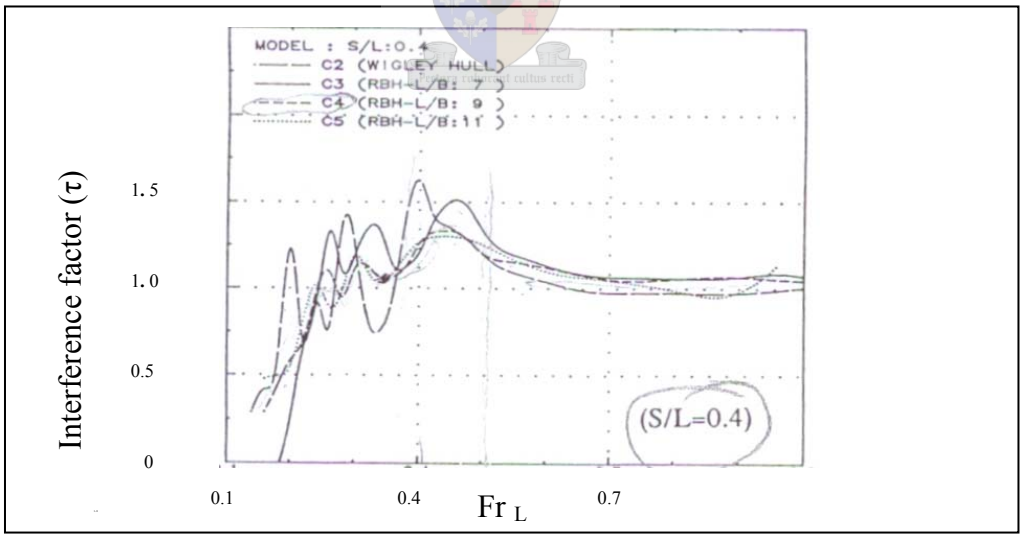

Figure 2.2 a) Graph of interference factor (τ) vs Froude (Fr) number taken from IM91

The wave patterns of the two demihulls may also affect each other depending on speed (Fr) and separation distance. A further effect is that asymmetric flow around the demi-hulls effects the viscous flow i.e. boundary layer formation. Referring to [IM91], this type of interference resistance is a function of separation distance and Froude number. The results of [IM91] show that wave interference causes large fluctuations in wave resistance below Fr = 0.5 and a virtually constant and small interference factor above Fr = 0.6. This effect is diminished

with increasing separation. Referring ahead to Chapter 2.8, the Froude number (Fr_L) range of the hull which was ultimately designed as our representative hull (RH1) is 0 -1.06. This corresponds to the range examined by [IM91].

Alternatively Turner et al. [TT68] provide a series of results from model testing to determine parameters affecting interference drag. The dependence on separation distance and Froude number is again shown and the following graph uses the data presented in [TT68]. It shows that at $Fr_L \approx 0.27$ and 0.33 there is minimum interference and at (B-2b)/L = 0.266 (same as RH1 – see 2.8) there are large fluctuations in interference with Froude number. These fluctuations are greatly reduced at higher separations.

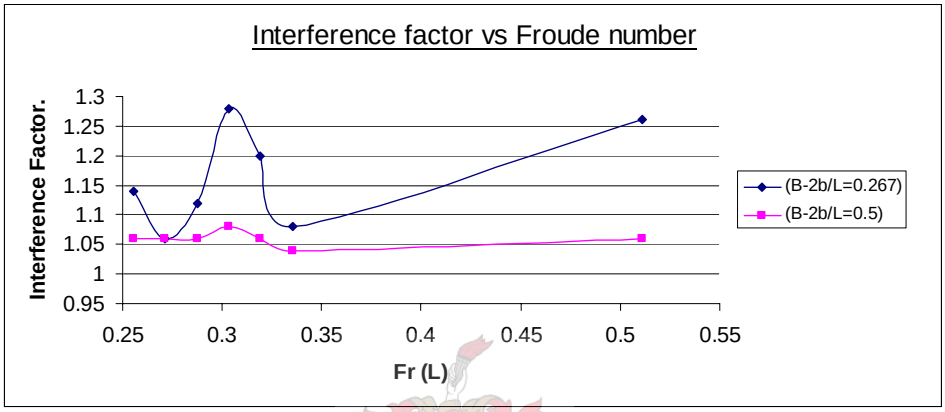

Figure 2.2 b) Graph of interference factor (τ) vs Froude (Fr) number plotted from [TT68]

2.2 Stability

Included in the main objective of this thesis is that the hydrofoil support system that is used in the final result will provide stable support throughout the given speed range. It is therefore important to consider the effect that the introduction of a hydrofoil support system will have on the stability of the sailing catamaran.

2.2.1 Pitch stability (Porpoising and Pitchpole)

As mentioned in chapter 1, pitch stability tends to be a problem for sailing catamarans due to the elevated thrust position and the fine demi-hull bows which offer very little buoyancy and planing effects to resist a forward pitching motion.

With the addition of the lifting foils, the COD would be lowered thus increasing the pitching moment arm between the thrust force and the hydrodynamic resistance. On the other hand the addition of the foils should reduce the resistance so it is unclear whether the pitching moment will be increased or reduced for a particular speed, depending on the positioning of the foils. What is clear is that the higher the hulls are raised by the lifting foils, the greater the angle at which pitchpole occurs. In addition to that the lifting foils should increase

the speed of the boat for a given condition so these two factors will increase the severity of the pitchpole if it were to occur on foil support.

The terminal velocity of a conventional sailing catamaran is determined by the speed at which the large pitching moment has lowered the bows sufficiently so that the deck starts to flood. This results in an unstable condition where the bows dig in completely and the boat pitch-poles.

Porpoising is a dynamic instability caused by the combined oscillations of boat pitch and heave, which either remains constant (not a comfortable ride) or increasing in amplitude (Risk of pitch-pole). The general rule for avoiding porpoising is to reduce the trim angle i.e. to move the COG forwards – counter trim by stern. For the case of a hydrofoil-supported boat, the hydrofoils act as natural dampeners for pitch and heave and so this instability may be avoided by careful balancing of the hydrofoils. Given the elevated position of the thrust force which will always tend to trim the bow down, it is unlikely that this will be a problem for sailing catamarans unless excessive lift is being produced on the hydrofoils which 'overpowers' the dampening of the free surface effects.

Since the dagger-boards (to which the main foil is attached) are found amidships the percentage of the lift force created by the aft foils is dependent on how far aft of amidships the COG is positioned. Ideally one would desire an even distribution of load on the foils for good pitch stability. The COG however is fairly dependent on the construction of the boat – particularly where inboard engines and water and fuel tanks are mounted. Practically it is found to be close to 45%, which implies very poor distribution of load.

2.2.2 Yaw Stability

Yaw stability is defined as the ability for an object to remain 'pointing' in the direction in which it is travelling. In terms of boats, it is defined as the tendency to resist rotation about the vertical axis (z-axis, as defined in naval architecture). Another definition [Ber02] is – "the ability to move straight ahead in the absence of external disturbances at one rudder angle"

Yaw stability is achieved by one simple criterion- The COG remains in front of the CLR. This may be illustrated by a dart or arrow. When travelling through the air in the conventional direction, it is easily seen that it remains yaw stable and the reverse can be said about a dart or arrow travelling backwards.
Most sailing catamarans are designed with the daggerboards amidships and rudders near the stern and the COG not far aft of amidships. As a result the CLR is usually well aft of the COG. The only condition where yaw instability is likely is when the boat begins to pitchpole so that the CLR is moved forward significantly. This is a case of pith instability in any case. The effect of hydrofoils of yaw stability is not likely to be significant if the

foils are attached to the rudders and daggerboards but a canard foil at the bow would shift the CLR forward, thus increasing the likelihood of yaw instability.

2.2.3 Sudden Loss in Foil Lift

The problem with foils as they near the surface is that of ventilation. This will be discussed in more detail in chapter 3 but in short, results in a sudden loss in lift. This would result in the section of boat supported by the ventilated foil dropping suddenly. This would increase the hull resistance at that point and may result in either yaw or pitch instability, depending on which foil becomes ventilated.

2.2.4 Other Aspects on Stability

Although these three aspects have been identified as the primary concerns with regard to the stability, there are many others. James Wharram [WB91] provides an interesting and insightful discussion on sailing catamaran stability, which stresses the importance of large displacement and that the CE (of the sails) is not too high above the waterline for maintaining good stability. The hydrofoils are expected to increase the displacement due to the added weight (and lower the COG) but also increase the height of the CE as the foils lift the hull out of the water. For a more complete evaluation of seaworthiness reference should be made to Marchaj [Mar86] and Krushkov [Kru81] For the purpose of future research, guidelines for assessing the Seaworthiness of a similar vessel is laid out by the ITTC in [IT99(ii)]. A means of quantifying stability (stability index or STIX calculations) for a small sailing monohull is given in appendix O. No equivalent was found for sailing catamarans.

2.3 Hullform Development.

Hullforms may be divided broadly into 3 categories; namely displacement, semi-displacement and planing hulls. These describe the range of speeds in which the hull is designed to operate and each will be discussed briefly.

2.3.1 Displacement hulls.

These are hulls designed to operate at relatively low Froude numbers, where the dynamic effects on the running conditions are very small. The hulls are typically ‘canoe-like’ in shape and they are characterised by large curvature in the aft section to allow for smooth flow that is split at the bow and rejoins at the stern. They also have round bilge station lines (the flow is too slow to separate cleanly off a hard chine hull) and thus vortex shedding at the chines is reduced at low speed. The boundary for this low speed is determined by the Froude

number of the boat and these hulls generally operate at below Fr_∇ = 0.35 as above this the drag curve is dominated by the hump resistance. [Mig97] Below in figure 2.3 is a typical displacement hull.

Since the Froude number range for displacement hulls is for low Froude numbers, hydrofoils are typically not used for these hull shapes as very large foils (large WSA) are required to generate significant lift. These in turn have large viscous drag components and thus an overall reduction in drag is practically not achievable unless the hull operates at speeds above conventional Froude number ranges for this hull; in which case a semi-displacement hull would have been a more appropriate hull shape.

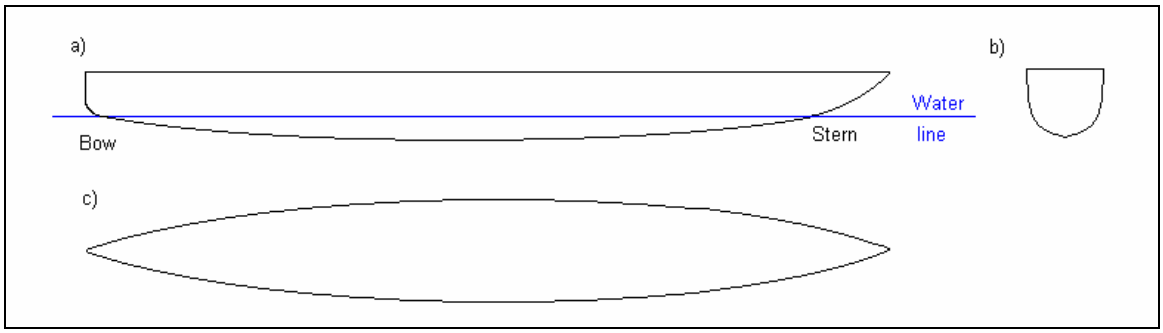

Figure 2.3 – Typical Displacement hull – a) Side view b) Mid-ship station c) Top View.

2.3.2 Planing hulls

Unlike displacement hulls these hulls are designed to operate at much higher Froude numbers (above the hump speed of displacement hulls) where the dynamic effects play a major roll in the running conditions of the boat. As a result, the large amount of curvature such as on the aft section of displacement hulls would result in large drag due to flow separation and suction. In order to avoid this, planing hulls have less curvature and a 'cut-off' or transom stern. In general, curvature of the buttock lines (a.k.a. rocker) and of the station lines create dynamic suction that induces dynamic sinkage and encourages vortex shedding, thus adding to the drag. Curvature is thus minimised on planing hulls but this will be discussed a bit more in 2.3.4. The WSA and dynamic effects are reduced with the incorporation of hard chines and spray rails. These allow for relatively flat sections in the station lines and the flow to be separated off the hull and create additional lift. The same separating effect is desired from the transom stern. Below in figure 2.4 is a typical planing hull.

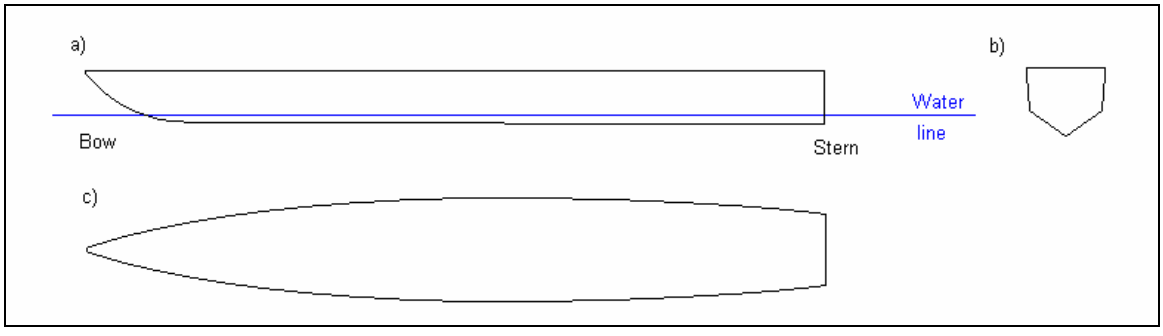

Figure 2.4 – Typical Planing hull – a) Side view b) Mid-ship station c) Top View.

Since these hull shapes are associated with operation at high Froude numbers, the use of Hydrofoils is very applicable to these hulls. Most of the lift force on these hulls is derived from dynamic forces and since hydrofoils are approximately twice as efficient as planing surfaces (as will be explained in section 3.3.1), their introduction is likely to reduce drag on the boat significantly.

2.3.3 Semi-displacement hulls

These hulls are a compromise between planing and displacement hulls. They typically have transom sterns, bows similar to displacement hulls and may or may not include hard chines, but seldom include spray rails. (Insufficient speed for spray generation) Sailing boats are almost exclusively in this domain of design, particularly since they operate over a large speed range and are required to perform well in all conditions. All the sailing catamarans produced in South Africa that were found during the internet survey (Chapter 1.9) were round bilge and transom stern in nature and typically had surprisingly large amount of rocker.

Since these hulls are designed to operate at a Froude number range spanning from where buoyancy forces dominate at low speeds to where dynamic forces dominate at upper speeds, hydrofoils are applicable to these hull shapes where the performance is reduced at low speed slightly due to increase WSA. As the speed increases the hull is raised out of the water and so the WSA and wave drag will be reduced, thus improving performance.

2.3.4 Rocker (Curvature of the buttock lines)

Rocker or curvature of the buttock lines is an important aspect of hull design and influences the wave-making resistance and seakeeping characteristics of the hull. Typically displacement hulls have lots of rocker while planing hulls have little or no rocker in the stern for planing effects (see following sections). This is because the curvature results in dynamic suction on the wetted surface of the hull, which in turn results in sinkage, increasing the drag on the hull. This effect is a function of free-stream velocity pressure (boat speed) and is therefore small at low speed. Displacement hulls have significant rocker since it reduces the cross-sectional area curve near the bow and stern and therefore reducing the wave making drag at low speed. At higher speed, the resulting sinkage is higher as the dynamic effect becomes significant.

Another aspect of rocker is the effects on seakeeping. Including some rocker in a hull design improves the performance of the hull in waves as it lowers the Centre of Buoyancy (COB) in relation to where the bow and stern enter and leave the water respectively. This allows the boat to respond more smoothly to waves by rocking so as to reduce the slamming and dragging of transom effects that would otherwise be experienced and

improve stability. On the other hand, too much rocker can result in hobby-horsing effect in waves which is obviously not desirable in terms of seakeeping. [Shut05 (i)]

Despite dynamic suction effects, rocker may be considered advantageous when a hull supported by hydrofoils is lightly loaded. This combination results in the boat lifting out of the water substantially at relatively low speeds and because of the rocker, the WSA decreases rapidly. If the hulls were compared with foils, they would have very low aspect ratios (since they are slender) and as a result do not produce large dynamic sinkage despite their large area. (Refer to Chapter 3.3.4)

2.3.5 Aspects of bow and stern design

Very fine bows, having deep V shape and narrow angles of entrance are associated with low wave making. This low wave making results in less disturbed flow in the tunnel which is where the foils are found, thus less of an effect on flow over foils. Another advantage is that the wave piercing characteristics of fine bows, results in reduced slamming and heaving of the bows in waves.

The disadvantage of fine bows (as discussed in 2.2.1) is their inability to resist pitchpole and the sharp bows mean the CLR moves forward rapidly as the boat pitches forward, reducing yaw stability. Fortunately for sailing cats, most of the lateral resistance comes from the rudders and daggerboards, diluting this effect.

Bulbous bows have been incorporated into some power cat designs, to reduce wave making resistance. The reduction in wave making drag is small on cats as it's already fairly small due to the narrow demihulls. [Mig97] They also tend to move the CLR forward, thus reducing yaw stability while also dampening pitching motion. Bulbous bows are almost never evident on sailing catamarans, and with therefore not be considered as part of the hull design.

The aft sections of power cats are usually designed in terms of stability and high speed performance. Stability is controlled more by the large rudders and daggerboards on sailing cats, and the high speeds achieved on power boats are only achieved in strong wind conditions. These aspects are therefore of less concern in the design of aft sections on sailing boats.

Since the sterns are generally broader and flatter, the effect of rocker is more significant on the mid to aft section. As a result rocker tends to result in natural trimming by stern which increases dynamically. This is to an extent desirable as it tends to counter the pitching moment but excessive rocker results in excessive induced and separation drag and sinkage as mentioned in 2.3.4.

2.3.6 Planing Effects

This dynamic effect acting on the hull is as a result of trim angle. It is not to be confused with planing speed but both are associated with relatively high speed (Froude number). As a result of trim angle, the hull rises out of the water. An analogy may be drawn between the hull and a flat plate at an angle of attack (See figure 2.5) where the effective downwash (as in a hydrofoil) results in a lift force on the hull. To ensure this trim angle, the LCG should be aft of zero trim position but this generally results in the transom dragging at low. (See 2.1.8)

Planing effects and dynamic suction resulting from hull shape (rocker and soft chines) will combine and result in the running conditions (trim and rise) which will vary with speed.

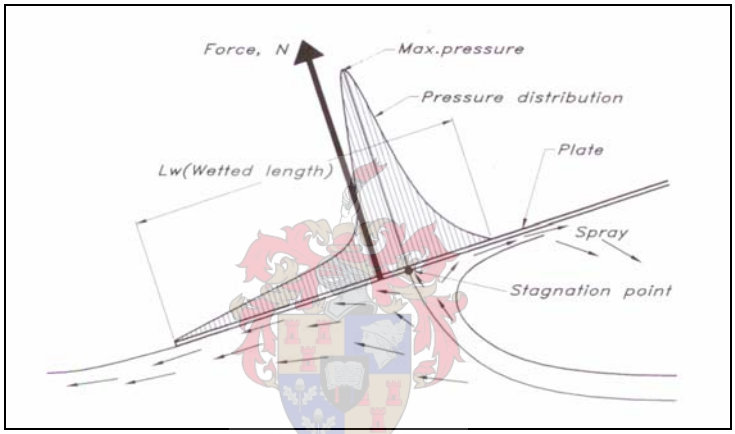

Figure 2.5 – Flat plate analogy of planing effects taken from [LE02]

2.4 Hull Selection

After the size of the yacht was determined in Chapter 1.5, two possible means of hull selection were determined. An existing hull shape of a sailing catamaran currently being produced in South Africa could be used, or a standard hull shape of suitable characteristics could be used. In either case, a representative hull shape would need to be found in order to determine these characteristics.

2.4.1 Finding a Hull

The first thing noted about sailing catamarans produced in South Africa is that the demihulls are symmetric. This is owed to the large separation between demihulls resulting in relatively small interference.

After consulting with local sailing yacht manufacturers, a hull was found but some concerns were expressed regarding the large amount of rocker this boat displayed. The associated dynamic suction on the hull would

need to be overcome by a lifting foil system if employed on this hull shape. Nonetheless, the characteristics of the hull were determined so that they could be compared to standard hull shapes. The hull characteristics were compared to the NPL [Bai76] and Series 64 [Yeh65] however no suitable match was found.

It was noted by the student that through his experience as a sailor, a fair amount of rocker is common in many sailing catamaran designs. As a result it was decided that the original hull shape would be used and if the problem of excessive rocker was overcome, this could be treated as a worst case scenario and even better results could be expected for applications to hull shapes with less rocker. Since the boat is fairly lightly loaded, this rocker may prove to be advantageous as discussed in 2.3.4.

Since no lines drawings were provided by the manufacturer, only 2D drawings and photos were provided, it was decided that demihulls based on the representative cat would be designed as part of this study. For the purposes of modelling the thrust force on the sails, details of the rig from the original hull are used. Since the hull generated by the student is aimed at being a representative hull of sailing catamarans produced in South Africa it was named Representative Hull 1 or RH1. (See figure 2.6)

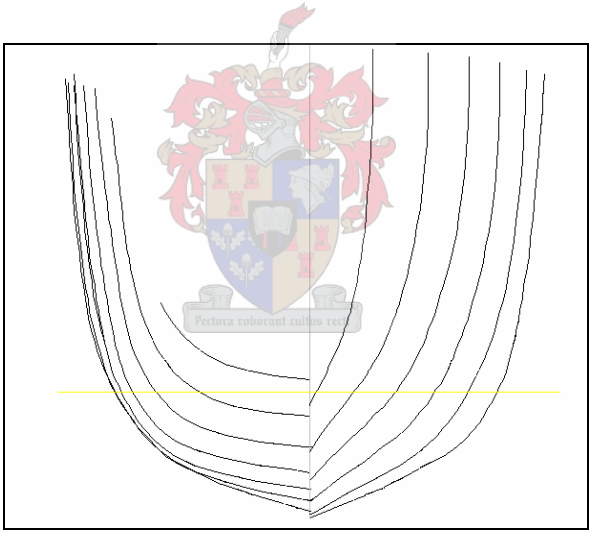

Figure 2.6 – Section plan of RH1

2.4.2 Discussing hull shape

According to Tom Speer [BD99], an expert in the field of sailing boat design, "*Since minimum wetted area and not form stability is the driving influence on multihull shapes, you can pretty well determine the lines yourself by taking the product of the profile and typical section shape.*" As a result it was decided that this method of determining the representative hull, although not accurate, should yield a suitably representative hull.

After referring to a discussion by Shuttleworth [Shut05(ii)] which explained how the buoyancy can be placed as a function of heave, so as to effect the trim of the boat, it was concluded that the bows were a little fine and

should have been flared slightly above the waterline. This would however only affect upper speed conditions when the boat tended to nose-dive as only flat water model testing would be conducted.

Since the main parameters of RH1 were based on the original boat, these are expected to be accurate and suitable. Since all other aspect were fairly well defined by the 2D drawings, the hull was deemed suitable.

As can be seen in figure 2.8, there is significant rocker all along the keel line of RH1. From the discussion in 2.3.4 and 2.3.5, we therefore expect a reasonable amount of dynamic sinkage at high speed and due to the large rocker (giving low effective trim angles on the aft section of the boat – where the hull is broad and flat) and narrow demi-hulls, we expect very little planing effects.

2.4.3 Evaluating performance

Larsson et al. [LE02] provides a few ratios for the evaluation of monohull sailing boat performance. Although we expect the performance ratios to be a bit higher for catamarans given their reduced displacement for a given sail area, these are nonetheless used as a yardstick.

The sail area to wetted area (Where the viscous forces are being compared to thrust force on sail) should be above 2 for reasonable performance and 2.5 is considered good. The waterline length- displacement ratio needs to be above 5.7 to ensure that the boat will reach semi-planing conditions. The sail area – displacement ratio (Where the wave drag is being compared to the thrust force on sail) should be between 20 and 22 for good performance. As can be seen in the table below, RH1 should have a very good performance based on these.

Ratio	Good performance range	RH1
S_A / S_w	2 - 2.5	2.86
$LWL / \nabla^{1/3}$	> 5.7	7.4
$S_A / \nabla^{2/3}$	20 - 22	32

Table 2.1 – Evaluating performance ratios of RH1

Hydrofoil Theory & Design

3.1 Foil Lift

Lift (L) is defined as the force produced at 90^0 to the free stream flow and in the plane of the foil cross-section. The lift produced by a two-dimensional hydrofoil in an ideal, unbounded fluid is given below.

$$L = \tfrac{1}{2} \rho V^2 A C_L \qquad (3.1)$$

Where ρ is the density of the fluid, V is the velocity of the fluid relative to the foil, A is the surface area of the foil and C_L is the lift coefficient. C_L varies linearly with angle of attack until the onset of stall (to be discussed shortly) and is a function of the foil shape and attitude. The value for C_L is given below for a simplified 2D, thin wing.

$$C_L = 2\pi \alpha_T \qquad (3.2)$$

Where α_T is the angle of attack relative to the angle of zero lift and the direction of flow. (See figure 4.1 below for a typical lifting foil cross-section)

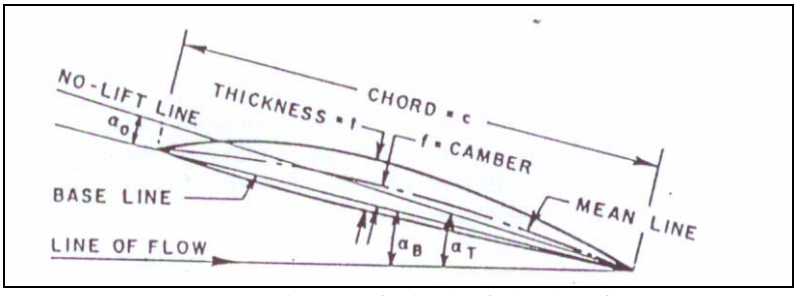

Figure 3.1 – Nomenclature of a hydrofoil taken from [Duc72]

From equation 3.1 it is clear that the lift increases quadratically with free stream velocity while only linearly with area. This means that for low speed applications, relatively large foils will be required to produce sufficient lift to raise the hull out of the water. This will result in a large WSA which in turn will mean large viscous drag (explained in more detail in 3.2.2). This means that hydrofoils are not applicable to low speed craft and will only

be beneficial to reasonably fast sailing craft when they are operating in the upper part of their speed range, i.e. in moderate to strong winds.

3.2 Foil Drag

Speer [Spe05] provides an excellent breakdown, with equations for the various components of drag on hydrofoils. Equation 3.3 below is presented by Speer and the components that each term represents are shown in italics below. The nomenclature has been changed from [Spe05] to maintain consistency.

$$D = (q \cdot C_F \cdot S_w) + (q \cdot N_j \cdot C_{Dj} \cdot t^2) + (q \cdot N_S \cdot C_{Ds} \cdot t^2) + (S_w \cdot q \cdot C_{DW}) + (\frac{1}{q} \cdot \frac{L^2}{[\pi \cdot (s^2 \cdot E)]}) \quad (3.3)$$

(Viscous) + (Interference) + (Spray) + (Wave) + (Induced)

$$C_{DW} = \frac{1}{2} \cdot k_W \frac{L^2}{s^2 \cdot h \cdot q^2 \cdot V^2} g \quad (3.4)$$

$$q = \frac{1}{2} \rho \cdot V^2 \quad (3.5)$$

Refer to the nomenclature for an explanation of all the symbols.

Alternatively, the total drag coefficient of the foils is broken down into its components by Migeotte [Mig97] in equation 3.6 below and then each coefficient is calculated separately. The component of drag is written in bracket below each coefficient and then explained in the sections that follow. All equations in each section are from [Mig97] unless otherwise stated.

$$C_D = C_{Di} + C_{DP} + \delta C_{DP} + C_{Dw} + C_{DS} + C_{DSep} \quad (3.6)$$

(Total) = (Induced) + (Friction & profile) + (Incremental profile) + (Wave) + (Spray) + (separation)

3.2.1 Induced

Induced drag is the drag associated with the lift created on the foil. Hoerner [Hoe65] gives an excellent summary of this and how aspects of configuration affect it – to be discussed in section 3.3. Figure 3.2 below shows how induced drag forms and equation 3.7 gives the simple equation for induced drag of a foil showing how it is related to lift for small angles of attack. (Excluding free surface effects on lift and trailing vortex system, excludes the presence of dihedral or sweep angles and assumes an elliptic lift distribution)

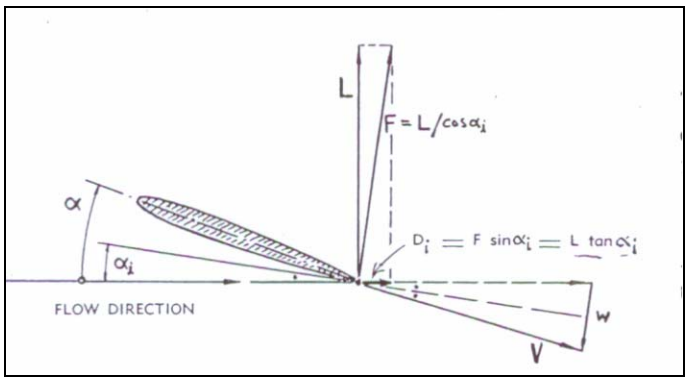

Figure 3.2 – Diagram demonstrating induced drag taken from [Hoe65]

$C_{Di} = C_L^2 / \pi\, AR$ (3.7)

Clearly, the larger the aspect ratio, the smaller the coefficient of drag and so less drag is produced for the same lift and area. Since sailing catamarans typically have large tunnels, the possibility of placing a high aspect ratio foil between the two demihulls means that a very efficient foil system is possible, while still keeping the foils relatively protected within the tunnel. All other forms of drag are not related to the lift produced by the foil and are therefore known as parasitic. (Present even when no lift is generated)

A more complete equation for induced drag is given below. [Mig97]

$$C_{Di} = \frac{C_L^{\,2}}{\pi AR \cdot K \cdot \cos\Lambda \cdot \cos^2\Gamma}(1+\xi)(1+\sigma) \qquad (3.8)$$

Where…

- K is the free surface effect correction (discussed in 3.3.1)

$$K = \frac{(16(\frac{i}{c})^2 + 1)}{(16(\frac{i}{c})^2 + 2)} \qquad (3.9)$$

(When i/c is small, P≈1/2)

- Λ and Γ are the sweep and dihedral angles respectively, as defined in 3.3.3.
- σ is Munk's correction factor for correction for the effect of the free surface on the trailing vortex system.

$$\sigma = 1.73 + 0.694\frac{i}{s} - 2.172\sqrt{\frac{i}{s}} - 0.514 \cdot e^{-\frac{i}{s}} \qquad (3.10)$$

- ξ is the plan form factor compensates for a non-elliptical lift distribution and is given as…

$\xi = a + b\ AR + c\ AR^2 + d\ AR^3$ (3.11)

$a = -5.9x10^{-4}$, $b = 8.47x10^{-3}$, $c = -5.9x10^{-6}$ and $d = -1.973x10^{-6}$

or Du Cane [DuC72] provides $\xi = 1 + (2/AR)$ (3.12)

3.2.2 Viscous / Frictional and Profile

This component of drag is associated with the boundary layer and the viscous forces on the surface of the foils. This is exactly as in hull drag where a form factor is applied to account for the shape of the foils being different from a flat plate.

C_{DP} is calculated from the equations that follow. For $Re < 5x10^5$ and thickness other than 0 or 0.2, the C_{DP} values can be interpolated or extrapolated from the values at these two thickness ratios. The following equations are taken from [Mig97] and follow from the methodology of Kirkman et al. [KK80] as described in 3.1.

<u>For $Re < 5x10^4$</u>

$C_{DP} = 1.46Re^{-0.507}$ (if t/c = 0.00) (3.13)

$C_{DP} = 0.466Re^{-0.259}$ (if t/c = 0.20)

<u>For $5x10^4 < Re < 5x10^5$</u>

$C_{DP} = 0.172Re^{-0.310}$ (if t/c = 0.00)) (3.14)

$C_{DP} = 181Re^{-0.810}$ (if t/c = 0.20)

<u>For $5x10^5 < Re < 1x10^7$</u>

$$C_{DP} = 2.93x10^{-3}\ (1 + 2(\frac{t}{c}) + 60(\frac{t}{c})^4) \qquad (3.15)$$

Re > 1x10^7

$$C_{DP} = 0.03\mathrm{Re}^{-0.1428}\left(1 + 2\left(\frac{t}{c}\right) + 60\left(\frac{t}{c}\right)^4\right) \qquad (3.16)$$

or

$$C_{DP} = \frac{0.075}{(\log_{10}\mathrm{Re} - 2)^2}\left(1 + 2\left(\frac{t}{c}\right) + 60\left(\frac{t}{c}\right)^4\right) \qquad (3.17)$$

The effect on profile drag due to the angle of attack of the foil δC_{DP} is calculated using the following formula [Mig97].

$$\delta C_{DP} = 0.005 C_L^2 \qquad (3.18)$$

3.2.3 Wave

This component of drag is associated with the formation of waves at the free surface. Equation 3.19 gives the component of drag coefficient resulting from wave drag of an individual foil.

$$C_{DW} = \frac{0.5 \cdot C_L^{\,2}}{Fr_i^{\,2} e^{2/Fr_i^2}} \quad \text{where} \quad Fr_i = \frac{V}{\sqrt{gi}} \qquad (3.19)$$

Depending on the placement of the foils and speed at which they are run, there may be positive or negative wave interference between the wave system of the hydrofoils and the hulls. The interference between the front and aft foils is described in 3.2.4.

Since this is a function of lift, it can be grouped with induced drag into a single equation.

3.2.4 Interference

- *Strut and the lifting foils*

Struts are vertical foils used to provide structural support to lifting foils. Apart from increasing the total viscous drag due to additional wetted area, the presence of struts result in an interference drag where they join the lifting foils. In the corners of the joints, the boundary layers of the two foils combine and the net result is a larger drag than the two foils taken separately. Additional pressure drag also arises from the pressure gradient

along the rear of the foils combining and retarding the boundary layer further. Hoerner [Hoe65] gives a good explanation of this and refers to various aircraft tail configurations for examples of interference drag. Furthermore interference between the foil and strut can result in cavitation, although this is not likely to be a problem for sailing catamarans (due to the low operating speeds see 3.3.2)

The drag coefficient is based on either thickness or chord length (subscript indicating which of the two) and equations for which are presented below.

$$C_{Dt} = 17(t/c)^2 - 0.05 \quad (3.20)$$

$$C_{Dc} = C_{Dt}\,(t/c)^2 \quad (3.21)$$

(t/c) is the thickness to chord ratio. If the angle between main axes of the foils differs from 90^0, the interference is worsened while if the foils are raked, the effect is seen to be reduced. The figure below is taken from Hoerner.

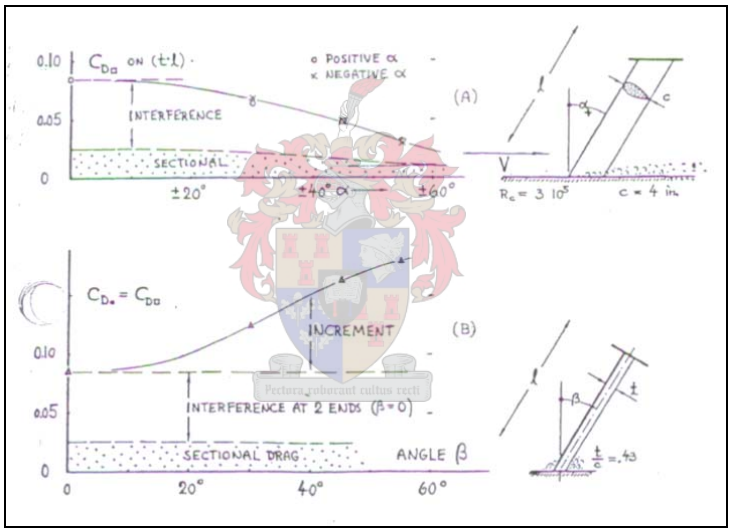

Figure 3.3 – Graphs showing effect of angling the join of foils on interference drag
Taken from [Hoe65]

Depending on the section, fairing the join of the foils with the correct radius (about 7% Chord) can reduce the interference drag by as much as 35%.

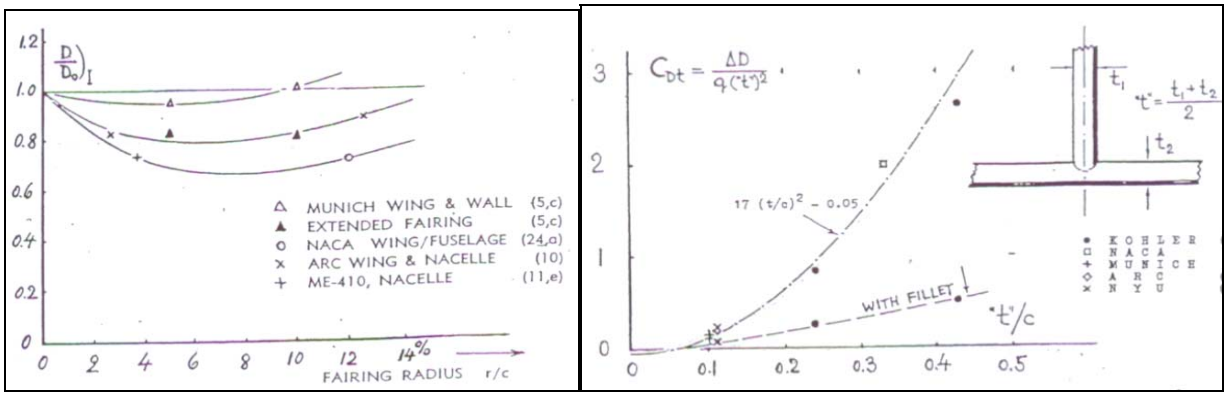

Figure 3.4 – Graphs showing effect of fillets on interference drag
Taken from [Hoe65]

The influence of struts on aspect ratio will be discussed in 3.3.4

A similar interference effect is found at the join of the foils to the hull and Hoerner also gives the following equations (assuming the wall is flat)

$C_{Dt} = 0.75(t/c) - 0.0003 / (t/c)^2$ (3.22)

$C_{Dc} = 0.8(t/c)^3 - 0.0003$ (3.23)

[Mig97] gives a graph showing the effect of interference drag in a corner on foil drag for a specific coefficient of lift and Reynolds number. It shows that when the joint is around 90^0 very little gain is achieved by adding a fillet radius and the magnitude of the interference drag is around 10%. As the angle at the joint decreases, the effect of fillet radius and magnitude of interference drag are shown to increase exponentially.

- *Front and Aft Foils*

As explained by Hoppe [Hop95], the wave interaction between the front and aft foils will usually result in the downwash from the front foil (creating a downwards velocity component to the flow) over the rear foil. This means that the effective AOA on the rear foils is reduced and this downwash effect varies with speed. At certain speeds however, the wave interaction will result in upwash on the aft foil.

Kolysaev et al. [KKL80] provide 3 criteria for the spacing of a tandem foil configuration, namely for strength, interaction with a design wave spectrum or for hydrodynamic optimisation. Since the latter is of most significance to this research project, it was only considered. It recommends the following limitations on the separation of the foils expressed in equation 3.24 for getting positive interference between the foils.

$$V\sqrt{\frac{s}{g}} < L_K < 3V\sqrt{\frac{s}{g}} \quad (3.24)$$

Where V is the speed of motion, s is the span of the front foil, g is the gravitational acceleration and L_K is the separation distance.

For the main and rear foil configuration of the preliminary design (See 3.4.2) the separation distance is 550mm (model scale) which yields an upper limit for model speed of 2.4m/s which is just about design speed. This means that wave interference only becomes significantly detrimental when the boat is fairly well supported by the foils and the hull drag has been reduced significantly. Since the rear foils of the proposed aircraft type configuration will be so much smaller than the main foil, their contribution to wave making and therefore ability to cancel the main foils wave system is very slight so this will only have a small effect on total drag.

For the final (canard) configuration (see 3.6.3) the wave making of the front foil is far more significant as more lift is generated than the rear foils of the previous configuration. The separation between the foils is 650mm, thus equation 3.24 yields an upper limit for model speed of about 4.9 m/s, well above the test speed range for our model.

Alternatively Matveev et al. [MM00] provides a methodology for determining the spacing of a tandem foil system such that the aft foil remains in the up-wash of the front foil. Since the wave length increases with speed, the separation distance required for this condition increases also. High speed craft require maximum spacing, impractical for most power boat applications with a HYSUCAT system. Sailing craft however, operate at lower speeds and may therefore be able to benefit from positive interaction. Equation 3.25 is from [MM00] and noting that beneficial up-wash on the rear foil occurs when ½ $L_H < L_k < L_H$, after substituting s of the model, the limits on the spacing between the foils is given by equation 3.26. This agrees with conclusions drawn from equation 3.24.

$$L_H = 1.95\ V\ (s / g)^{1/2} \qquad (3.25)$$

$$0.13V < L_K < 0.26V \qquad (3.26)$$

- *Hull and Foils*

An important aspect which must be taken into account when calculating the lift of the foils is the interaction between the hulls and foils. The interference drag between hulls and foils due to interference of the boundary layers was already discussed in but there is a further interference. As explained by Ishikawa [Ish91], the low pressure on the upper surface of the lifting hydrofoil, creates a downward suction force on the hulls. As a result, a certain amount of the lift generated by the hydrofoil is cancelled out by this interaction.

Referring again to [Ish91], for the given experiment of a monohull with lifting hydrofoil, the lift is reduced to 40% at low $F_{R,\nabla}$ and 75% at high $F_{R,\nabla}$. Clearly this is a very significant reduction. It is however also discussed that this reduction is dependent on how close the foil is to the bottom of the hull and obviously, what percentage of the foil is situated below the hull. For the test case mentioned above, the hydrofoil is situated at h/c = ½ i.e. the clearance between the foil and hull is half the chord length. Also the beam of the boat is equal to the span of the foil i.e. 100% of the foil is directly below the hull.

For our preliminary design (see 3.4.2) the main foil submergence is 80% of its chord length below the hull (h/c = 0.8) and 24% of the main foil is below the static water-plane area. The rear foils are 100% below the hull but are at 183% of chord length below the hull (h/c = 1.83). As defined in [Ish91] the effective lift ratio (unity at infinite separation) is reduced as the separation between hull and foil (h/c) is reduced and results for their given configuration were as follows. There was an effective loss in lift of about 23 – 30% at h/c = 0.5 and 10-20% at h/c = 2. (Depending on speed, at higher Froude numbers, the effect was lessened). We therefore expect a loss of lift

on the rear foil of about 20%, but as the hull is raised out of the water, this effect will be reduced. Although the main foil is very close to the hull, only a small % of that foil is under the submerged demi-hulls so the loss in lift is expected to be of the order of 8%. Since the bulk of the loading is on the main foil (more than 80%) the overall loss in lift will be of the order of 10%. This will be reduced as the hull rises out of the water and so will be neglected in the computational model. This will allow the hulls and foils to be analysed separately.

3.2.5 Spray

Energy is required for the generation of spray and as a result, there is a drag component associated with this. The following empirical formula can be used to determine the spray generated by any surface piercing strut.

$$C_{DS} = C_F[7.68 - 6.4(\frac{t \cdot \cos\beta}{c})] \qquad (3.27)$$

C_F is the skin friction coefficient as defined by the ITTC. (See chapter 5.1), t and c are the thickness and chord of the strut respectively and β is the angle away from vertical that the strut is inclined.

3.2.5 Separation

Separation is introduced in 3.3.2 and separation drag due to thin airfoil stall must be included as thin aerofoil theory assumes potential flow. Migeotte [Mig97] gives a brief outline of how the component of the coefficient of drag due to separation is calculated. For a thin foil at small AOA with laminar separation (no reattachment) the equations for this calculation are given below.

$t_e = t + c \sin\alpha$ (3.28)

$C_{D,sep} = 2C_f\, 70(t_e/c)^4$ (3.29)

For turbulent and transitional flow regimes ($Re > 5x10^5$) the flow is able to reattach after separation and the separation drag is given by the following equation. [Mig97]

$$C_{D,sep} = \frac{\sin^2\alpha}{0.222\sin\alpha + 0.283} - \frac{(\frac{\sin\alpha \cdot \cos\alpha}{0.222\sin\alpha + 0.283})^2}{\pi AR} \qquad (3.30)$$

Where AR is the aspect ratio, as explained in section 3.3.4 by equation 3.35

3.3 Effect of Varying Foil Configuration

3.3.1 Free Surface Effects

As sub-cavitating foils near the surface, the downwash mass flow is reduced (Refer to [Hop95]) and as a result, the lift generated by the foil is reduced. This reduction in lift is presented below in figure 3.5 (taken from [DuC72]) in the form of lift factor (K) versus fraction of chord length below free surface. Lift factor is the then multiplied by the coefficient of lift (C_L) in equation 3.1 to account for the free surface effects. K is calculated from equation 3.9 [DuC72]

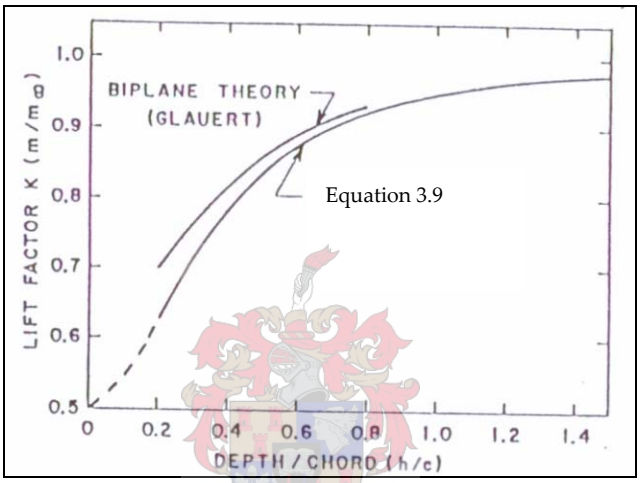

Figure 3.5 – Graph of lift factor (k) versus depth of foil as fraction of chord length.

From figure 3.5 it can be seen that the lift loss is only 5% at a depth of 1 chord length while this loss increases to 50% at the surface (where the foil acts as a planing surface only)

This has very significant implications regarding the stability of a foil-supported craft. Apart from the obvious heave stability, there is added pitch and roll stability. If for example a boat is fitted with front and rear foils, if both the foils are situated relatively close to the surface, as the boat pitches forward the front foil will sink deeper and the rear foil will be raised to a shallower level. As a result, there will be a relative increase in lift on the front foil and a righting moment will be created, thus correcting the forward pitching motion and vice versa. In the same way, now considering roll stability, when the boat begins to roll there will be more lift generated on the more deeply submerged side. This then creates a righting-moment which would tend to counteract the roll.

3.3.2 Separation, Cavitation and Ventilation

In all three cases (cavitating, separating or ventilating foils) the flow over the foil is non-ideal and results in poor lift to drag ratios (L/D). Each case will now be looked at individually.

- *Separation:*

Separation refers to the case of when the boundary experiences an adverse pressure gradient. The name comes from the fact that the flow no longer follows the surface of the foil, i.e. separates from it. This effectively changes the shape of the foil thus increasing the drag and reducing the lift. In the case of laminar separation a separation bubble forms on the surface of the foil (see figure 3.6 a) and the flow may reattach when it trips to turbulent flow. In fully turbulent flow (only under conditions of high angle of attack), an area of recirculation forms (see figure 3.6 b) and there is not reattachment. Laminar separation is only significant for model scale foils where the separation bubble is relatively large. At full scale the separation bubble becomes relatively small (most of foil is in turbulent flow) so laminar separation may be ignored at full scale

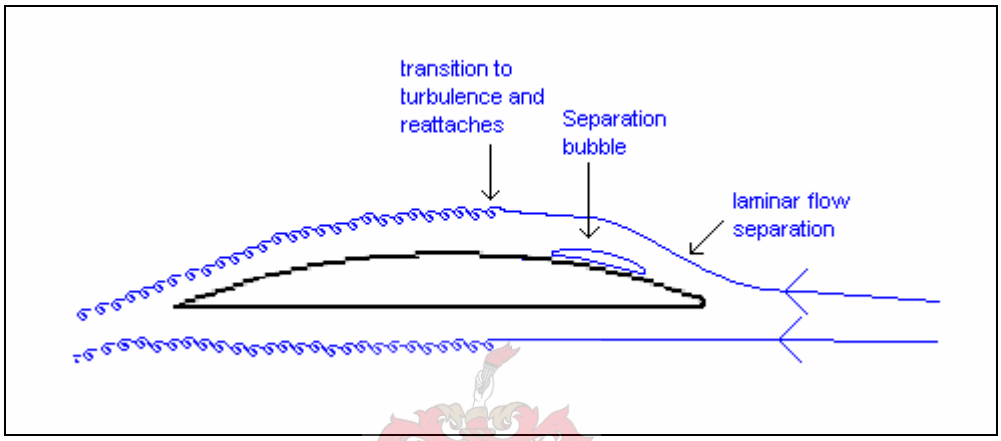

Figure 3.6 a) – Hydrofoil with lamina flow separation and reattachment

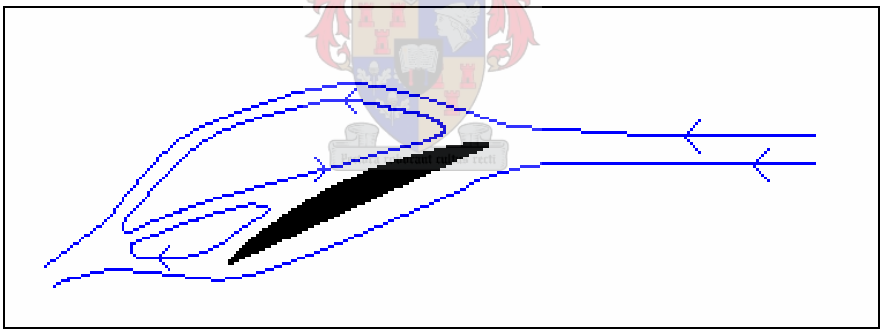

Figure 3.6 b) – Hydrofoil with turbulent flow separation

- *Cavitation:*

Another problem associated with the low pressure on the surface of the foil is that if this pressure falls below the vapour pressure (boiling point) of the water at the given temperature, bubbles of water vapour start to form on the surface of the foil. This results in the flow pattern around the foil being disturbed, with a resulting loss in efficiency and lift. The formation and collapse of vapour bubbles often results in erosion that will also ultimately affect the strength and hydrodynamics of the foils; roughness due to erosion will increase viscous drag. Intuitively, sailing catamarans are not expected to operate at the speeds required for cavitation, although the addition of lifting foils is expected to increase the operating speed and so calculations for cavitation are included for completeness.

Depending on the AOA of the foils, the minimum pressure may occur in different positions. For low or negative AOA, cavitation may occur on the lower side of the nose, while for normal AOA the cavitation occurs just behind the mid-chord on the upper surface. This then shifts to the leading edge at high AOA. Below is a typical cavitation bucket showing the three regions of cavitation. The onset of cavitation can be accurately predicted for C_L values between 1 and 2 on the figure below so the foils are designed to operate in this range of C_L values. For the other values of C_L, experimentation is required to determine the onset of cavitation.

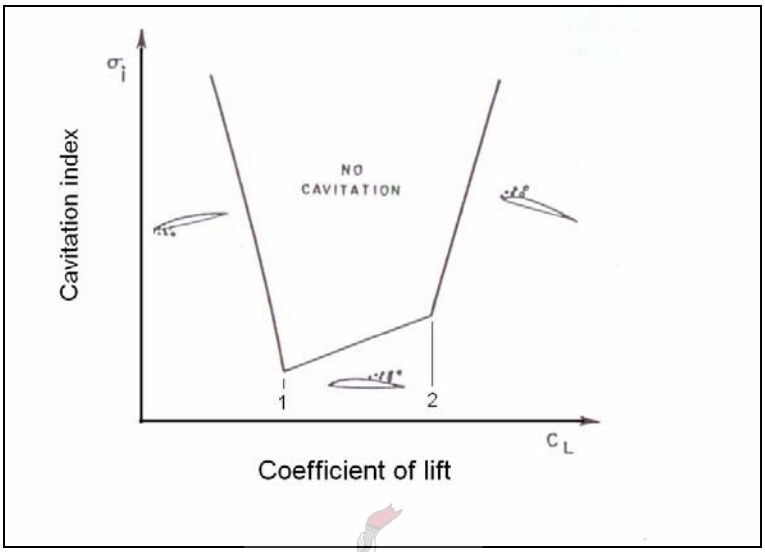

Figure 3.7: A typical cavitation bucket taken from [DuC72]

Since the pressure on the upper surface is a function of the lift and depth below free surface, we expect that at a certain speed (V_{crit}) the foil will begin to cavitate and since deformation of the surface increases the pressure on the upper surface, the shallower the foil, the higher this critical speed, so our worst case scenario will be the foil well below the surface. Equation 3.31 below gives V_{crit} in knots and equation 3.32 provides a means of determining the cavitation index (σ_i) for a circular arc cross section [DuC72].

$$V_{crit} = \frac{27}{\sqrt{\sigma}} knots \qquad (3.31)$$

$$\sigma_i = 2.55(t/c) + 0.64(C_{Li}) \qquad (3.32)$$

C_{Li} is calculated from equation 3.1 and the point of cavitation will occur when $\sigma = \sigma_i$.

- *Ventilation*

A third problem associated with the low pressure on the surface of the foil is that of ventilation. This happens typically on surface piercing foils or foils with surface piercing struts. The low pressure on the top surface of the foil basically sucks the surface of the water down until an air pocket is formed on that surface all the way down the foil (until the static pressure of the water minus the dynamic pressure on the foil, equals the atmospheric pressure). Dissolved air in the water also forms bubbles in the low pressure region and may build up in time.

This again breaks down the flow around the foil and reduces its effect. Ventilation is a problem at medium to high AOA and the resulting loss in lift is high (> 50%)

A solution to the problem of ventilation is fences (Refer back to figure 1.6 for examples of fences). These are perpendicular divisions in the foil that prevent the downward progression of the air pocket. The air pocket would then need to travel around the fence, away from the foil where the suction pressure is less. Ventilation is most serious near the leading edge of the foil, where the curvature (and therefore low pressure) is greatest. For this reason fences are usually only situated around the front edges of foils. In Figure 1.6, the rudder and surface piercing main foil have fences on them at various intervals so that they provide resistance to ventilation across the range of elevations.

3.3.3 Dihedral and Swept Foils

The concept of a dihedral foil was introduced in section 1.4.2 and is best illustrated in figure 3.8 that follows. The dihedral angle thus creates a side component to the lift force. Since the configuration is symmetric, the side components to the force on the hydrofoils cancel so only a net upwards force is created, but a loss in efficiency will be experienced. The motivation for this sacrifice in efficiency is that they provide a more stable system in terms of pitch, heave and roll, and also provide better performance in waves. They are almost exclusively used as surface piercing foils. This means that as the foils rise up to the surface, not only do the surface effects reduce the lift but the amount of foil in the water is also reduced. In a similar manner, the righting moment created by heel or trim is higher than in the case of fully submerged foils.

The equation for the induced drag including the effect of the dihedral angle is taken from Hoerner [Hoe65] and is shown below.

$$C_{Di} = C_L^2 / (\pi\, AR \cos^2\Gamma) \qquad (3.33)$$

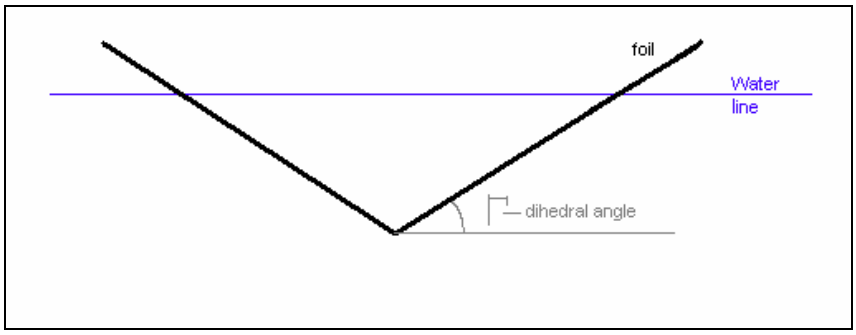

Figure 3.8 – Front view of a dihedral foil.

Hydrofoils can also be swept forwards or backwards. This means that the foils remain in a horizontal plane but their mean chord line is angled from the conventional perpendicular to the flow. This may be required for three purposes – they provide a smoother re-entry if the foils exit the water due to waves or too much lift, they shift

the COP forward or aft if they are swept accordingly and sweep delays the onset on cavitation. (See figure 3.9 below)

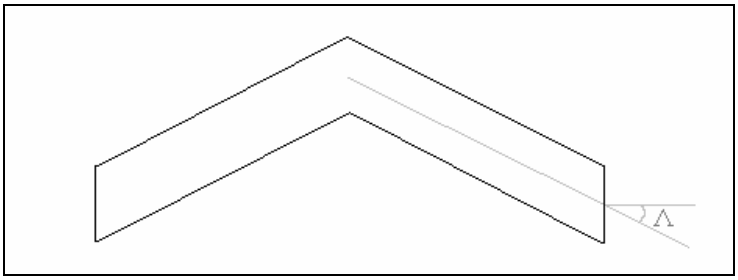

Figure 3.9 – Top view of a swept foil.

In both cases there is a loss in efficiency and additional strength requirements as more bending moments are introduced onto the foil system. The increase in induced drag due to sweep is given by Hoerner [Hoe65] in the following equation.

$$dC_{Di}/dC_L^2 \approx 1/\cos(\Lambda) \qquad (3.34)$$

3.3.4 Flow around tips, Aspect Ratio and Strut Effects.

One of the characteristics of a lifting foil is that the pressure on the upper surface is lower than that on the lower surface. The net result of this pressure difference is the desired lift. As a result of this pressure difference, the fluid will tend to flow around the tip of the hydrofoil so as to provide pressure recovery. This results in a loss in efficiency, which is highly dependent on aspect ratio.

Aspect ratio is defined in equation 3.35 where AR is the aspect ratio, s is span of the foil and A is the projected area. For a square foil this becomes s/c where c is the chord length. It follows logically that the lower the aspect ratio, the more the relative flow around the tip will reduce efficiency. It therefore follows that in order to create efficient foils a high aspect ratio is desired. There are, of course strength limitations as the higher the aspect ratio, the greater the bending moments induced in the foil and the greater the thickness ratio required. A large thickness ratio will also reduce the efficiency and maximum speed before cavitation (equation 3.31), so a balance must be found.

$$AR = s^2 / A \qquad (3.35)$$

The effect of the placement of struts on the effective aspect ratio is explained in [DUC72], but will be reiterated briefly here. In figure 3.10 below, the two support struts are separated by a lateral distance (a), which is some fraction of the span (s). Equation 3.36 then gives the effective aspect ratio AR for a given depth (h) and chord length (c). From this equation, it can be seen that for a given depth and chord length, the aspect ratio is doubled

if a single central strut is replaced by 2 struts situated on the ends of the foil. This is logical since the flow around the tips will be inhibited by the presence of struts.

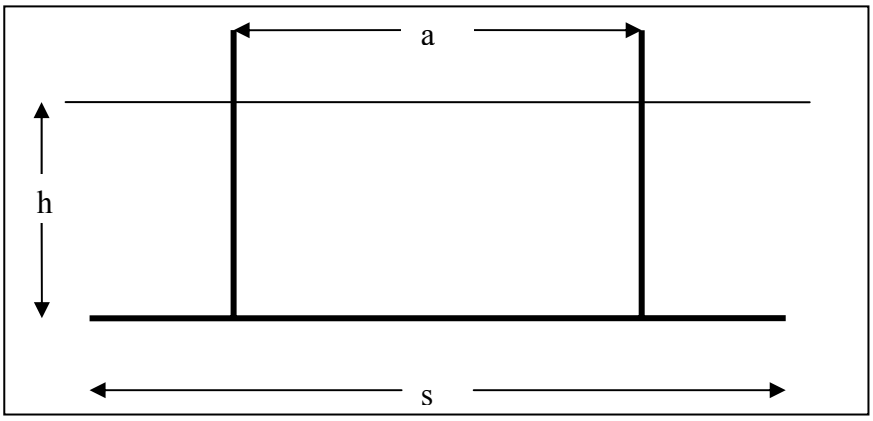

Figure 3.10 – Fully submerged foil with varied strut position

$$AR = \frac{s}{c}[1 + (\frac{a}{s})^3 \frac{h}{s}] \qquad (3.36)$$

As presented by Hoerner [Hoe65] for low aspect ratio foils it was found by tapering the foils, an improvement in induced drag is made and that the tip to root chord ratio should be in the order of 1/3. This corresponds roughly to aircraft wings. Figure 3.11 below is the graph given by Hoerner where the correction factor k (for the resulting non-elliptical lift distribution) divided by projected area (A) is plotted against tip to root chord ratio. From equation 3.37 it can be seen that it is desirable to minimize k and thus C_{tip}/C_{root} must be near 0.3 for an optimal aspect ratio. Tapering the foil also aids strength issues as the centre of lift on the foil is shifted towards the root, thus reducing bending moments.

Tapering does however make the manufacture of the foils more complicated as it is difficult to build up such foils from plates. Typically this requires machining or moulding if the foils are made from composites which add to the cost of the production.

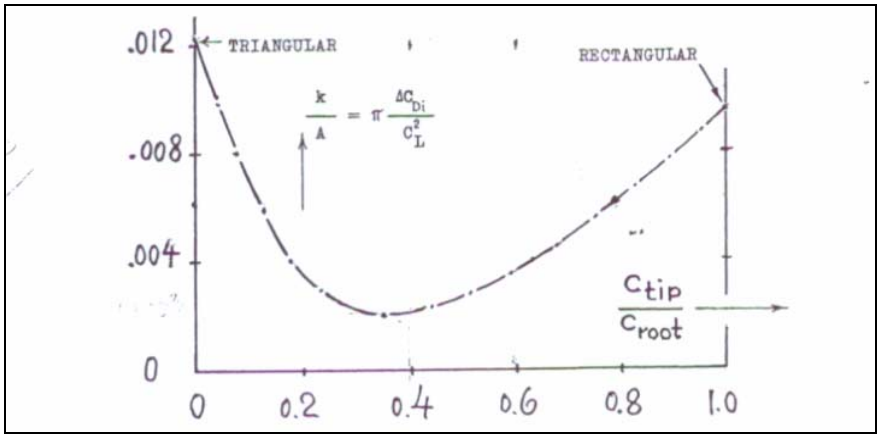

Figure 3.11– The effect of taper ratio on the induce drag of a foil taken from [Hoe65]

$$C_{Di} = (1 + k)\, C_L^2/\pi AR \qquad (3.37)$$

3.4 Design

3.4.1 Methodology

The first aspect of the design is to determine the design speed (and range) and then from the geometry of the prototype hull, a preliminary foil configuration is designed. The placement of the foil may be determined on experience or in this case, the existing geometry. By balancing the moments, about the LCG, the loading of the foils is then calculated. Now that the placement and loading of the foils has been determined, the areas, nose radii, thickness ratios and foil profiles are optimised for the given configuration. (For example, one of the factors affecting nose radii is that the smaller it is relative to chord length, the smaller the angle of attack required for ventilation. [DuC72])

The configuration may then be optimised iteratively to provide better stability or a more efficient foil system e.g. improve hull-foil interaction or foil-foil interaction (See 3.2.4)

The structural aspect of the design must then be checked to insure that the foils can safely take the loading. This is then iterated with the foil profile and configuration as the thickness may have to be increased or struts included, which will reduce bending moments on high aspect ratio foils. These in turn affect the hydrodynamics of the foil system. The methodology for designing the foil system is shown in the figure 3.12.

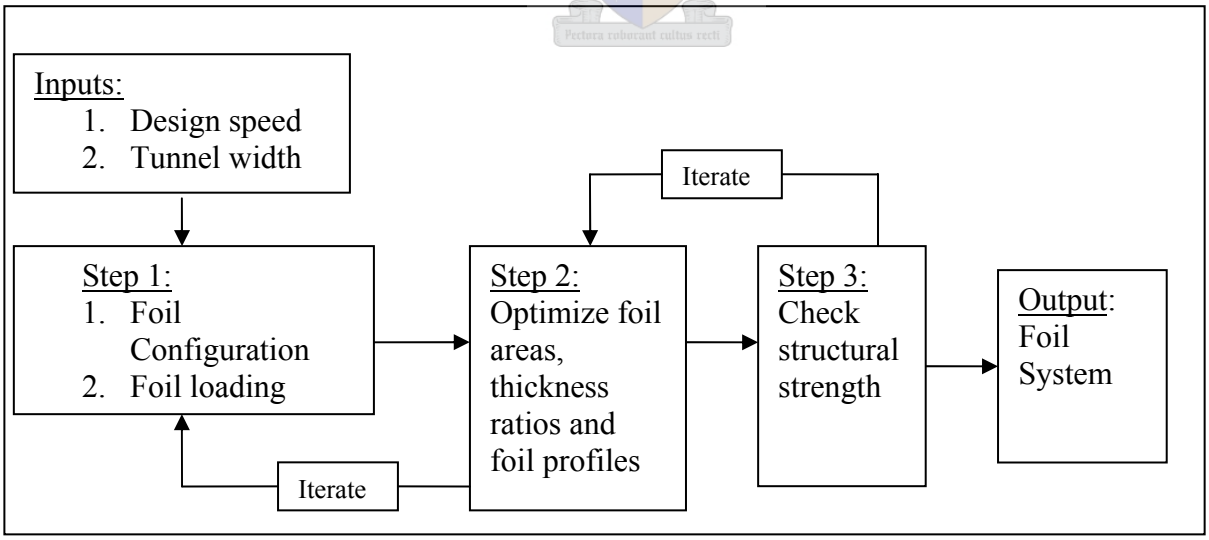

Figure 3.12 – Flow diagram of the design methodology for foil system.

3.4.2 Preliminary Design

As mentioned in section 1.7, the simplest option for the arrangement of the foils would be to attach them to the rudders and daggerboards. This poses a serious limitation on the flexibility of the system, but this would provide a simple configuration and was investigated first. It was therefore proposed that a main foil spanning

the tunnel is attached to the two daggerboards and two T-foils are placed on the rudders. In order to ensure the rear foils provide pitch stability, they must be located near the 1 chord length depth below the surface, in order to take advantage of free surface effects. This means that they will not be placed at the end of the rudders. Based on the hydrostatic tests on the hull (Appendix G) an LCG was determined and the load distribution was calculated as mentioned above.

For this configuration, most of the load was located on the main foil, which is obviously bad in terms of pitch stability, since the change in lift (with pitch) on the rear foils would be small and not provide much of a righting moment. In order to spread the load more evenly, one could shift the LCG aft but this would result in an inefficient hull shape for low speed applications (drag the transom – see section 2.1.8). Alternatively, the centre of lift of the main foil could be shifted forward by sweeping the main foil but this would result in a loss in efficiency and in order to keep the design simple, an unswept main foil was chosen. Testing a swept main foil may however form part of a future optimisation project.

A further short-coming of this preliminary design is that the T-foils are problematic in that they have 4 corners each where they join onto the rudders and thus produce a large amount of interference drag relative to their lift capability. Another disadvantage of this configuration is that the lift on the rear foils is a function of the rudder angle. (See figure 3.13 below) Equation 3.38 approximates the effect of rudder angle on lift however the effects of the rudder on the flow have not been considered.

A problem with many sailing catamarans, as mentioned in chapter 1.2, is that they lack manoeuvrability, especially in tacking. The effect of a hard rudder angle to tack the boat would result in a loss of lift on the rear foil. This in turn would trim the stern down and as a result, shift the CLR aft. This would then upset the balance of the boat, causing it to tend to 'bare-off', countering the intended manoeuvre and making the boat even less manoeuvrable. It was however noted that different rudder system (like the one used in the 1955 patent (see Appendix A, figure A.1) could be used. It is also important to note that the speeds at which the foils will be providing substantial lift will be predominantly during downwind sailing, where tacking is not required.

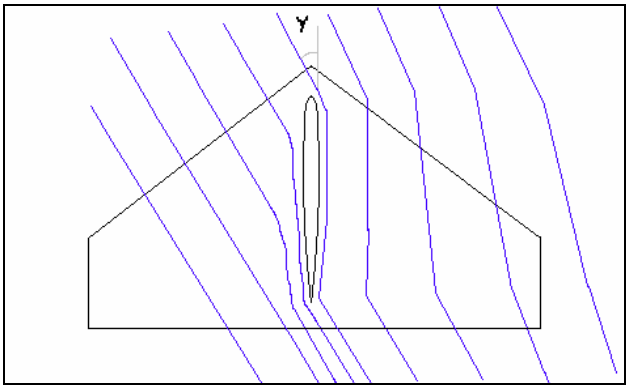

Figure 3.13 – Top view of rear foil attached to rudder.

$$L(\gamma) = L(0) \times \cos(\gamma) \qquad (3.38)$$

- *Cavitation and Ventilation*

Since the main hydrofoil is attached to the dagger-boards and rear foils to the rudders, well below the surface, ventilation is not likely to be a problem until the boat is nearly fully supported and the lifting foils near the surface. Large rudder angles will increase the likelihood of ventilation on the rear foils and an air pocket may be sucked down the low pressure side of the rudder and onto the rear foils. Since the elevation due to foil support will reduce the aspect ratio and area of the rudders, greater foil angles will be required, except that if greater speeds are achieved this effect may be counteracted to an extent (see equation 3.1). This may mean that fences are incorporated into the design of the rudders and on the main foil near the daggerboards to prevent the advance of ventilation.

As already mentioned, cavitation is generally not considered a threat to foils of sailing craft. The thickness ratios and coefficients of lift (equations 4.30) were calculated for the foils proposed. As a result it was calculated that cavitation would first occur on the rear foils, at a speed of about 47 knots and the main would experience cavitation at a slightly higher speed. Since this is well above our expected operating range, cavitation is not expected to be a problem for these hydrofoils. In fact the world speed record for sail driven craft is of that order. [YW02]

Although the hydrodynamic aspects of the foil design are the main focus of the thesis, stress analysis was taken briefly into consideration as this may iteratively affect the hydrodynamics. For example, the main lifting foil, being of such high aspect ratio, may require a central strut for added support. This would then add to the drag but also to the lateral resistance of the configuration.

After making some assumptions regarding the manufacture of the main foil based on existing manufacturing techniques, a strength calculation yielded an acceptable maximum stress (with a safety factor of about 3) in the main foil, however considering fatigue and impact loading due to waves, it was felt a more conservative design, including a central strut on the main foil would be advisable. This would also provide additional lateral resistance, thus reducing the leeway angle, which could compensate in part for the loss in lateral resistance resulting from the lifting foil system elevating the hull, rudders and daggerboards partially out of the water. On the other hand this would increase the WSA (and therefore viscous drag) at low speeds.

For simplicity of manufacture, the main strut was given the same cross-section as the daggerboards, however usually circular arc cross-sections used for surface piercing foils as they have low spray generating characteristics.

In order to produce maximum lift, the main foil will be placed at the end of the daggerboards but if found through experimentation the foil is needed closer to the surface (for stability) other depths may be investigated.

From computational analysis, it was estimated that the lift from the foils should carry 60% of the boat's weight when travelling at 12 knots. This would indicate that the expected results would appear to be good, so long as the drag resulting from the foils remains low to start with. From hydrostatic testing, the full scale wetted surface area was calculated as 18.3m^2, depending on trim with zero heel angle and drops off to about 12.9 m^2 when heeled at 6.5^0 so that the windward hull is clear of the water. The foils increase the WSA and therefore primarily increase the viscous drag, however are expected to have only small additions to other forms of drag (wave, form, spray, interference between vertical and horizontal foils) except for the induced drag. The increase in wetted surface area is approximately 4.716 m^2 (25.7% of 18.3 m^2)

3.4.3 Design Modifications

It was found during experimentation (see chapter 6) that the configuration in the preliminary design was unsuitable as the pitching moment proved to be too high and there was strong tendency for the boat to pitch forward and pitch-pole at above displacement speeds. As a result of this, a foil was placed at the bow, in the middle of the tunnel (see figure 3.14 below). It was found that this provided a far more stable configuration. The rear foils were then removed to test if they were necessary. It was found that the drag was in fact reduced by doing this. This is explained in more detail in Chapter 6.

Since all of the front foil lies in the tunnel, the reduction in lift on that foil due to hull-foil interaction should be zero. From the calculations in 3.2.4 we expect a positive wave influence from the front foil on the rear foil.

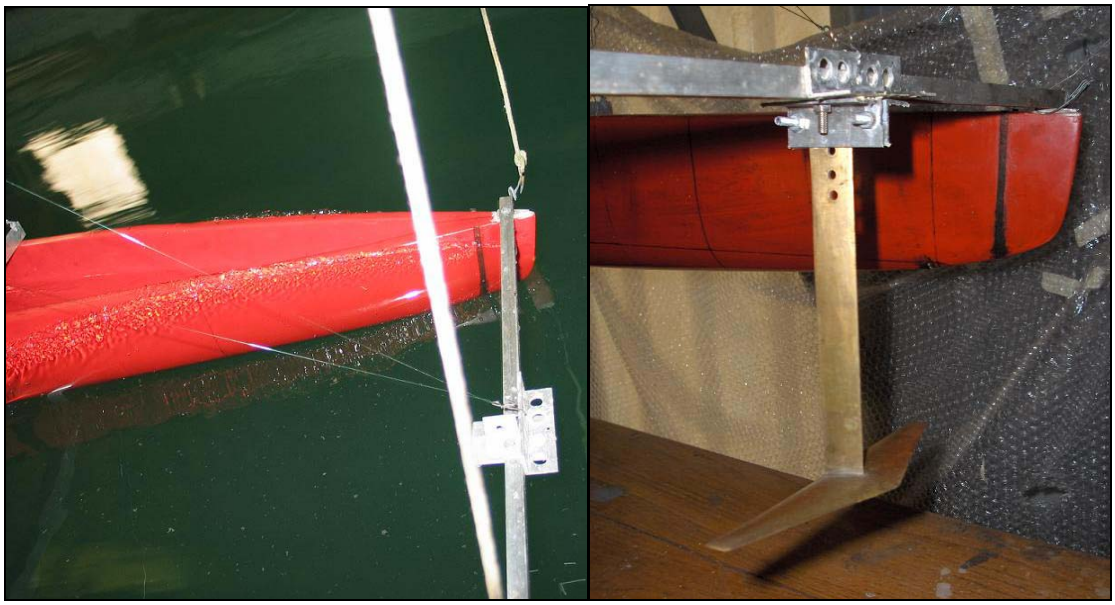

Figure 3.14 a) Model pitch-poling at 3.5 m/s b) Front foil

The lift on the front foil will raise the bow and this in turn will increase the AOA on the main foil. Once the front foil reaches the surface it will not be able to rise any further. The main foil will then continue to raise the hull out of the water and pivot the boat about the front foil. In doing so, the AOA on both foils will be reduced, thus stabilising the foil lift and reducing induced drag on the foils. The only threat to stability in this running condition would be ventilation as discussed in section 2.2.3. Since cavitation is not likely in the given speed range, only ventilation is of concern. This was experienced during testing at about $Fn_{\nabla} = 3.2$ (22 knots prototype speed, which is on the upper limit of the speed test range) and so fences will be required as part of the design on the prototype.

Calculations for cavitation were conducted as in the preliminary design and the maximum speed before cavitation was even higher than before (52 knots), which not likely to cause problems for even the sailing catamaran with lifting foils.

Chapter 4

Computational Analysis

4.1 Thin Ship Theory

Thin ship theory is a potential flow model and a direct application of Michell's integral equation which was derived by him in 1898. One of the advantages of catamarans, when it comes to computational modelling is that their narrow demihulls allow for the use of thin ship theory. As described in [Tu87], the only requirement is stated that the hulls rate of change of thickness must be small. In other words, so long as the hull has a high length to beam ratio (L/B) and the entry angle on the bow is narrow, this theory is accurate. No means of quantifying this is given but an example hull is presented. Since the L/B and B/D ratios of this example hull are comparable to that of RH1, it was considered a suitable method for determining the resistance of the hull.

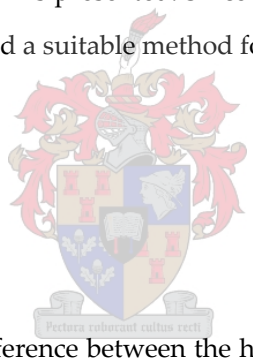

4.2 Procedure

Since section 3.2.4 concluded that the interference between the hull and lifting foils is expected to be small, the computational analysis of the vessel is made much simpler by analysing the hull and foils separately.

Since the computer modelling of RH1 may be computed using thin ship theory which is computationally and in terms of setup, far less time consuming than a complete CFD (RANSE) model. A package using thin ship theory, known as MICHLET [Laz97], which has been used in the past for such research, was therefore selected for computing the resistance on the hull. This does however require several inputs which can only be determined experimentally. Such inputs are running trim, sinkage and WSA across the speed range being calculated. Since towing tank tests are being conducted, these inputs may be measured during towing tank tests and then placed in the input file.

Unfortunately, the option to model heel and leeway has not been incorporated into this program. After searching on the internet and corresponding with the author of MICHLET (Mr L. Lazauskas), it became apparent that only complete potential flow programs at present, allow for such inclusions. One such program that was recommended by Mr Lazauskas, called SPLASH, involved a detailed modelling of both the aerodynamic and hydrodynamic aspects of the boat. The problem with this program is that it is complex

(beyond the scope of this research), designed specifically for monohulls and is expensive. It was therefore decided that the results for tests without heel or leeway could be modelled in MICHLET and so long as those tests corresponded, the model testing methodology can be proven valid and the results achieved for the leeway and heel tests can be presumed correct. It is, after all, desired that a trend regarding the effect of these parameters be found rather than the exact values.

As in past research conducted at the University of Stellenbosch [Mig01], the foils will be modelled using a program known as AUTOWING [KT05]. This will provide the lift and drag on the foil system, including the effect that the foils have on one another for a given configuration. (See section 3.2.4)

The depth at which the foils run at various speeds may be determined by the sinkage and trim results taken from the towing tank experimentation.

Both AUTOWING and MICHLET are potential flow based programs and will therefore not pick up viscous scaling effects. The viscous drag is therefore added on empirically in the calculations. Both programs also do not account for spray drag, but this is expected to be small as sailing catamarans are observed to produce little spray in most sailing conditions.

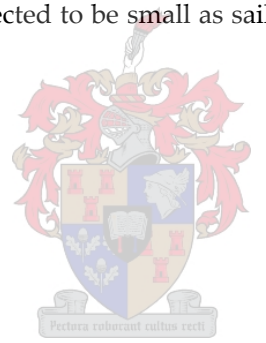

4.3 MICHLET

As mentioned before, MICHLET is a computer package that utilises thin ship theory The hull configuration is fed to the program via an input file (Appendix I) which in turn refers to a text file containing points that define the shape of the hull/s. Included in this input file is the speed range and the corresponding running data (WSA, trim and sinkage taken from experimentation)

Some sources of error are derived from the assumptions made by the program. MICHLET assumes that the sides of the boat are vertical from the points defined at the water surface. This may cause error particularly in the region of the bow wave as it is seen in experimentation to be very large with respect to draft. Fortunately there is no flare or tumblehome near the bow so error won't be very large. Similarly, errors may be large for large sinkages however this is not a problem in our case as seen in results – sinkages even without foils are very low.

The form factor of the hull is not known but since the demi-hulls are slender, it is expected to be close to unity. [CMAP97] gives some examples of form factors of slender boats and demonstrates that they are usually significantly higher than unity (note form factors reduce with speed). Also noted that the form factor acquired

from towing tank, wind tunnel and CFD analysis provided large variation in results, towing tank test being the highest. [CMAP97] concludes that the most important factor for determining form factor of high speed, round bilge, transom stern vessels is the $L/disp^{1/3}$ ratio and that it is reasonably independent of speed and demihulls separation. From the table provided a linear interpolation yields a form factor of about 1.25.

The MICHLET calculations are set for a particular sinkage and trim, which affects the underwater shape (slenderness) and in turn the form factor. For boats without much rocker, the hull becomes very slender as it rises out of the water, thus the form factor tends to 1. RH1 does however have substantial rocker and thus the slenderness doesn't necessarily tend to infinity as the boat emerges, thus the form factor doesn't quite tend to 1. There has apparently been much debate regarding the calculation of form factor. As a result, the form factor was first set to 1 in the calculations and the results compared to determine accuracy.

The convergence of the MICHLET solutions was tested by varying the number of n-theta values (angular division in the hull) which are used to calculate the wave drag on the hull. The value was set initially according to the recommendations of the MICHLET user manual and the number increased until a variation of less than 10% was achieved.

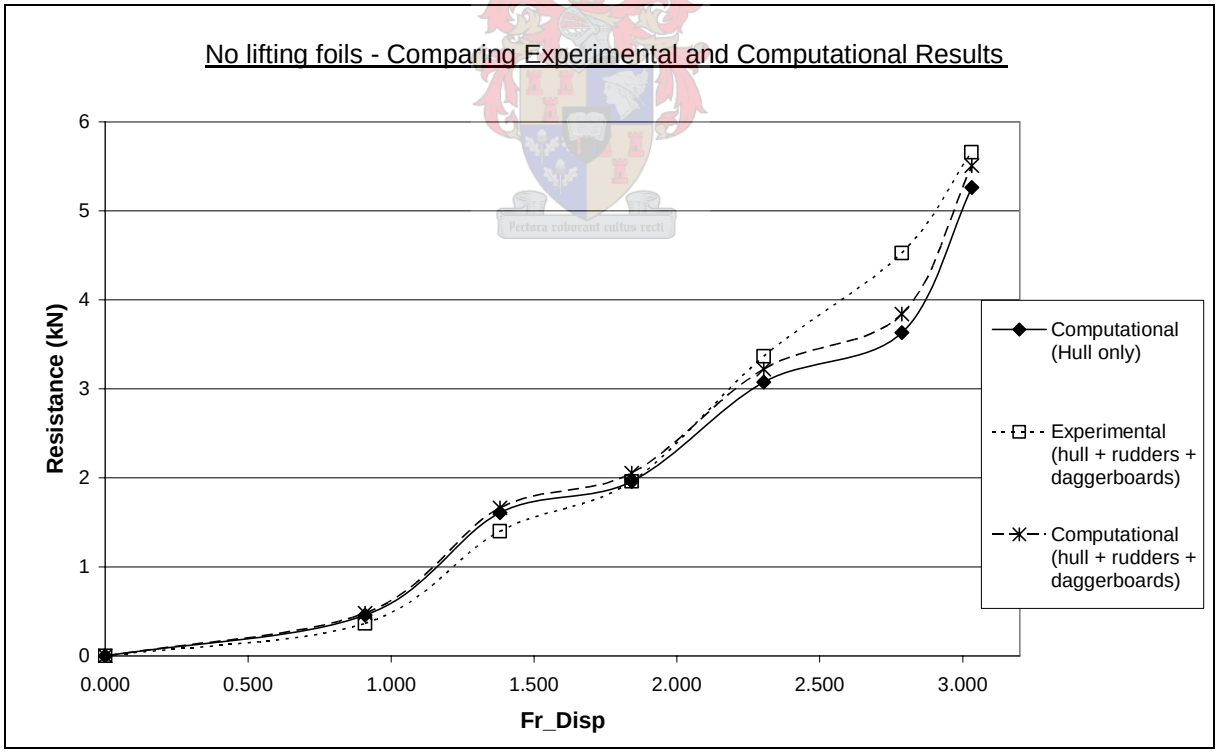

Figure 4.1 – Comparing the experimental and computational (MICHLET) resistance curves of RH1

The experimental results of RH1 tested across its speed range are compared to the computational results in figure 4.1. The viscous drag of the rudders and daggerboards (as calculated in appendix H) have been added on to the result of MICHLET and a strong correlation between the results is observed. The correlation between the experimental results and those predicted by MICHLET is excellent and the only major deviation occurs at $Fr\nabla$

where MICHLET under-predicts the resistance by 15%. This may be attributed to assumptions of MICHLET, as mentioned earlier.

4.4 AUTOWING

This is a vortex panel method program, designed specifically for calculating the lift and drag on a given hydrofoil configuration. The cross-sections of each foil are entered first and then a series of points are used to describe the configuration of those foils. The effects of compressibility and viscosity are considered negligible [Dev98]. Since the viscosity is assumed negligible, the residual drag generated by the foils is calculated only and the viscous drag is calculated using the ITTC equation 5.1.

Planing theory may also be applied in this program, thus making it possible to model planing hulls in this program. Unfortunately this does not apply to RH1 as over almost all of the speed range, buoyancy forces dominate over planing forces. This is why the hulls are modelled separately in MICHLET.

Since the foils and hull will be modelled independently, the interference between the two will not be taken into account. This will result in a slight under prediction in the total drag and a slight over prediction on the lift. The lifting foils increase the mass flow rate above their upper surfaces. This will increase velocity of the water in between the foils and the hull, thus increasing the effective form factor. No means of quantifying this effect was found in the literature study, but since it affects only a small portion of the boat, it is not expected to influence the resistance greatly. Where the foils join onto the hull, the hull would act as a turbulent stimulator, thus the transition to turbulent flow may occur sooner. Another effect of the hull's boundary layer would be to reduce the speed of the flow over that section of the hull. This would then reduce the Reynolds number of the flow over the foil. These effects are assumed to cancel.

[KT99] provides a test case where the results of AUTOWING are in good agreement with the experimental results, which verifies the accuracy of the program. A comprehensive analysis of the use of AUTOWING was conducted by Migeotte [Mig01], where the accuracy of AUTOWING was validated and criteria for insuring convergence of the solution were provided. These criteria were then applied to the computational model of the foils modelled in AUTOWING and are summed up in table 4.1.

Large Froude number methodology (often used in hydrofoil calculations) assumes the wave pattern above the foils has a negligible effect on the lift of the foils. This saves vast amounts of computation as the vortex sheet at the surface does not then need to be calculated. According to the AUTOWING manual, this approximation is reasonable only when the Froude number based on the chord of the foils is greater than 4.5. This is often the

case for high speed power catamarans but unfortunately the bulk of speed range used for this testing procedure results in Froude numbers lower than this.

For this reason, a linearised free surface calculation was used in AUTOWING, which includes in its calculations the free surface deformation. Since there will be interference from the upstream foil, this free surface condition will best capture these effects.

General Convergence	1. Domain – distance in front of foil 2. Domain – distance behind foil 3. Iterations	2 chords 10 chord lengths 70 iterations
Hydrofoil vortex lattice	Spanwise density Chordwise density (Including free surface effects)	12 32
Free surface panel density	Per chord length	40

Table 4.1 – Summary of criteria for convergence of AUTOWING taken from [Mig01]

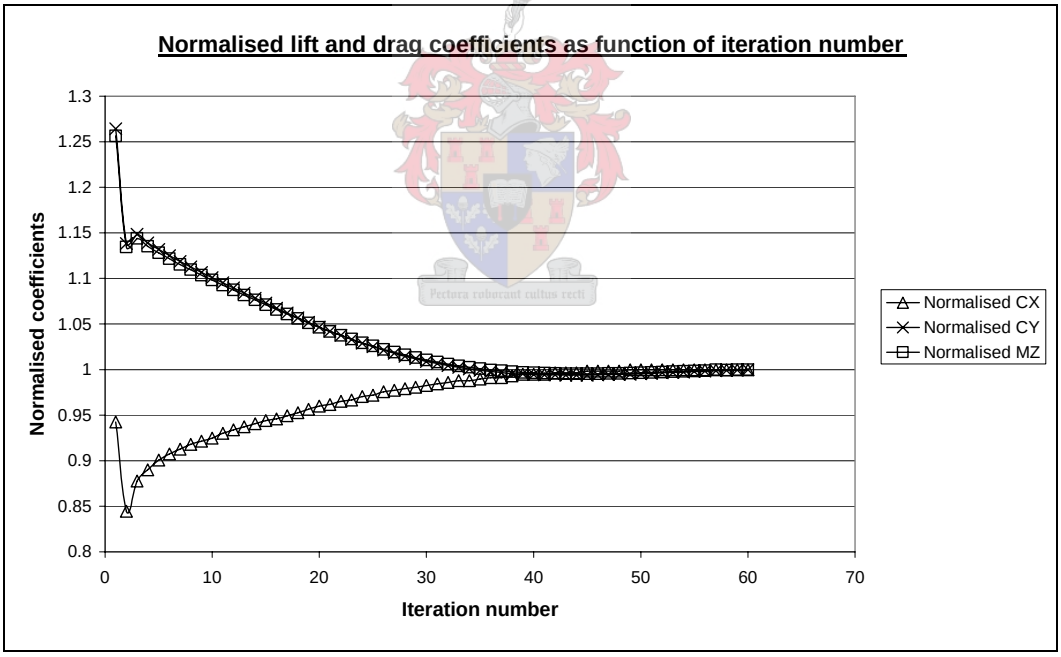

Figure 4.2 – The normalised coefficients of lift, drag and trim moment plotted against iteration number

In order to check the convergence of the solution, the coefficients of lift, drag and trim moment on the foil system were plotted against the iteration number. Since lift and drag (and the resulting trim moment) are the outputs which will be used to verify experimental results, it is important that these coefficients are converged. Figure 4.2 below shows the convergence of these coefficients occurs at 40 iterations but since the trim and sinkage were left at zero for this test case, a larger number of iterations (65) was chosen to ensure convergence. For each speed, the convergence of these coefficients was monitored and it was found that 65 iterations was sufficient throughout the speed range.

The centreline wave pattern was also plotted after various iterations (see figure 4.3). It was found that convergence of the centreline wave pattern was only achieved above 75 iterations, but since this was not required for this research, a great deal of computational time was saved by using only 65 iterations.

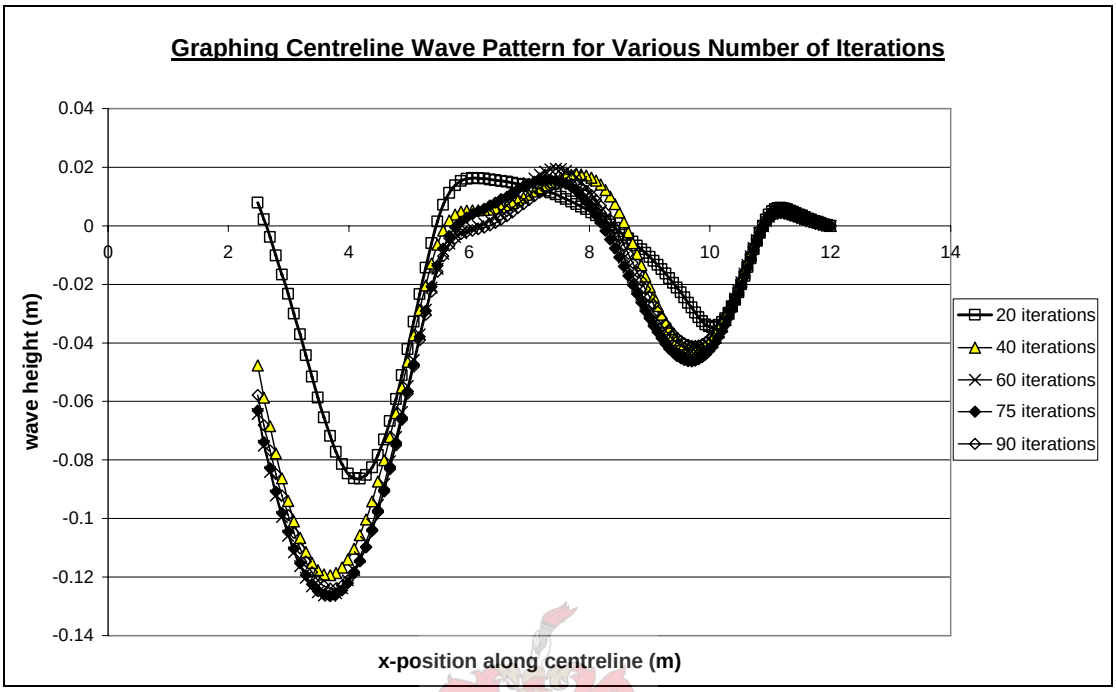

Figure 4.3 – The centreline wave pattern for various iteration numbers
(Same input values used for speed, trim, sinkage)

Chapter 5

Experimental Methodology and Set-up

5.1 Requirements and Concepts of Towing Tank Testing

A scaled model of the prototype to be tested was manufactured. In order to design an appropriate model, the standard methodology of Froude, used by the ITTC (International Towing Tank Convention 1957) was adopted [Ber02]. The basis of this concept for scaling hull resistance is that both Reynolds and Froude similarity cannot be achieved simultaneously and so the resistance is decomposed into frictional (R_F) and residual (R_R) components. Froude similarity is then used to ensure that the coefficient of residual resistance remains constant while the frictional resistance coefficients (associated with Reynolds similarity) for both is calculated using the equation 5.1.

$$c_F = \frac{0.075}{(\log_{10} \mathrm{Re} - 2)^2} \qquad (5.1)$$

The calculation of full scale resistance using the ITTC'57 method is as follows…

1. From the resistance measured in the towing tank test, the models total coefficient of resistance may be calculated.

$$c_{Tm} = \frac{R_{Tm}}{\frac{1}{2}\rho_m \cdot V_m^{\,2} \cdot S_m} \qquad (5.2)$$

2. The residual resistance is determined by subtracting the frictional resistance calculated from 5.1 for the model.

$$C_R = C_{Tm} - C_{Fm} \qquad (5.3)$$

3. The total resistance coefficient of the prototype is then calculated by adding the frictional resistance and roughness allowance coefficients (C_A), calculated for the prototype vessel.

$$C_{Tp} = C_R + C_{Fp} + C_A \qquad (5.4)$$

4. The total resistance of the prototype is then determined.

$$R_{Tp} = c_{Tp} \frac{1}{2} \rho_p \cdot V_p^{\,2} \cdot S_p \qquad (5.5)$$

The viscous drag on the foils doesn't scale in the same way as the hull, as the Reynolds numbers are different for the foils as pointed out by Kirkman et al. [KK80]. In order to scale the drag correctly, the drag on the hull and foils must be separated, scaled using respective techniques (taking into account the fact that the foils at model scale operate in mainly laminar flow) and then summed to produce an accurate full scale resistance (see figure 5.1). The star superscript indicates model scale whereas no superscript indicates prototype scale.

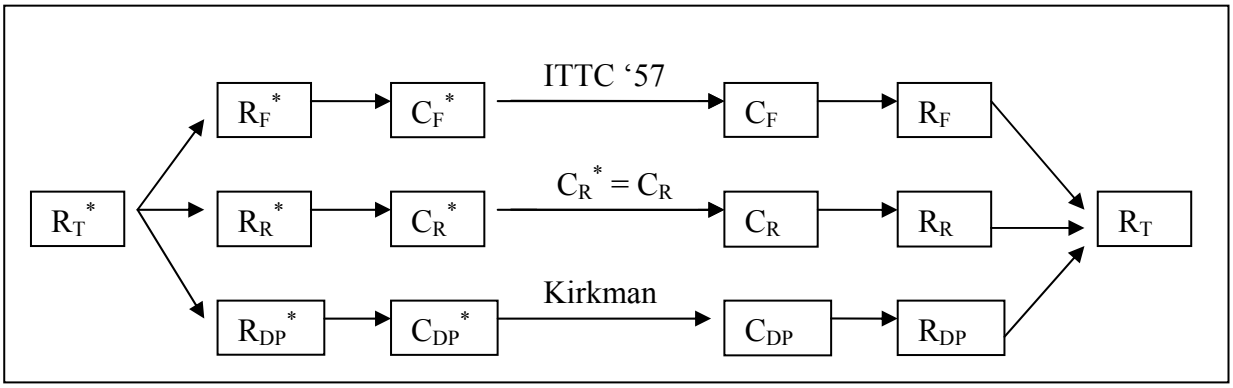

Figure 5.1 – Scaling procedure used to determine full scale resistance

Since the drag on the foils scales differently to the hull, the drag on the foils will be proportionally higher due to laminar separation. As a result, the Centre of Drag (COD) would be relatively lower for the model than for the full scale prototype and as a result, the running condition (predominantly trim) would be incorrect, requiring prototype testing for more exact results. A more direct implication of this is that the terminal speed at which stability breaks down and pitchpole occurs would be lower for the model than for the prototype. The model test will therefore provide a conservative estimate of the stability limits in terms of pitchpole.

5.2 Sizing the model

5.2.1 Introduction

In manufacturing a model, the first aspect would be to decide on the scale. The scale of a model is determined by both practical and accuracy limitations but from practical experience [Mig05] it has been found that model scales of up to 20 can provide suitable accuracy.

5.2.2 Practical Limitations

Although the addition of lifting foils in reality would increase the weight and therefore displacement of the vessel, this increase would not necessarily scale correctly and so a better comparison would be made if the displacement is kept constant and this increase in displacement borne in mind when comparing results.

One of the limitations on model size is cost. It would obviously be more cost effective to make the model as small as possible. In addition this would make handling of the model easier. Of course the model would have to be small enough to fit into the towing tank but this is seldom a determining factor as accuracy limitations (blockage and shallow water effects) require the model to be much smaller than the tank cross section. (See 5.2.3)

In terms of manufacture there may also be some practical limitations depending on the means of manufacture and coupled with that is the weight specification of the model. The displacement of the model must scale appropriately (divided by the cube of scale factor) so is may be difficult to manufacture models of low displacement hulls that are light enough to meet this requirement.

5.2.3 Accuracy Limitations

The viscous scaling effect is an important limitation in terms of scaling accuracy. Since full scale boats typically operate in fully turbulent flow across most of their hull even at low speed, whereas models have large sections of their hull still in laminar flow, it is desirable for accuracy to make the model as large as possible. A solution to this is to trip the flow to turbulent through any number of stimulating devices, the most common of these being strips of sandpaper placed 5% of the wetted length aft of the bow, as recommended in 'Principles of Naval Architecture' [SNA88]. This leaves a small amount of laminar flow to compensate for the added resistance of the turbulent stimulators. For a completely turbulent model, [Ber02] recommends that the Reynolds number based on length (Re_L) > 5 x 10^6, but this proved to be impractical for the towing tank size provided. Migeotte [Mig05] stated that with the inclusion of turbulent stimulators, a minimum Re_L = 5 x 10^5 will provide sufficient turbulent flow over the model to yield accurate results.

[Whi91] gives the following equation for a minimum Reynolds number based on roughness height for the stimulation of turbulence.

$$Re_k = \frac{U \cdot k}{\upsilon} \geq 120 \qquad (5.6)$$

Another accuracy limitation is the errors which may occur due to blockage and shallow water effects. Shallow water increases the flow around the model which would give incorrect values for resistance, sinkage and trim. The blockage effect is when the largest cross section of the model is large enough to set up a return flow around the model, thus having a similar effect of resistance. Migeotte [Mig97] provides the following limitations for negligible shallow water (5.7) and blockage effects (5.8). It is therefore desired that the model is small enough so as not to exceed these limits.

$L/h > 1$ for negligible shallow water effects (5.7)

$A_x^{0.5} / R_h < 0.2$ for negligible blockage effects (5.8)

Where: L = length of model h = depth of tank

b = width of tank A_x = maximum cross-sectional area of model

p = max wetted girth of model (WSA tests) R_h = hydraulic radius = $\frac{b \times h - A_x}{b + 2h + p}$

5.2.4 Determination of Scale Factor

It was first proposed that a model length of 0.78m (scale factor of 14.4) is used as this would then fit entirely in the limits of the bed of the NC milling machine that was available. It was then discovered that by comparing the weight of similar sized models that the weight requirement for such a small model would be difficult to achieve. Sailing yachts are relatively light compared to their motorized counterparts so even conventional model manufacturing methods would produce overweight models for all reasonable sizes. It was then decided to investigate a larger scale (bearing in mind that it would be desirable to have a fair percentage of the weight as deadweight which could be moved so as to manipulate the COG) and to investigate lighter methods of manufacture.

An alternative method of manufacture was then proposed. A balsa frame generated from CAD drawings of the model would define the shape of the hull. Surfboard foam would be placed in between the frame and the hull faired by hand. An expert surfboard shaper was available for the fairing and this method appeared to provide a light and simple solution. More detail on this is given in section 5.3. Assuming this method, weight estimations were calculated (see table 5.1) so as to assess the percentage dead weight for the required displacement at various scale factors.

Model length	Scale factor	Estimated Percentage Deadweight
0.78	14.4	- 19.1
1	11.2	4.14
1.3	8.6	23.3
1.5	7.5	31.6

Table 5.1 – Estimated deadweight for proposed manufacturing process at various scale factors

It was then decided that a model length of 1.3m would be suitable in terms of weight requirement. Calculations to determine whether is would meet the other criteria were then made. A model of this length would have a weight of 4kgs and BOA of about 66cm. This would be easy to handle and fit easily into the towing tank.

The blockage and shallow water effects were checked. It was found from the calculations (see appendix D) that neither of these effects would affect the resistance of a model of this size.

For a model length of 1.3m at low speed (equivalent to 6 knots full scale), the Re_L of the model is about 1.5×10^6 which is greater than the required 5×10^5. Since this is the lowest speed to be measured, this size model will be sufficient to provide accurate resistance values.

The roughness of the turbulent stimulators was also checked at that same low speed. If k is estimated at about 0.5mm, we get $Re_k \approx 600$, and therefore based on equation 5.6 our roughness is sufficient. We therefore expect a large percentage of our model to be in turbulent flow, even at low speed.

It was therefore concluded that a scale factor of 8.6 (yielding a model length of 1.3m and displacement of 4kg) would be suitable for the RH1 model.

5.3 Process of Design and Construction

As mentioned in section 2.4.1, a representative hull was designed and named RH1. The 2D drawings of the original hull were used in the program MAXSURF [Max03] to generate a 3D CAD drawing of this approximate hull. Hydrostatic tests were then conducted for various Longitudinal Centres of Gravity (LCG's) in MAXSURF. (See appendix G) Since the wetdeck is well clear of the water for flat water applications and simplicity in manufacture the hull shape was modelled by considering the demi-hull shape independently and the cross-beam structure of the boat was not included.

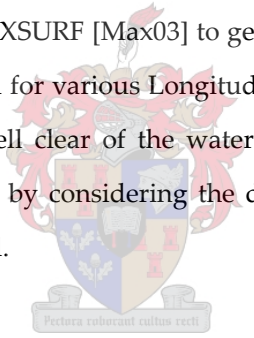

This CAD drawing was exported to another program – RHINOCEROS, which is more appropriate for manipulation of the drawing. From this, stations at 10cm intervals were introduced. From these, bulkheads at these points, spines and deck stiffeners (see appendix E, figure E.1b) for each hull were drawn and then printed out on a 1:1 scale. These were then cut out from balsa wood to give a frame that ensures the hulls are faired correctly (see figure E.1a). Surfboard foam was then fitted in between the bulkheads and then faired before glassing over. An aluminium frame of angle iron was used to form the cross-beams and aluminium strips were glued to the deck stiffeners to ensure sufficient strength where the crossbeams are screwed onto the hulls. After glassing the hulls were painted and sanded down to a grit size of 20,000, which provided well faired and very smooth hulls. (See figure E.2)

The rudders and daggerboards were sized according to typical dimensions used on the original design (see Appendix F) and the profiles were, as recommended by Larsson et al. [LE02], standard NACA 0010 profiles, scaled to fit the chord length of the foils. Since minimizing weight is of utmost importance, the material selected for manufacturing the foils was aluminium (as opposed to brass – the standard material used for model foil manufacture). The 3D models of these foils (as well as the lifting foils) were generated in RHINOCEROS and

then transformed into solid CAD models in PROENGINEER. Cutter paths were then generated for these profiles and they were then cut from an aluminium sheet on an NC machine.

A suitable fairness on the foils was achieve by sanding down the foils to a grit size of 600 and then a polish called WADPOL, designed specifically for aircraft applications, was used to give an excellent finish.

The rudders and daggerboards were located in the hull with 1.7mm pins. The vertical alignment was ensured by the use of templates drawn from the CAD model of the boat. A keel line was drawn with a thin pen and the foils were aligned with this. They were then glued into place using an epoxy with a fillet of radius approximately 4mm. (See figure E.3)

Figure 5.2 – Photo of a complete model after testing
(See Appendix E for more photos of model during testing)

The rear foils were super-glued into place which gave a good bond while being brittle enough to be broken off and re-glued if positioning was deemed unsuitable. While gluing, the rear foils were aligned by resting them on polystyrene blocks, strapped to the daggerboards. This gave a smaller fillet (about 1mm). The main foil was pin joined onto the daggerboards and the join filleted with press-stick. This allowed easy fairing and adjustment of the main foil angle of attack (AOA). The effect of drag on the press-stick was checked visually and no deformation was detected during testing.

After manufacture, the two hulls were weighed at 1.435kg and 1.445kg leaving 1.12kg for the crossbeams, foils and deadweight. After assembly, the structural weight was 3.961kg and 3.457kg for the case of with and without lifting foils respectively.

5.4 Modelling a Sailing Catamaran

As mentioned in section 1.2, the thrust force of a sailing boat acts at an effective position known as the Centre of Effort (CE). This was then calculated for the three common points of sail, and tabulated. (See Appendix J) It was noted that despite the changes in sails and settings, the height of the CE above deck level remained nearly constant.

As mentioned in the section 1.2, two important variables for modelling sailing vessels are heel and leeway. Both are dependent on the sideward component of the thrust force on the sail, and therefore the sheeting angle or point of sail of the boat. The leeway angle is also a function of speed[3] (refer to equation 3.1 in section 3.1) and therefore the two cannot be coupled directly.

It was first thought that the model could be simply towed from the exact CE for the three basic points of sail (beating, reaching and running) and the boat should naturally reach an equilibrium position with a certain heel and leeway angle. As mentioned in section 1.3, balance is maintained with rudder angle. The correct rudder angle would then need to be determined for each sailing condition. This would be difficult and may require a large number of trial runs and 'tweaking'.

It was therefore decided that a more sensible approach would be to model the boat without heel and leeway angles, and simply tow it from the correct elevation height, without the lateral component of CE. (Since the heel and leeway angles were fixed, lateral components of the CE would have no effect) This would give the appropriate bow down effect as drag increases. The effect of leeway and heel were then measured separately so that their individual effects may be determined and the combined effect postulated. The change in flow due to rudder angle required for the above mentioned equilibrium was however not accounted for. This was considered to have little effect as only small rudder angles are maintained for straight line sailing. In practice, if the boat is heeling greatly, resulting in large weather helm, the sail is allowed to 'luff' in a gust or the area is reduced by reefing in strong wind, thus making the boat more manageable and the required rudder angle smaller. The induced resistance and change in flow over the hull is expected to be small for small rudder angles and would have little effect on the results as the induced drag is small (Refer to Appendix H) and only a small percentage of the submerged hull lies in the wake of the rudders

The proposed testing methodology was then compared to those already in use. The two main approaches are described in [LE02]. The first is similar to what we have described - towing from the exact CE with an active rudder system and is called free-sailing. The second uses a dynamometer and is called semi-captive. The

[3] As speed increases, less leeway angle (angle of attack on non-lifting foils) is required to get the same side force.

advantage of the first is that the number of test points is kept to a minimum and direct insight into the behaviour of the boat under different sailing conditions may be gained. The second is a more systematic approach (but complex and requires a relatively large number of tests and a dynamometer) where the boat is fixed in all degrees of freedom except pitch and heave and the speed, yaw angle and heel angle are then varied. This method requires both a complex experimental setup and a specialised Velocity Prediction Program (VPP) into which all the side forces and moments are computed, to give a complete analysis.

The proposed approach uses elements of both methods and allows for a better understanding of the effects of heel and leeway separately. Since it overcomes the problems associated with the other two test methodologies while still providing reasonable accuracy, it was deemed suitable. It would provide a simple, reasonably accurate experimental setup, with relatively few tests required and a greater understanding of the effects of heel and leeway, separately.

The effects of waves were not tested as this did not fall within the scope of this research project, although the expected effects are discussed in chapter 2.

5.5 Equipment and Model Setup

Towing Tank particulars

Length:	90m
Breadth:	4.5m
Water Depth:	2.7m
Max Carriage speed:	8.2m/s

During testing, the air resistance was minimized (with the use of a Perspex screen in front of the trolley) as this wouldn't scale correctly with the hydrodynamic forces. In reality however, air resistance plays a major role and forms a sizable component to the total drag [Shut05 (ii)]. The air resistance of the hull and rigging is therefore computed with the forces on the sail and this is then translated into forward and sideward components.

The model was towed from an appropriate height as determined by the CE calcs (see appendix K). This was achieved by attaching a light mast to the main crossbeam and using wire and nylon (fishing) line to support it against bending or buckling. (See figure 5.4) The leeway (yaw) angle was set using a pair of side arms, with ball joints at both ends, turnbuckles to adjust their length and an adjustable counterbalance to ensure the mass of the side arms didn't influence the displacement of the model. (See figure 5.3) The heel angle was set by setting the angle of the mast at the appropriate angle with a lateral line (non stretch rope). The position of this lateral line was set so as to ensure minimal vertical or forward components while running. The height at which the side arms were attached to the trolley depended on the level of the water and the running height of the model

(particularly when supported by foils). This and the length of the tow rope were adjusted to ensure the side arms had virtually no directional component in the vertical or forward direction, so as not to affect, displacement, trim and resistance readings. Reference beams were mounted above the side-arms so a visual check of the alignment of these side-arms was made easier.

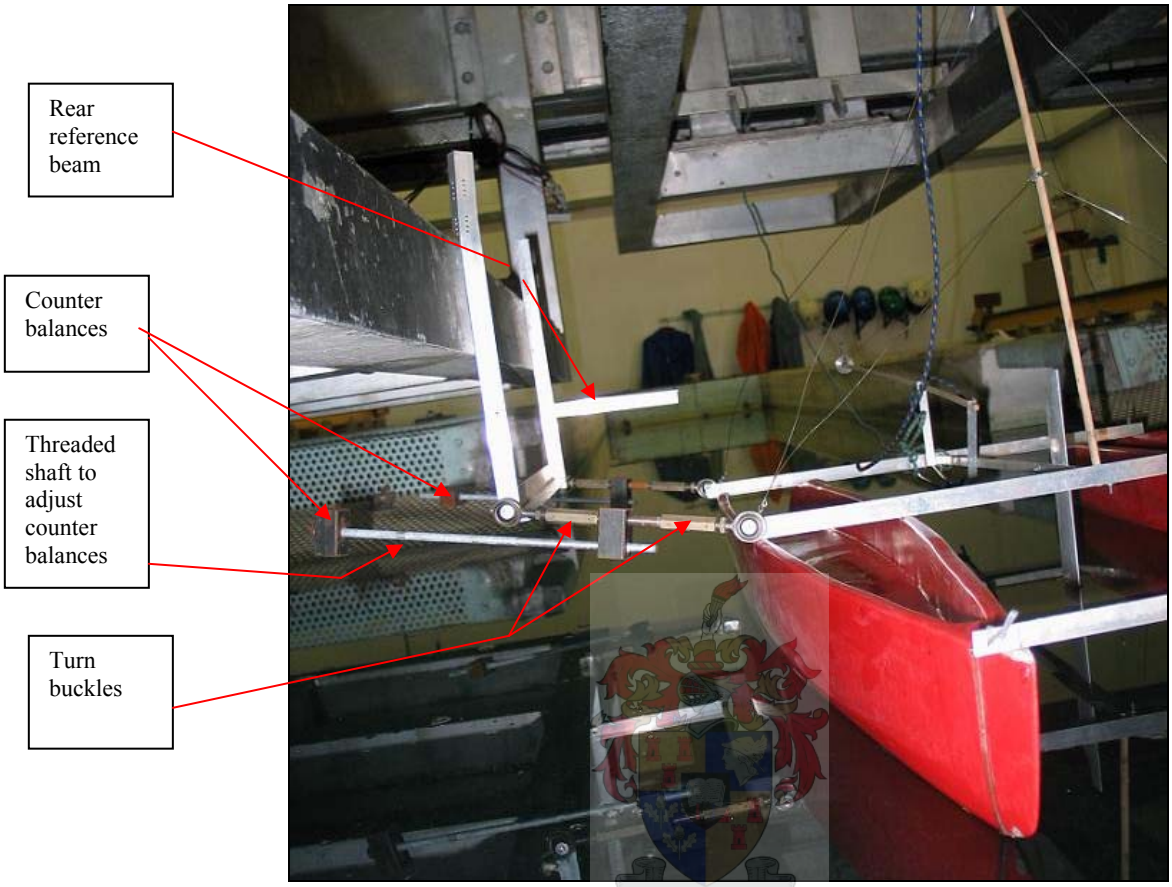

Figure 5.3 – Photo showing front view of side-arms

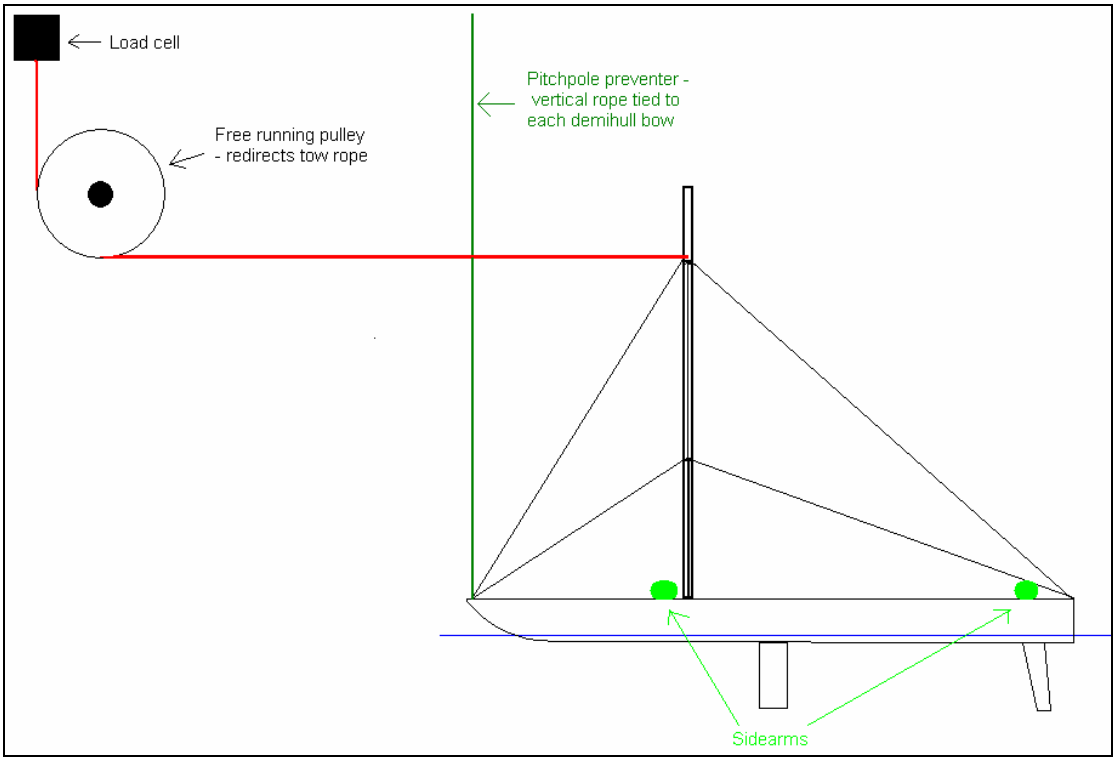

Figure 5.4 – Side-view of experimental setup

The height of the towing point was adjusted to ensure an almost horizontal towing rope and the boat was positioned centrally to ensure no lateral components to the tow rope. To ensure that the boat does not nosedive, as was experienced during initial testing, a safety line was connected to each bow; the length of each was adjusted to become taught as the deck of the bows near the water level.

Although the addition of lifting foils in reality would increase the weight and therefore displacement of the vessel, this increase would not necessarily scale correctly and so a better comparison would be made if the displacement is kept constant and this increase in displacement borne in mind when comparing results.

5.6 Measurement

The trolley is equipped with front and rear trim sensors (displacement sensors) as well as a resistance load cell. The displacement sensors are preset to a certain displacement (midrange) so that a large amount of rise or sinkage of bow and stern can be measured. A computer is linked to these sensors via a DAQ (data acquisition system) and is used to capture these readings as well as the speed of the trolley.

The model was weighed throughout the testing to ensure that water absorption and or leaks as well as changes to the model, did not result in excessive changes in displacement. The total weight of the model never exceeded 4.3% over the design weight (scaled displacement) and since this small error would affect the WSA (viscous resistance) and displacement (wave resistance) by a very small order of magnitude, it will have little effect on the hull resistance.

The speed of the trolley is measured by a counter, which counts the rate at which the wheels of the trolley are turning. The errors resulting from this method would be from expansion of the wheel due to temperature changes and slipping of the wheel. Once at full speed, the slippage is expected to be near zero (since the motors then merely need to overcome the air resistance while the weight of the trolley is significant enough to provide good traction). The coefficient of thermal expansion for steel is 12×10^{-6} / ^{0}C [GT97] and the change in temperature is conservatively estimated as 20^{0}C resulting in a change in diameter of less than 0.03% and the change in speed measurement will be directly proportional to that. The speed was calibrated several years prior to testing but due to the small expected error in the measurement, it was decided not to recalibrate the speed before testing.

5.7 Testing procedure

The model was first tested without lifting foils and then the lifting foils were attached so that their effect of hydrodynamic resistance across the speed range could be determined.

5.7.1 Model testing without lifting foils

- *Determining LCG*

The COG of the hull was not known and in reality, will vary during use, as the volume of fuel and water held in the respective tanks change and the placement of cargo and crew varies. A hydrodynamically efficient submerged hull shape is obviously desirable and the aim of the designer. If the COG is set too far aft, the hull will be inefficient at low speeds (see section 2.1.8) but will benefit from planing effects more at moderate to high speeds, and vice versa. A compromise is therefore desired to give a good overall performance. It must also be borne in mind that from a stability perspective, it makes sense to distribute the load on the foils as evenly as possible. It would therefore be better in that sense to have the Longitudinal Centre of Gravity (LCG) relatively far aft.

Since the LCG was not known, it was decided to run a few tests over the speed range to determine a suitable LCG. Three LCG positions were tested (44%, 46% and 47%) which were determined from the hydrostatic tests to yield reasonable trim angles. (0.8^0, 0.4^0 and 0^0 respectively) The waterline was deduced from the hydrostatic tests for these trim angles and they were deemed suitable based on the experience of the student, since he is a relatively experienced sailor.

- *Straight line tests*

Once the suitable LCG has been determined, the straight (testing without heel and leeway) could commence. This involves measuring the resistance, bow and stern rise (which can be used to calculate the overall rise and trim of the boat) and WSA at various speeds. A curve of the resistance versus speed is then be plotted and compared to the computational results. The trim and rise are required for the computational analysis.

- *Determining effects of heel and leeway*.

Only the total resistance (hull and foils) is measured at various speeds, for three heel angles. The same is then done for three leeway angles. The effect of these two angles on resistance is then plotted independently. (See figure E.4a-c)

5.7.2 Model testing with lifting foils

- *Determining a suitable configuration*.

The next step is to determine a suitable configuration for the lifting foils. This involved varying the depth of the main foil and angles of attack of all foils, and if necessary, changing the foil configuration completely. Once this is done, the straight line tests are completed as before.

- *Determining effects of heel and leeway*

Finally, the effects of heel and leeway are computed on the boat with hydrofoils (lifting foils) attached. The testing procedure is the same as without lifting foils.

The model resistance can then be scaled up and compared to the computed resistance. It is hoped that these discrepancies can then be explained.

5.8 Assessment of Accuracy

A detailed study of the sources of error in the experimental set-up was conducted and a number of sources were identified. (See appendix K for details) Each resulting error was then quantified and in all cases except the calibration of the load cell, the errors were considered negligible.

The accuracy of the calibration of the load cell measuring the resistance of the model was checked across the speed range. This showed that at measurements corresponding to the low speed measurements, the calibration becomes very inaccurate. In order to limit the error caused by this non-linearity at low speed measurements, the load cell was recalibrated (see figure 5.5). The curve fit for these low speed measurements is shown and has strong agreements with good repeatability. The results of the tests were then corrected by applying the equation of the recalibration curve. Since the scaling up methodology (explained in section 5.1) is only an empirical approximation, any errors due to the slight variance in the readings will have a negligible effect on the accuracy of the measurements.

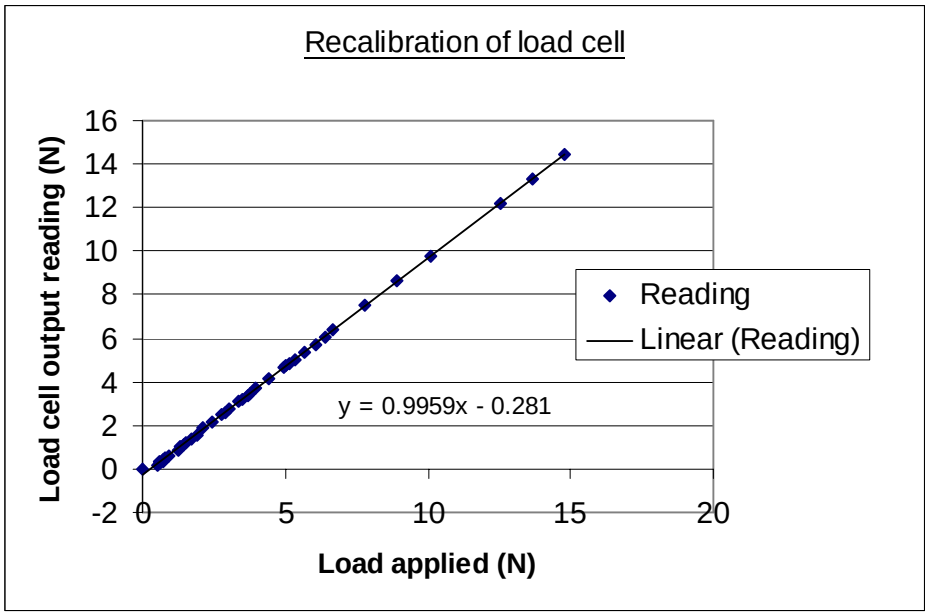

Fig 5.5 – Graph of curve fit used to recalibrate the load cell for resistance measurement

Chapter 6

Results

6.1 Determining LCG

From the results shown in figure M.1, (appendix M) the change in resistance across the speed range due to a shift in LCG is not very significant for the given range of LCG. Since the LCG of 44% gave the best resistance characteristics and would also provide the most even loading of the hydrofoils (and therefore highest stability when the foils were attached to the daggerboards and rudders) this LCG was chosen for testing.

6.2 Validation of Resistance Curve

In order to predict and verify the model testing results, a set of model testing results of a model catamaran of similar parameters was sought out. After the model had been designed (See section 2.4.1) a similar model was found in a paper by Insel et al. [IM91] (see table 6.1) and from the graphs provided, the resistance across the speed range of RH1 was computed.

Model	**C4 (NPL series)**	**RH1**
L	1.6	1.3
L/B	9	8.24
B/T	2	3.7
$L/\nabla^{1/3}$	7.417	10.3
C_B	0.397	0.39
C_P	0.693	0.559
C_M	0.565	0.718
$A(m^2)$	0.338	0.24 (Hydrostatics results)
LCB (%L aft amidships)	-6.4	-6
S/L	0.4 (chosen to match)	0.3875
S/B (resulting)	3.6	3.19

Table 6.1 – Comparing parameters of C4 to RH1

One of the principle differences between the C4 and RH1 models is their towing positions. As a result RH1 will tend to nose-dive at high speeds, increasing WSA and drag, while C4 will not. The high speed drag of RH1 is therefore expected to increase relative to C4. Since C4 is more heavily loaded (smaller $L/\nabla^{1/3}$), the viscous and

wave drag in general is expected to be higher on C4 but, on the other hand C4 does not have large rudders and daggerboards which increase the viscous resistance of RH1, thus countering the above effect to a certain extent. As explained in section 1.5 we expect a more prominent displacement hump at Fr∇ of 1.5 on the more heavily loaded C4. The beam to draft ratio of the two are significantly different but this is expected since C4 is more heavily loaded. Referring to figure 6.1 (also shown more clearly in Appendix M, as figure M.2) there is a fairly strong agreement in the results, given the above mentioned differences. A reasonable confidence is therefore placed in the results.

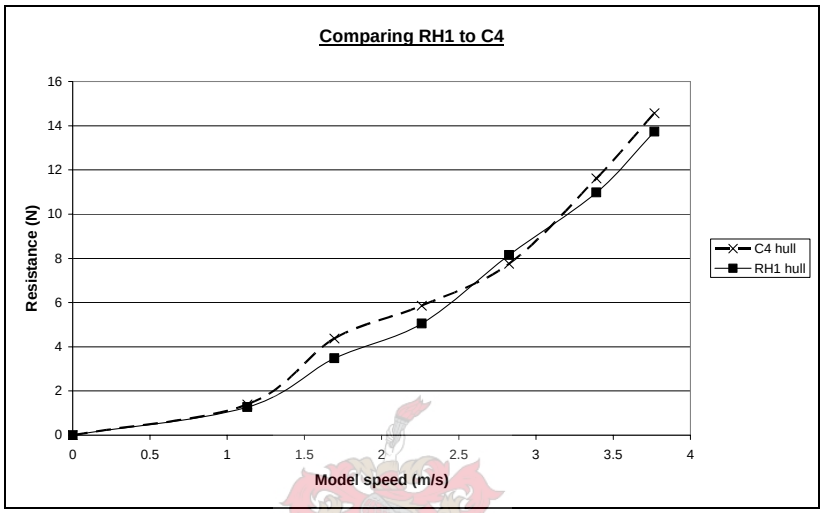

Figure 6.1 – Comparing experimental resistance characteristic of C4 [IM91] to that of RH1 without lifting foils

Since the equation defining the resistance on the hull is given by equation 5.5, we expect a roughly quadratic increase of resistance with increasing velocity. Deviations from this parabolic curve will result from variations in WSA (due to the wave system and changing running conditions) and coefficient of resistance due to wave interference (as discussed in section 2.1.9). This is in agreement with the curve shown in fig 6.1.

Since the resistance is expected to increase with speed, the pitching moment is also expected to increase. This means that the maximum speed obtainable by the boat without the assistance of following seas and a wave pushing from aft (thus lowering the effective position of thrust) is determined by the speed at which pitchpole occurs. From practical experience this is expected to be around 25 knots for conventional sailing catamarans of this size. Since the drag forces on the foils do not scale correctly with the hull (as discussed in 5.1) we expect the model to pitchpole at a model speed equivalent to slightly less than 25 knots. The model was found in experimentation to pitchpole at a speed equivalent to about 22 knots full scale speed.

6.3 Determining Suitable Foil Configuration

Initially the HYSUCAT type configuration (as discussed in section 3.4.2) was investigated. The depth of the main foil was varied and the AOA on the foils was also varied. It was found that installing the main foil at the end of the daggerboards lowered the COD to such an extent that the pitching moment was increased significantly, tending to cause the boat to nose-dive and a very poor performance was achieved (see figure E.5a). Raising the main foil 1.5 chord lengths higher (see figures E.5b-f) on the daggerboards reduced this problem, increased the heave stability due to surface effects and provided much better results, but the stability of the boat was still very poor and still tended to pitchpole (see appendix, figure E.6 f) unless the boat was tweaked for each speed (adjusting the trim by hand). In addition, there are some practical issues with attaching the main foil at a fraction of the daggerboard length, as the daggerboards can no longer be retracted fully. The practical aspects of the design and a full optimisation were however left for a future research project.

As a result of these stability problems, a canard foil was installed, to provide lift at the bow so as to counter the tendency to pitchpole. This proved successful and a stable running configuration was found. It was then supposed that the rear foils may not be necessary and since they are attached at only a fraction of the length of the rudders, they have '4 corners' providing a large amount of interference drag, and were therefore removed. The result was that the resistance was reduced (≈2.5%) after the rear foils were removed and so the final configuration was determined as a canard foil at the bow and a main foil amidships, connected between the daggerboards (see figure 6.2).

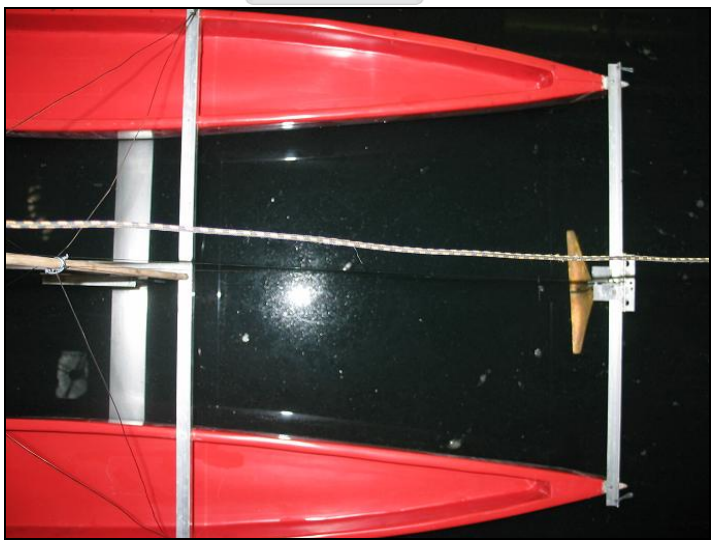

Figure 6.2 – Photo of canard configuration
(See appendix E, figure E.7a and E.7b)

The angle of attack (AOA) of both foils were then adjusted in an attempt to minimise resistance while still maintaining a stable configuration throughout the speed range (see appendix M, figure M.3). The best results were achieved with a main foil AOA of 0.89 degrees and canard foil AOA of 2.7 degrees (both relative to the

static waterline). This result did however give a large hump resistance, which could be reduced by increasing the AOA on the main foil, but this resulted in instabilities due to porpoising and ventilation at high speed. Ideally a fully controlled foil system (trim and ride height control) would be ideal in providing an optimal resistance curve but this would be both costly and difficult to implement in a working prototype and not the objective of this thesis.

a) b)

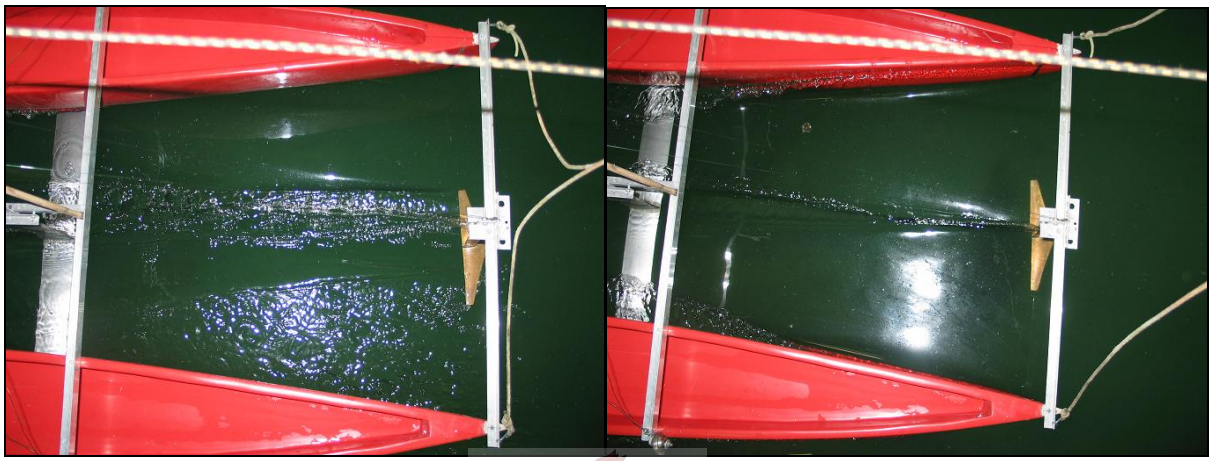

Figure 6.3 – Pictures showing - a) bow up running condition b) bow down running condition (See appendix E, figures E8a-d)

During experimentation it was observed that there were two stable foil-borne running conditions. The first was with the bow raised and the boat supported mostly on the foils and the second was with the bow lowered and the boat balanced between the foil support (with low AOA) and the buoyancy of the bow. This is shown in figure 6.3. where in 6.3 a) the boat is running in the bow up condition with the canard at the surface (often ventilated and uneven flow off it propagates down onto main foil, thus reducing efficiency) and very little WSA and bow wave, while in 6.3 b) the model was accelerated, pitched forward and is now running in the bow down condition with the canard deeply submerged and significant spray on the bow. The latter resulted in much poorer performance and the boat required some tweaking in order to re-establish the bow up running condition. The bow down running condition is also not very stable as the CLR would move far forward and the area and aspect ratio of the rudders would be reduced. As a result the boat would be unstable in yaw and the yawing moment created by the off-centre CE on the sails would undoubtedly result in yaw instability. The threat of pitchpole when sailing in waves under this running condition would also be a problem. This running condition was therefore determined to be unsuitable and the resistance values were taken for the bow up running condition only. Practically this would imply a trim control system is required for this configuration to maintain stability as well as performance, but practical issues were not considered in this project. Since practical issues were not considered and this configuration provides a stable bow up running condition throughout the speed range (so long as no sudden acceleration is applied) this was determined to be a suitable configuration.

It was noticed during experimentation that almost all the hydrofoil support was provided by the main foil and the boat could in fact (if balanced carefully) run at certain speeds on the main foil only with the canard foil just above the surface. If the main foil was swept back so that the hydrofoil support is spread more evenly between the foils the pitch stability is expected to be improved, however this was left for an investigation of a more complete design in future research.

6.4 Comparison Between Total Resistance curves of With and Without Hydrofoils

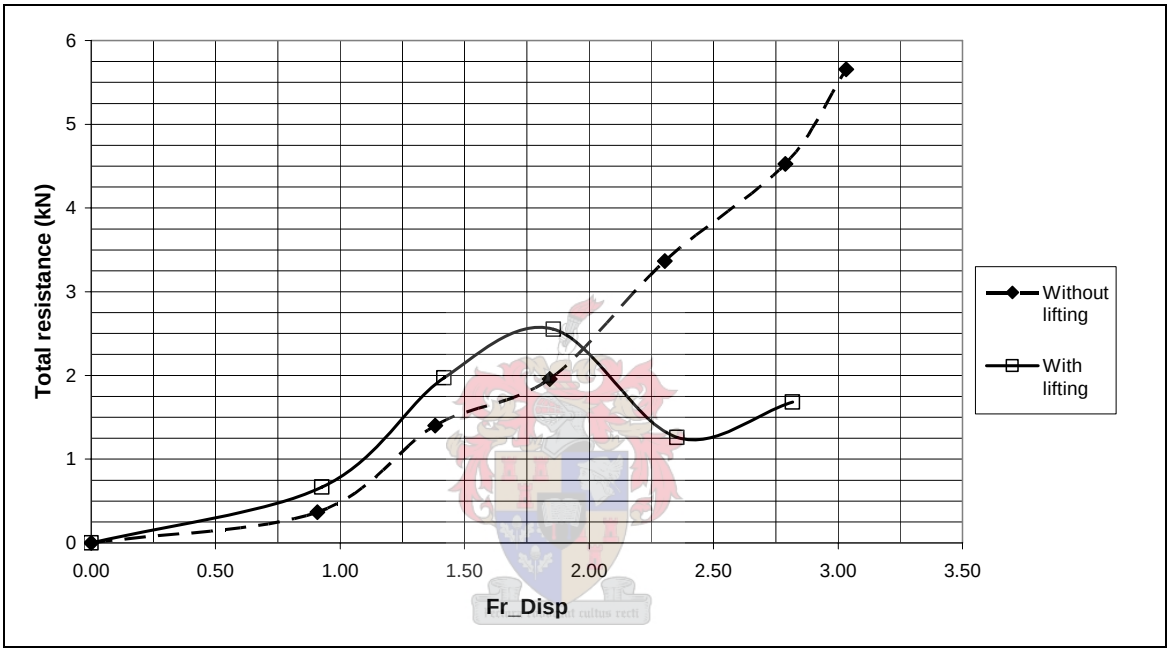

Figure 6.4 – Comparing the full scale resistance measured experimentally and scaled using the methodology of section 5.1, across the speed range, for both with and without lifting foils

Figure 6.4 above is shown again in figure M.4. The full scale resistance was determined experimentally using the methodology described in chapter 5.1. From this figure it may be concluded that a reduction in resistance due to the attachment of lifting foils, is expected above a displacement Froude number of 2 (approximately equivalent to 14.2 knots for our full scale prototype). Below this speed the resistance is increased due to the added viscous and induced drag of the hydrofoils while the hull is not raised sufficiently to reduce the total drag. At the hump speed around 13.5 knots (displacement Froude number of 1.9) there is a maximum increase in resistance of about a 44%, due to the addition of the hydrofoils. A maximum reduction in resistance of 63% was measured at an approximate displacement Froude number of 2.3.

This reduction in hydrodynamic resistance above a displacement Froude number of 2 is in agreement with the results of several other research projects that investigated hydrofoil supported catamarans with semi-displacement type demi-hulls ([Hop80], [Hop91], [Miy89] and [Mig01]). This implies that although the

configuration was not fully optimised, it is unlikely that a significant improvement below this Froude number is possible (even for catamarans with very wide tunnels that allow for very high aspect ratio foils to be used).

6.5 Investigating the Effects of Leeway and Heel.

The qualitative effects of heel and leeway were investigated. The results were taken directly from model scale rather than scaling up, as in reality, these two phenomena seldom occur independently (as they are both linked to the sideward component of the aerodynamic force on the sail) and all that was sought from this investigation was an insight into their effect.

6.5.1 The Effects of Leeway

For the case of without lifting foils, the induced drag on the rudders, daggerboards and demihulls would increase with increasing leeway angle. The induced drag of the rudders and daggerboards was calculated in appendix H and is calculated to be relatively small when compared to the total resistance of the hull. From the results of [CWM97] it was shown that the induced drag on hulls at reasonable leeway angles is also small compared to the total resistance. An additional effect of leeway is that it offsets the bows of the demihulls and this will effect the wave interaction between the demihulls. A large change in wave pattern was observed for large leeway angles.

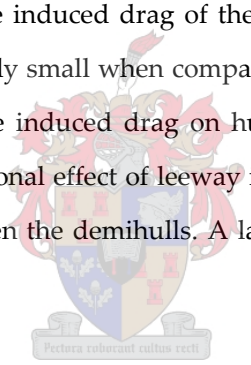

In order to establish what effect this would have, attempts were made to relate this phenomenon to the effects of positioning of the outriggers on trimarans. After referring to the following papers [DWD05], [BBBCCFTZ05], [SD05], and [Dub04], it was concluded that since the wave interference resistance is a function of hull shape, separation between outriggers and speed, no fixed means of quantifying this effect on wave interference was made. All that could be concluded from this is that variations in wave resistance interference, as a result of changing the positioning of the outriggers, are expected. A further conclusion for low speed was that the optimal positioning of the outriggers is when their bows are in line with the bow of the main hull.

If these conclusions are applied to the catamaran, the effect of leeway on wave interference drag is to cause unknown variations in resistance at above low speed and at low speed the minimal resistance is expected to occur at a yaw angle of zero.

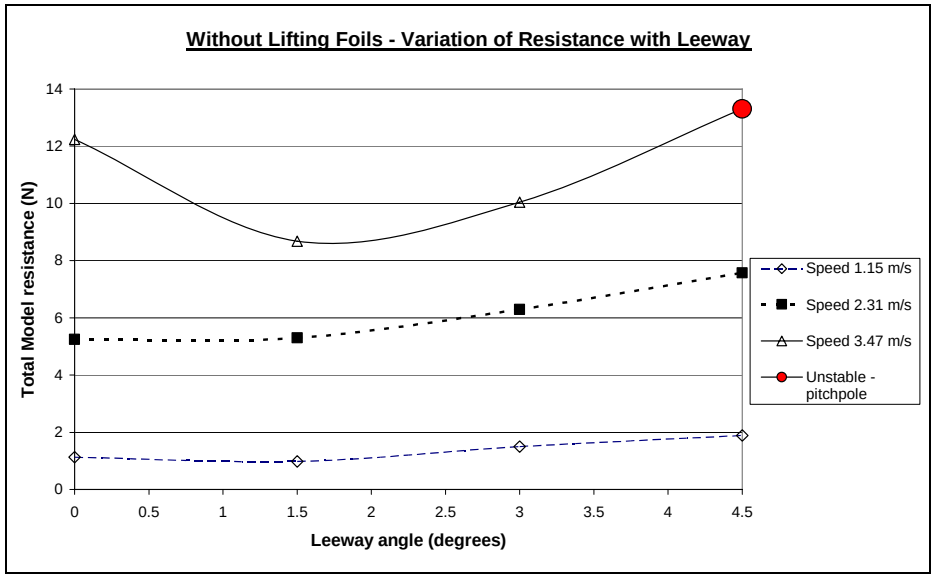

Figure 6.5 - Experimental resistance plotted against leeway angle of RH1 without lifting foils
Shown more clearly in Appendix M, figure M5

Figure 6.5 shows the effects of leeway on the resistance of RH1 without lifting foils. The change in wave interference resulted in a slight increase in resistance with leeway angle for low and moderate speeds. For high speed ($Fr\nabla \approx 2.8$) a reduction in resistance is observed at moderate leeway angles.

For the case of with lifting foils the effect of leeway is expected to be much the same as without lifting foils but there is will a slight loss in lift on the foils due to the leeway angle. This was discussed in section 3.4.2 and is described by equation 3.38, but since leeway angles are expected to be small, the loss in lift will be only slight.

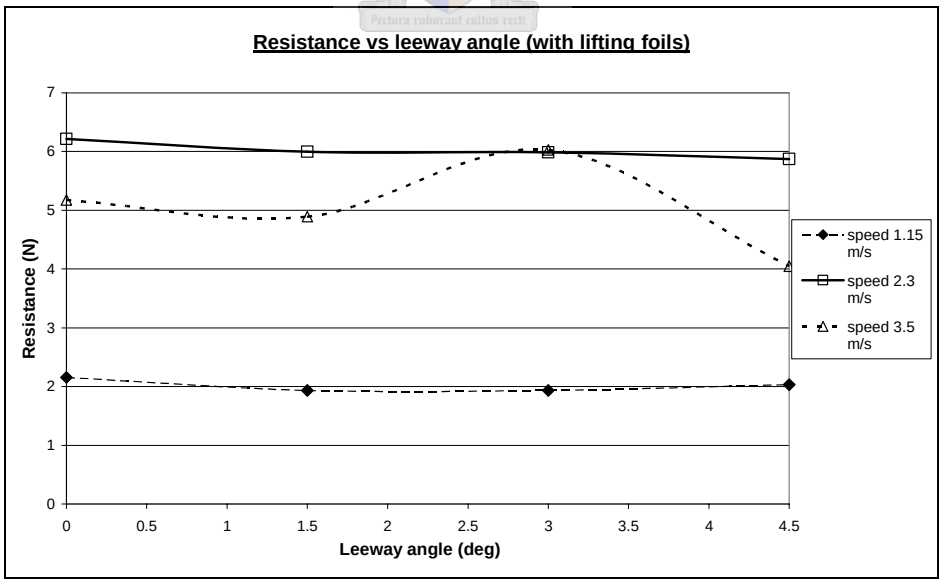

Figure 6.6 – Experimental resistance plotted against leeway angle of RH1 with lifting foils
Shown more clearly in Appendix M, figure M6

From figure 6.6 it was determined that for RH1, with the addition of this lifting foil configuration, the effect of leeway on resistance is small for low speed, a slight decrease at moderate speed and at high speed, the resistance is less at leeway angles of 1.5^0 and 4.5^0 , but is increased at 3^0.

Large leeway angles are associated with large sideward aerodynamic forces, which in turn result in large heel angles. In order to maintain a straight motion with large heel angles, a large rudder angle is usually required which will add additional induce drag. Since this is not modelled, it is expected that the drag in reality would be much higher for both large heel and leeway angles.

During experimentation, the strong sideward forces on the foils (see calculations in appendix H) combined with the slight flex in the rigging of the experimental setup resulted in a slight heel angle (about 2^0 at its maximum) at high speed and leeway angle. Although it was attempted to compensate for this when fastening the boat in place, this was noted as a source of error. Since only a qualitative effect of leeway was sought it was felt that this error was acceptable as absolute accuracy was not required to provide insight into the effect.

6.5.2 The Effects of Heel.

From the hydrostatic analysis conducted in appendix G, we expect the WSA and therefore viscous drag to decrease with heel. Since RH1 has significant rocker, as the windward hull emerges from the water, its FP will move aft with increasing heel. This will affect the wave interference resistance in a similar way to the effects of leeway, but a far more drastic change is expected as the FP of the windward hull will move all the way back to amidships before the windward demihull is emerged completely.

After referring to the results of MICHLET (appendix I), the wave interference resistance was relatively small compared to the viscous resistance component (between 0.4% at high speed and 15% at low speed for no heel). The wave interference is expected to change with heel angle but from these results, the reduction in viscous drag due to change in WSA with heel is expected to be more significant at high speed.

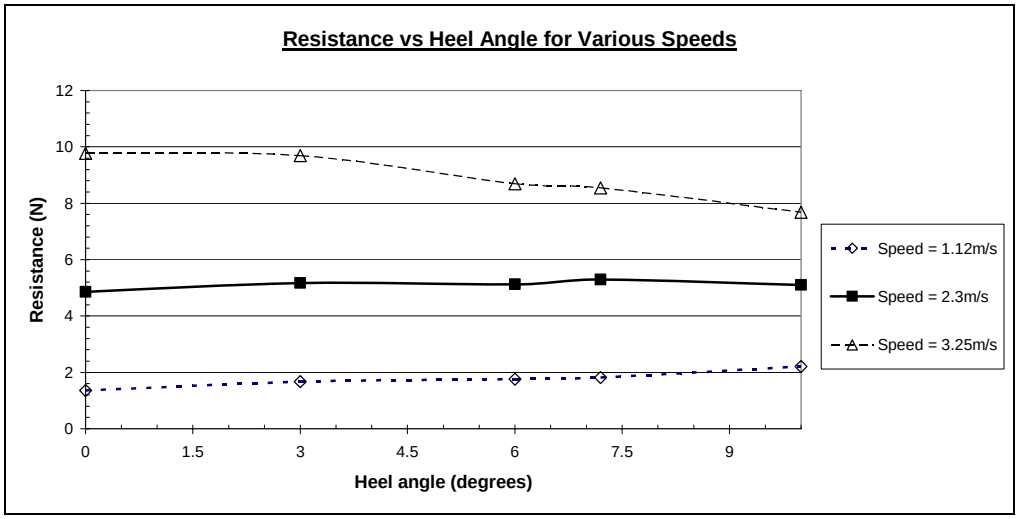

Fig 6.7 - Experimental resistance plotted against heel angle of RH1 without lifting foils
Shown more clearly in Appendix M, figure M7

From figure 6.7 it can be seen that the effects on wave interference seem to cancel the reduction in viscous resistance at low and moderate speed but at high speed, the reduction in viscous resistance dominates as expected.

Since heel brings the leeward hull deeper into the water, and therefore its deck closer to the surface, the trim angle resulting in the deck of the bow flooding (initiating pitchpole) would be smaller. This implies that pitchpole may occur at a lower speed. On the other hand, as mentioned earlier, the viscous drag is expected to drop with heel angle implying a reduction in drag, which in turn reduces the pitching moment that causes pitchpole and so the net effect is not directly obvious and would need to be determined experimentally. A further aspect effecting the pitching moment is the change in its lever arm. The increase in draft of the leeward hull due additional loading with increasing heel angle would tend to raise the Centre of Drag on the hull, thus shortening the lever arm. On the other hand, the CE is also raised by increasing heel angle, therefore increasing the lever arm. From some simple hand calculations it was determined that the effect of heel angle on the pitching moment lever arm is expected to be small with respect to the above mentioned effects. In experimentation, the speed at which pitchpole occurred was reduced to the equivalent of about 19 knots (from 22 knots without heel) when the boat was heeling at 7^0.

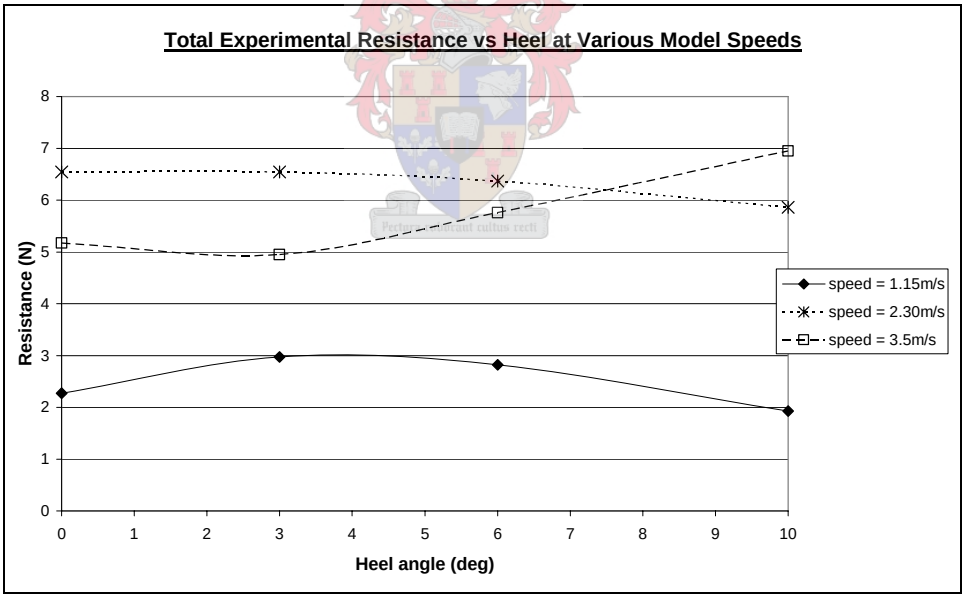

Fig 6.8 - Experimental resistance plotted against heel angle of RH1 with lifting foils
Shown more clearly in Appendix M, figure M8

The addition of the hydrofoils resulted in a slightly more complicated relationship as there is a loss in lift due to heel angle (therefore increasing WSA). For example in conditions of almost complete hydrofoil support, the heel angle would lower the leeward hull, thus increasing the WSA (reversing the effect of heel demonstrated without hydrofoils at high speed). The heel angle also brings the main foil to the surface on the windward side, reducing lift and encouraging ventilation, thus reducing performance. The use of a slight dihedral angle on the main foil would provide a better righting moment and foil support at heel angles and the central strut prevents spread of ventilation to the leeward side, but this was left for a more complete design in future research.

At low speed, there is little lift generated on the lifting foils so the change in resistance is not expected to be very different from without lifting foils. A slight change in resistance is shown in figure 6.8 due to the change in foil efficiency, wave interference and WSA. At moderate speed more lift is generated and both demihulls are partially supported. The change in WSA is expected to be much like without lifting foils as the main foil is still fully submerged. At high speed, the hull is well supported and heel angle results in an increase in WSA and the main foil piercing the surface. Here the resistance is expected to increase with heel angle due to extensive loss in lift on the main foil due to heel. Figure 6.8 is in agreement with expected trends.

6.6 Analysis of Computational and Experimental Results

Referring back to figure 4.1, there is a very strong correlation between the computational and experimental resistance curves for RH1 without lifting foil. A reasonable amount of confidence is therefore placed in these results. Referring now to figures 6.9, there is a reasonable correlation (not as strong as for without lifting foils) between the experimental and computational resistance curves but this is to be expected due to the added complexity of modelling both hull and foils. The discrepancies may be explained by a number of factors. The MICHLET calculation uses the assumption of vertical sides above the waterline and although this is accurate for the front and mid sections of the boat, the aft section is fairly angled near the waterline and would therefore result in errors in the wave resistance calculations near the stern. A larger error is expected with increasing rise as RH1 is flatter near the keel and since rise is far more significant with lifting foils, this error will be larger and increase with speed. For very large values of rise, the underwater hull shape is no longer slender due to the large rocker of RH1 and therefore the thin ship theory of MICHLET is no longer appropriate and will have resulting errors. For large values of rise however, a greater percentage of the drag comes from the foils, thus this error will be 'diluted' when summed together with the foil drag results. Also since the interference effects between the hulls and foils are ignored, the lift cancellation and interference drag is not accounted for in the calculation.

Since the hull-foil interaction has been ignored, the hump speed is expected to be under-predicted as the hull-foil interaction is strongest there (The last section of boat to leave the water is directly above the main foil). This trend is demonstrated in figure 6.9.

At high displacement Froude numbers (above 2.3) the prediction becomes poor. This may be explained by the following. The stability of the AUTOWING calculation tends to 'break down' as the foil system nears the surface. This resulted in an unconverged solution for the top speed, so no foil drag prediction was made for that speed. Since the main foil is already close to the surface at the second to last speed, the results for the foil drag

may not be very accurate. On inspection of the wave surface output from AUTOWING for the second to last speed, a rather unrealistic surface was predicted, thus not much confidence was placed in the solution.

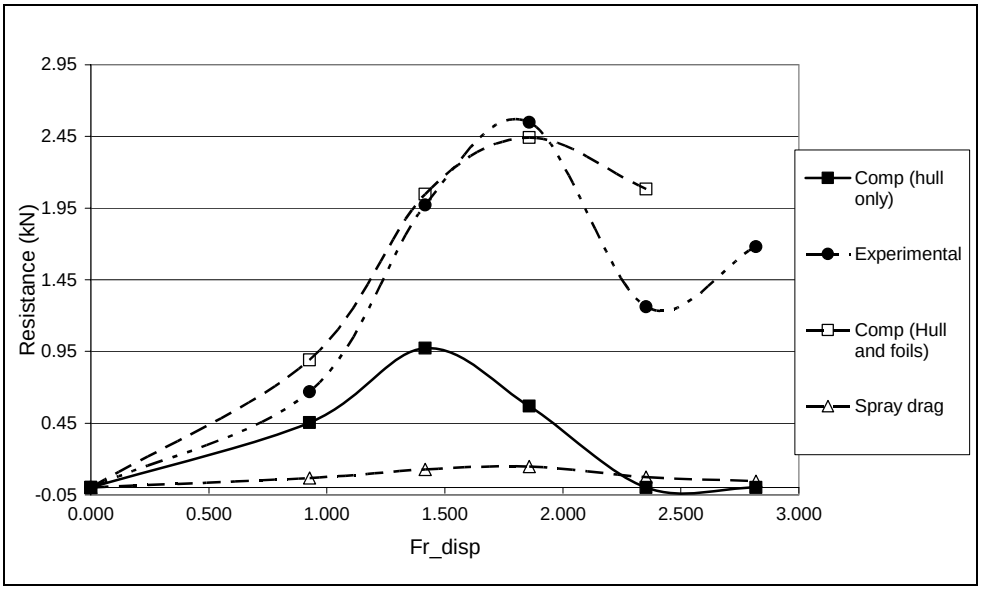

Figure 6.9 – Comparing the experimental and computational resistance curves of RH1 with lifting foils
The hull resistance was determined using MICHLET, the foil drag was determined using AUTOWING and the spray drag on the surface piercing struts was calculated using equation 3.27.

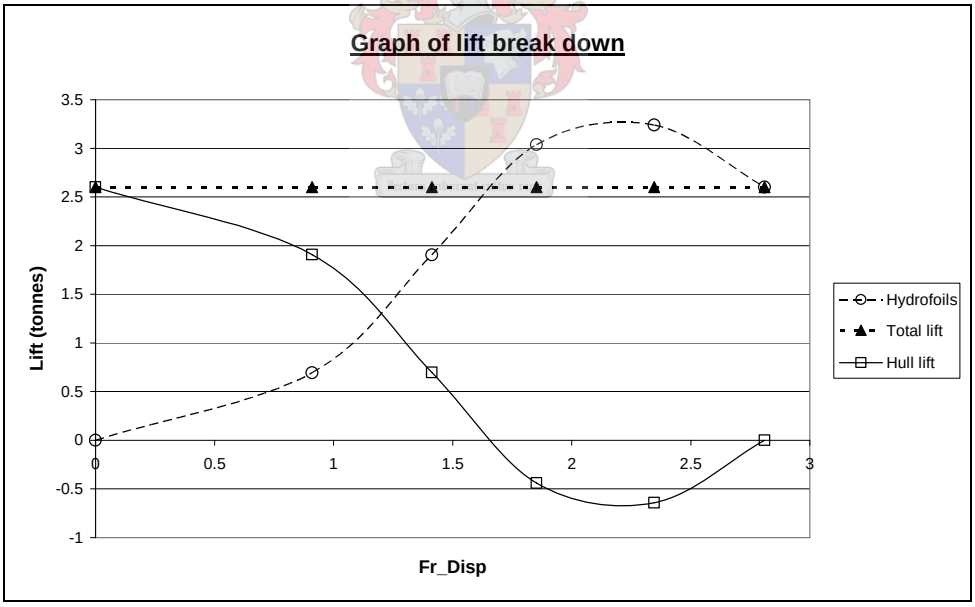

Figure 6.10 – Graph of lift breakdown varied with speed. Foil lift calculated theoretically.
See appendix M, figure M.14

From the theoretical calculations made in AUTOWING, the lift produced by the lifting foils (see figure 6.10) is larger than the total displacement of the boat above a displacement Froude number of about 1.65. This would indicate a strong interference and lift cancellation at this speed (as described in chapter 2.3.5) but as already mentioned the results on the last two speeds are not reliable due to the instability in the AUTOWING calculation resulting from the close proximity of the foils to the surface.

6.7 Analysis of Change in WSA

From figure 6.11, the WSA (and therefore viscous drag) is reduced above a displacement Froude number of about 1.6. With the addition of induced and spray drag created by the foils, we expect an improvement in performance at above this Froude number. A reduction in total resistance above a displacement Froude number of 2 is therefore a reasonable expectation. Change in WSA of the hulls only is shown in appendix M, figures M.9-10.

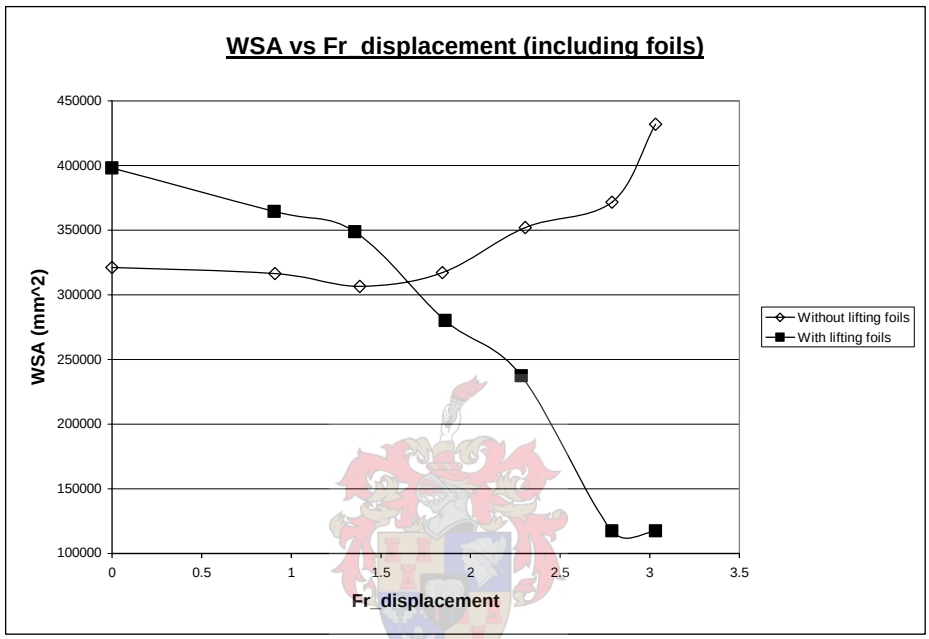

Figure 6.11 – Graph showing effect on WSA due to addition of foils

After the boat is fully supported by the foils, the drag is expected to increase as the wave drag increases as the foils near the surface and the viscous drag on the foils increases with increasing speed. This agrees with the experimental results.

Chapter 7

Conclusions and Recommendations

7.1 Achievement of Objectives

The *main objective* of the thesis was achieved. A hydrofoil system without trim and ride height control was developed that maintained a stable running condition throughout a typical speed range. The change in resistance across that range as a result of the addition of the hydrofoil system was determined.

The achievement of the *secondary objectives* is commented on below.

- A representative hull (RH1) was designed based on an existing design sailing catamaran and the speed range was determined from data obtained from that existing design.
- The resistance characteristics of RH1 were tested, verified and explained. A roughly quadratic increase in resistance is experienced with speed with fluctuations due to wave interference was found.
- A canard configuration with the main foil attached to the daggerboards and front foil at the bow was found to provide suitable support throughout the speed range without any form of trim or ride height control.
- The resistance characteristics of RH1 with the canard configuration was tested and compared to the resistance characteristics without the lifting foils. The AOA on the foils was adjusted until a maximum portion of the speed range experienced a reduction in resistance, while stability was still maintained throughout the speed range.
- The effects of leeway and heel on the total hydrodynamic resistance were investigated at low, moderate and high speed. It was found that because both of these are a function of wave interference, these effects are complicated and highly dependent on hull shape, so no general conclusions were drawn. The effects of leeway and heel were however determined specifically for RH1.

7.2 Important Conclusions Drawn from Experimentation

Originally proposed configuration with lifting foils attached to the rudders and daggerboards did not provide sufficient stability for RH1. As a result the configuration was changed to a canard type configuration. This provided 2 stable running conditions, one with the bow trimmed up and one with the bow down (providing lift through buoyancy). The latter was found to be unsuitable and so the former was only considered. Although this bow up running condition remained stable throughout the speed range, it was found in experimentation that

the pitch stability was not robust and sudden accelerations (or perturbations in trim) would result in the boat moving to the bow down running condition. Practically this meant that a trim control system would be required to provide adequate performance and stability.

The results concluded that an improvement in performance (reduction in hydrodynamic resistance, resulting in an increase in speed) is expected only above a displacement Froude number (Fr∇) of 2. From other examples of hydrofoil supported catamarans, not much change in this is expected if the foil configuration is optimised further. For this configuration, a maximum increase in resistance was achieved at Fr∇ ≈ 1.9 of 44% and a maximum reduction in resistance was achieved at Fr∇ ≈ 2.3 of 63%. The hump resistance (maximum increase) could be reduced by varying the main foil AOA but high main foil AOA yielded instabilities at higher speeds.

It was also noted that most of the foil loading for this canard configuration is on the main foil and so very little pitch stability is achieved. Better pitch stability would be achieved for this configuration if the main foil was swept backwards.

The presence of the strut of the canard configuration would move the CLR forward, thus creating a potential problem with regard to yaw instability. An alternative would be to reinvestigate the HYSUCAT type configuration but move the main foil forward (sweeping it forward or making it independent of the daggerboards) which would provide more pitch stability.

7.3 Recommendations for Future Research

From the above conclusions, the following is recommended for future research.

- The design of a retractable hydrofoil system could be investigated. Since the speed of sailing craft is dependent on wind speed, there will often be conditions of relatively low boat speed (below displacement Froude number of 2). From the results it was therefore concluded that it would not be desirable to have a fixed (permanently submerged) hydrofoil system as it would not be beneficial in terms of total resistance for a significant portion of the speed range.
- The HYSUCAT type configuration is reinvestigated but the main foil is moved forward as suggested. This could form part of a more complete design and optimisation. Since the canard foil disturbed the flow over the main foil (which provides most of the lift), an improvement in performance is expected. Judging by the experimental results, there would need to be a significant shift forward of the COP of the main foil to provide adequate stability so sweeping it forward is not likely to be practical. An independent strut system is therefore recommended which would provide much more freedom in

terms of design. The balance of the system would be affected by the addition of the struts on the main foil so this would need to be compensated for.

- If the canard configuration is investigated further, the main foil should be swept back to provide better pitch stability. It would also be more practical to have two canard foils, one under each demihull bow as heel tends to lift the canard out of the water, thus making it less effective at providing pitch stability.
- Due to the significant pitch instability of sailing catamarans, it is suggested that a trim control system is included in a full hydrofoil system design. A significant reduction in the hump speed was achieved by varying the main foil AOA. It is therefore suggested that a ride height control system is also included in such a design.
- The reduction in hydrodynamic resistance at a particular speed would in reality result in an increase in speed. Since this would affect the apparent wind and aerodynamic drag on the hull and rigging, a full Velocity Prediction Program (VVP) assessment would need to be conducted to quantify this increase in speed. This fell beyond the scope of this thesis, but the complexity of a VPP was investigated (see appendix L) so that it may be fully investigated in future.
- Although stability was investigated, a full investigation into the effects on stability and seaworthiness by the addition of lifting foils could be investigated.
- The incorporation of a dihedral main foil. Since initially, little was known with regard to the dynamics of a hydrofoil supported sailing catamaran, the configuration investigated was kept very simple. Since roll and heave stability are important for sailing catamarans, and a dihedral angle is known to improve this, it is suggested that this aspect is investigated.
- Since the low speed model resistance yielded very low readings it is recommended that a slightly larger model is used so that greater accuracy can be obtained for low speed measurement. This would also improve accuracy in terms of viscous scaling effects, but other factors limiting the size of the model (refer to section 5.2) must be considered.

References

[Bai76] D. Bailey. The NPL High Speed Round Bilge Displacement Hull Series, Resistance, Propulsion, Manoeuvring and Seakeeping data, National Maritime Institute, Royal Institute of Naval Architects, 1976.

[BBCCFTZ05] E. Begovic, A. Bove, D. Bruzzone, S. Caldarella, P. Cassella, M. Ferrando, E. Tincani, I. Zotti. Co-operative investigation into resistance of different trimaran hull forms and configurations. *International Conference on Fast Sea Transport.* FAST 2005. June 2005. St. Petersburg, Russia.

[BD99] Boat Design.net website. Forum. http://forums.boatdesign.net .1999.

[Ber00] V. Bertram. Practical Ship Hydrodynamics. Butterworth-Heinemann.2000.

[Bir03] A. Biran. Ship Hydrostatics and Stability. Butterworth-Heinemann.2003.

[Cae06] CAE Marine Website. http://www.sovereign-publications.com/caemarine.htm Last modified January 29, 2006.

[Cha00] EJC and GC Chapman. Design and Development of a 4.9m Hydrofoil Catamaran. Catalyst Magazine, Vol. 1 No. 2 July 2000. (Originally presented to a conference in Hobart in January 1999). http://homepages.rya-online.net/ejcchapman/HobartPaper/ HobartPaperWeb.htm. 2000.

[CMAP97] P.R. Couser, A.F. Molland, N.A. Armstrong and I.K.A.P. Utama. *Calm Water Power Predictions for High Speed Catamarans*. Fast '97 Papers. (pgs 765-773)
1997.

[CWM98] Dr P.R. Couser, Dr J.F. Wellicome and Dr. A.F. Molland. Experimental Measurements of side force and induced drag on catamaran Demihulls. In *International Ship Building Progress* Vol 45, pgs 225-235 , 1998.

[Dev98] William Devenport. "Panel Method Applet". Instructions for a Vortex Panel Method Applet. (http://www.engapplets.vt.edu/fluids/vpm/vpminfo.html
Last update - 1998.

[Dub04] V. Dubrovsky. Ships with Outriggers, Backbone Publishing Company, Fair Lawn, USA. 2004.

[DuC72] P. du Cane. High Speed Small Craft. David and Charles: Newton Abbot.1972

[DD97] L. Doctors and A. Day. *Resistance prediction for transom stern vessels*. Fast '97 Fourth international conference on fast Sea Transportation, Vol. 2, pages 743-750, Sydney, 1997

[DL01] V. Dubrovsky and A Lyakhovitsky. Multi-Hull Ships. Backbone Publishing Company. 2001.

[Doc98] L. Doctors. Intelligent regression of resistance data for hydrodynamics in ship design. In *Twenty Second Symposium on Naval Hydrodynamics*, Pages 21-36, Washington D.C. 1998.

[DWD05] N. Degiuli, A. Werner, Z. Doliner. Determination of optimum position of outriggers of trimaran regarding minimum wave pattern resistance. Faculty of Mechanical Engineering and Naval Architecture, University of Zagreb, Croatia. 2005.

[Gil55] R. Gilruth. Hydrofoil Craft. United States Patent Office. Patent number 2,703,063. 1955.

[Gro87] *J.Grogano. ICARUS*, the Boat That Flies, *Adlard Coles Ltd London,1987*

[GT97] J.M. Gere and S.P.Timoshenko. Mechanics of Materials (4th Ed.) PWS Publishing Company. 1997.

[Hoe65] S. Hoerner. Fluid Dynamic Drag. Published by he Author, 148 Busteed Drive, Midland park, New Jearsey, 07432, 2nd Edition, 1965.

[Hop80] K.G. Hoppe. *The Hydrofoil Supported Catamaran*. Progress Research Report 1980-2, University of Stellenbosch, Mechanical Engineering Dept., University of Stellenbosch, South Africa. 1980.

[Hop91] K.G. Hoppe. Performance evaluation of high speed surface craft with reference to the HYSUCAT development (part 2). *Fast Ferry International, 1991*

[Hop95] K.G. Hoppe. *Optimization of Hydrofoil Assisted Planing Catamarans.* Presentation delivered to the Third International Conference on Fast Sea Transportation (FAST '95) in Lubeck-Travemunde, Germany.

[IM91] Dr M. Insel and Dr. A.F. Molland. An investigation into the resistance components of high speed displacement catamarans. *The Royal Institute of Naval Architects. 1991*

[Ish91] S. Ishikawa. Study on hydrodynamic Interaction between Hull and submerged Foils. Spring meeting of SNAME, 1991.

[IT02(i)] ITTC website. Resistance, Uncertainty analysis spreadsheet for speed measurement http://ittc.sname.org/2002_recomm_proc/7.5-02-02-04.pdf. 2002.

[IT02(ii)] ITTC website. Resistance, Uncertainty analysis Example for resistance test. http://ittc.sname.org/2002_recomm_proc/7.5-02-02-02.pdf 2002

[IT99i] ITTC website. Testing and extrapolation methods, General uncertainty methods in EFD, Guidelines for resistance towing tank tests. http://ittc.sname.org/2002_recomm_proc/7.5-02-01-02.pdf.1999.

[IT99ii] ITTC website. Testing and extrapolation methods High Speed marine vehicles Sea keeping tests. 1999.

[KHK00] Takeshi Kinoshita, Koutarou Horiuchi, Hiromasa Kanou, Yasuhiro Sudo and Hiroshi Itakura. Prototype of a Single-HandedHydrofoil Sailing Catamaran. http://ketch.iis.u-tokyo.ac.jp/twinducks/protype_test.html. 2000.

[KK80] K.L.Kirkman and J.W.Kloetzli. 'Scaling Problem of Model Appendages' ATTC. University of Michigan, Ann Arbor. 1980.

[KKL80] B.A. Kolysaev, A.I. Kosorukov and V.A. Litvinenko. Some recommendations for choosing the distance between hydrofoils. Handbook on the design of ships with dynamic principle of supporting. Sudostroenie, Leningrad. 1980. Pp 472.

[Kru81] U.S. Krushkov. Dynamic Stability of Sailing Multihulls. Edited and appended by H. A. Myers, January 1981.

[KT99] N.V. Kornev and A.E. Taranov. Investigation of a vortex wave wake behind a hydrofoil. *Ship Technology Research,* 46(1):8-13, February 1999.

[KT05] N.V. Kornev and A.E. Taranov. The AUTOWING 3.0 website. http://www.cl.spb.ru/taranov/Index.htm Date of publishing unknown but found in 2005.

[Laz97] L. Lazouskas. A note on the drag of hulls with transom sterns. Published on the internet: http://www.maths.adelaide.edu.au/Applied/llazausk/hydro/hydro.htm 1997 – Website no longer in operation

[LE02] L. Larsson and R. E. Eliasson. Principles of Yacht Design, 2nd Edition, Adlard Coles Nautical, A & C Black Publishers Ltd, 2002

[Mar86] C.A. Marchaj. Seaworthiness the Forgotten Factor. Adlard Coles Ltd. U.K. 1986

[Max03] MAXSURF Websites.
http://www.formsys.com/Maxsurf/MSIndex.html.
http://www.kastenmarine.com/maxsurf.htm
2003.

[Mig01] G. Migeotte. Design and Optimisation of Hydrofoil-Assisted Catamarans. PhD Thesis, Department of Mechanical Engineering, University of Stellenbosch, Nov 2001

[Mig97] G. Migeotte. Development of Hydrofoil supported catamaran with semi displacement hulls. Master's Thesis, Department of Mechanical Engineering, University of Stellenbosch, December 1997.

[Mig05] Communications between Dr. G. Migeotte and the author.
January – December 2005.

[Mil97] R.Miller. The Miller Hydrofoil Sailboard. http://www.foils.org/miller.htm
1997.

[Miy89] H. Miyata. Development of a new type hydrofoil catamaran. *Journal of ship research*, 1989.

[MM00] K.I. Matveev and I.I. Matveev. "Tandem Hydrofoil System" *Ocean engineering*, 28(2):253-261. January 2000.

[Muc87] W. Muckle. Muckle's Naval Architecture. 2nd Edition. Butterworth and Co Ltd. 1987.

[Pe01] J. Perry '*A Hydrofoil Sailing Dinghy.*' http://www.btinternet.com/~sail/boatbuild02.htm
2001.

[SD05] P. K. Sahoo, L.J. Doctors. The waves generated by a trimaran. *Eighth International Conference on Fast Sea Transport.* FAST 2005. June 2005.

[Spe05] T. Speer. *Tom Speers' Home Page (website).* Generic Hydrofoil Trade Study.
www.tspeer.com\hydrofoils\generic.pdf.
Date unknown but found in 2005.

[Shut05(i)] J. Shuttleworth http://www.john-shuttleworth.com/Articles/NESTalk.html . Multihull Design Considerations for Seaworthiness. 2005

[Shut05(ii)] J. Shuttleworth. http://www.john-shuttleworth.com/Dogstar50-article.html. 2005

[SNA88] Society of Naval Architects and Marine Engineers. Principles of Naval Architecture, Second Revision. 1988.

[SO03] Alexander Sahlin and Jens Österlund Swedish Speed Challenge.
http://www.trampofoil.com/speedsailing/boat.html
Date of publishing unknown but found in 2005.

[The95] A.Thebault. L'Hydroptere. http://www.hydroptere.com. Channel crossing record broken in 1995.

[TT68] H. Turner and A Taplin. 'The resistance of Large Powered Catamarans' SNAME transactions, vol 76. 1968.

[Tu87] E. Tuck. *Wave Resistance of Thin Ships and Catamarans*. Website of University of Adelaide, Department of Applied Mathematics.
http://internal.maths.adelaide.edu.au/people/etuck/pdfiles/t8701.pdf
1987.

[Uni06] Unistel Website. http://admin.sun.ac.za/kie/unistel/technologies/publications.htm
Date of publication unknown but found in February, 2006

[Vea05] R. Veal. Website on The Moth Class of sailing dinghy.
http://www.rohanveal.com/moth.html..
http://www.rohanveal.com/articles/foil_setup.html
Date of publishing unknown but found in 2005.

[WB91] James Wharram and Hanneke Boon. Catamaran Stability.
http://www.wharram.com/introduction_to_catamaran_stability.shtml
http://www.wharram.com/catamaran_stability.shtml
1991.

[Wik05] Wikipedia – The Free Encyclopedia. http://en.wikipedia.org/wiki/Gravity.
2005

[Yeh65] H.Y.H. Yeh. Series 64 Resistance Experiments on High-Speed Displacement Forms. David Taylor Model Basin. Marine technology, pages 248-272, July 1965.

[YW02] Yachting World Magazine. *Article entitled 'Greed for Speed'*. May 2002

A

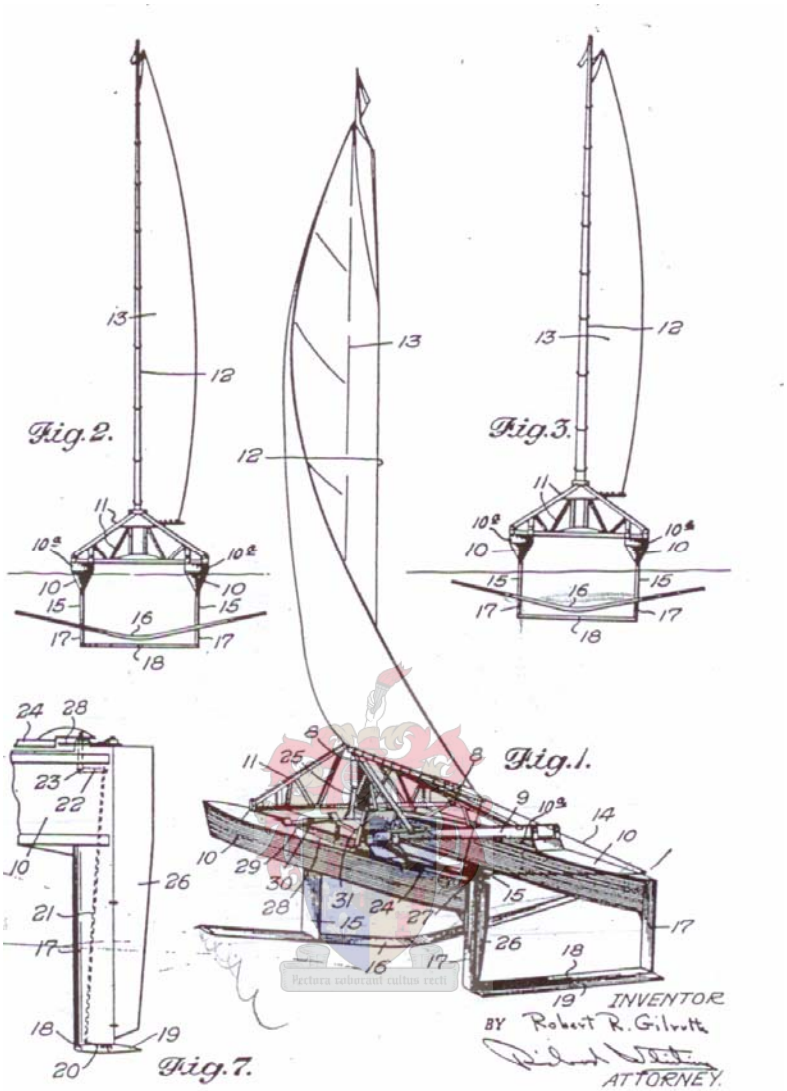

Figure A.1 – Patent #2 703 063 Hydrofoil craft designed and patented in 1955 [Gil55]

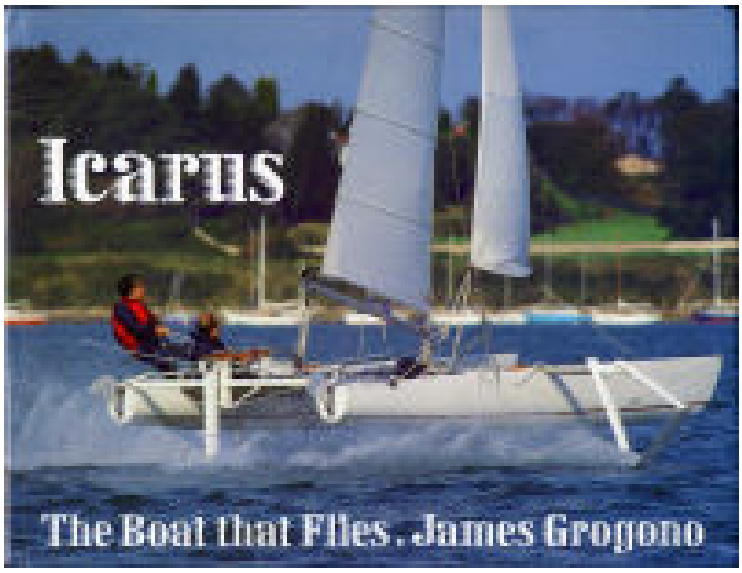

Figure A.2 – Icarus [Gro87]

Figure A.3 – Mayfly [YW02]

Figure A.4 – Ceres – top speed nearly 22 knots [Cha00]

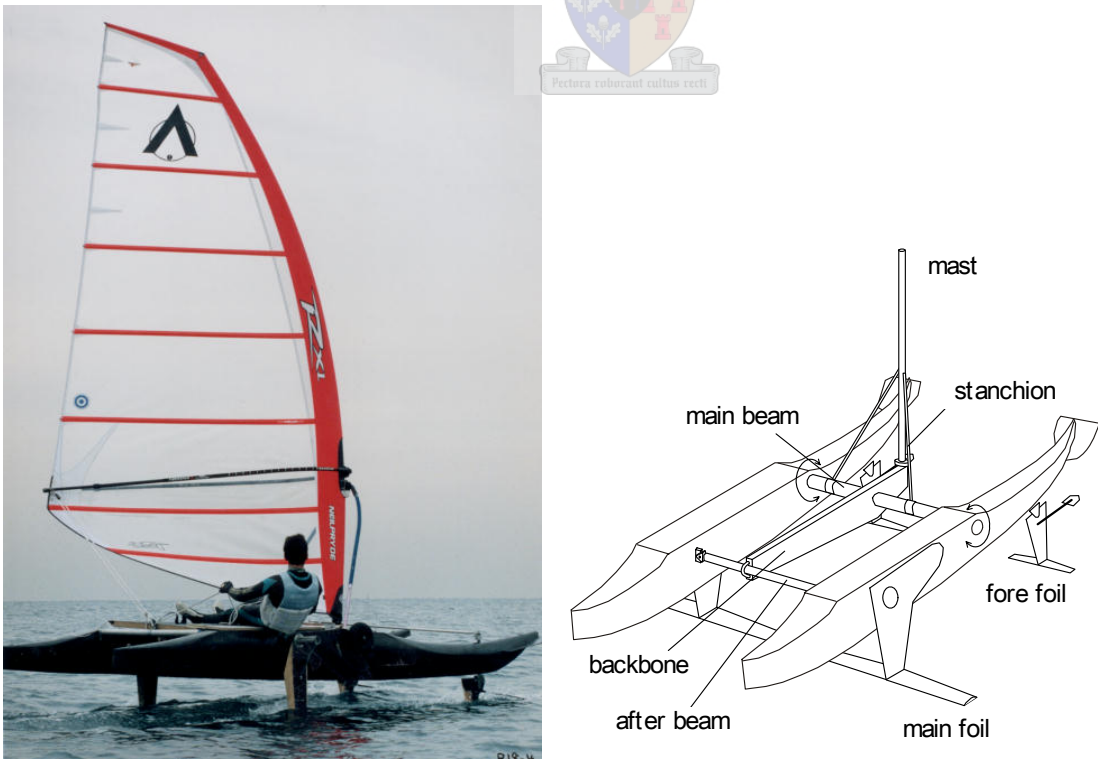

Figure A.5 – 'Twin Ducks' [KHK00]

Figure A.6 – Rohan Veal's Moth Design. [Vea05]

Figure A.7 – L'Hydroptere [The05]

Figure A.8 – The Miller Hydrofoil Sailboard [Mil97]

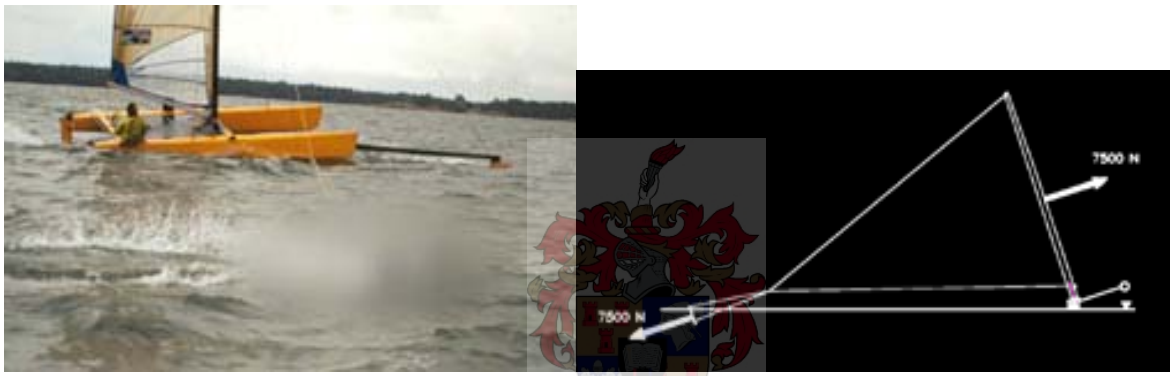

Figure A.9 – 'The Paravane Speedsailer'[SO03]
Demonstrating the use of a hydrofoil connected with wires (paravane) to the mast, to counter the heeling moment.

B

Comparing the WSA of a catamaran to that of an equivalent monohull.

Subscripts
M = monohull
DC = demihulls of catamaran
C = catamaran hull (both demihulls)

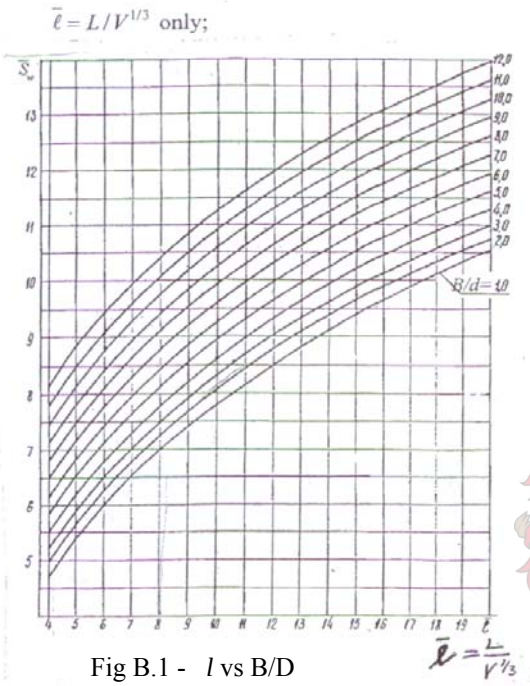

Fig B.1 - *l* vs B/D

Firstly comparing WSA for monohull and cat with same LOA and Displacement

$V_M = V_C = 2V_{DC}$ & $L_M = L_C = L_{DC}$

The following beam-to-draft ratios (B/D) are reasonable estimates for cats and monohulls…

$(B/D)_M = 4$; $(B/D)_{DC} = 2$

$\ell_M = L_M / (V_M)^{1/3} = L_{DC} / (2V_{DC})^{1/3} = 0.794\ \ell_{DC}$

Using RH1 $\ell_{DC} = 10$ (approx) => $\ell_M \approx 8$

From figure B.1 above (taken from [DL01]) we get $\acute{S}_{W,M} = 8.1$ and $\acute{S}_{W,M} = 7.75$

Therefore: $Sw_M = 8.1(V_M)^{2/3} = 8.1(2V_{DC})^{2/3} = 12.86\ (V_{DC})^{2/3}$

$Sw_{DC} = 7.75\ (V_{DC})^{2/3}$

$Sw_c = 2Sw_{DC} = 15.5\ V_{DC}$

$Sw_C / Sw_M =$ **1.21** i.e. for a catamaran of same length and displacement as a monohull, the WSA is about 21% higher.

Using the example of the YD40 from [LE02], about 40% of the medium load displacement is ballast. This means that that monohull will have an increase in displacement of around 40%. Substituting a factor of 1.4 into V_M results in …

$Sw_C / Sw_M =$ **1.08**.

The increase in WSA of the cat is now only slight. The increase in wave generation on the monohull due to added displacement and larger angle of entry on bow is expected to increase more substantially.

C

Figure C.1 – Original boat shown at anchor with rudders and daggerboards in raised position

Figure C.2 – Original boat sailing with main sail and asymmetric spinnaker

Principal Dimensions

LOA	11.2m	36.7’
DWL	10.3m	34’
BOA	5.7m	18.7’
Draft (Daggerboard up)	0.35m	14 inches
Draft (Daggerboard down)	1.6 m	5.2’
Displacement	2600 kg	5700lbs
Wet-deck Clearance	0.85m	2.8’
I	12.3m	40.3’
J	3.8m	12.5’
P	13.0m	42.6’
E	4.7m	15.4’

Sail Areas

Main	41m2	442sqft
Jib	20m2	215sqft
Screecher	57m2	615sqft
Asymmetric Spinnaker	89m2	960sqft

D

Blockage and shallow water effects

Inputs		Units	Comment
b =	4.5	m	Width of tank
h =	2.7	m	deph of tank
Ax =	0.012395	m^2	max x-sectional area of model
L =	1.3	m	length of model
p =	0.31	m	max wetted girth of model (WSA tests)

Shallow water effects

(for L/h < 1 the effects become negligible)

L/h =	**0.481481**	**negligible effect**

Blockage Effects

(for ((Ax)^0.5)/Rh < 0.2 the effects become neglegible)

Rh =	1.188796	
Ax^0.5 / Rh =	**0.093651**	**negligible effect**

E

E.1 Balsa frame used to shape demihulls

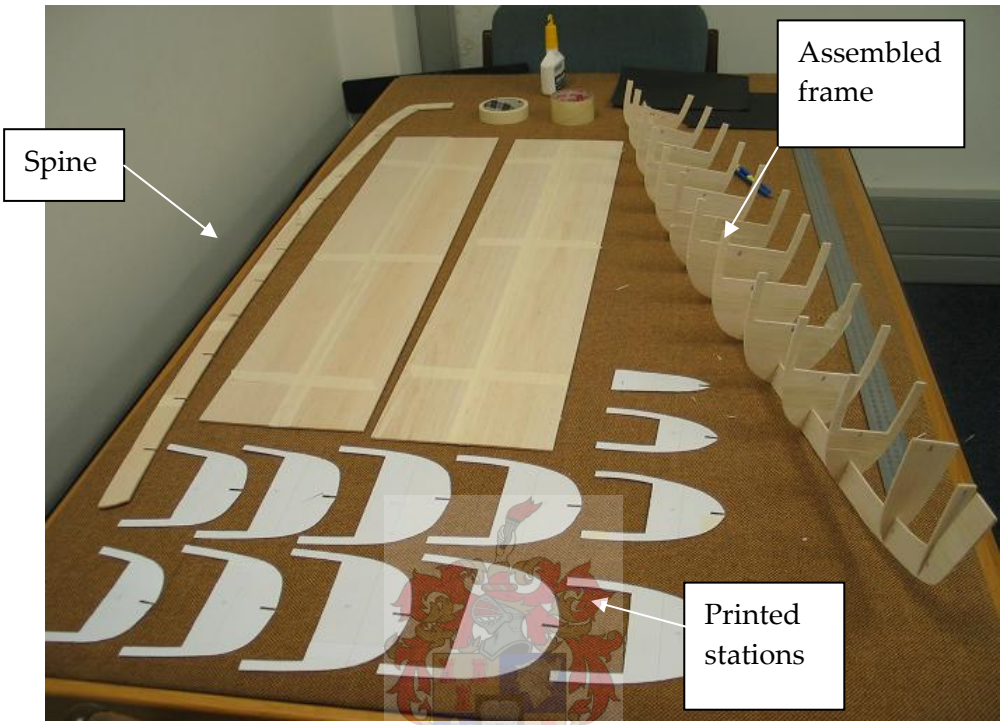

Figure E.1.a) Balsa sheets are cut into stations and spines and then assembled

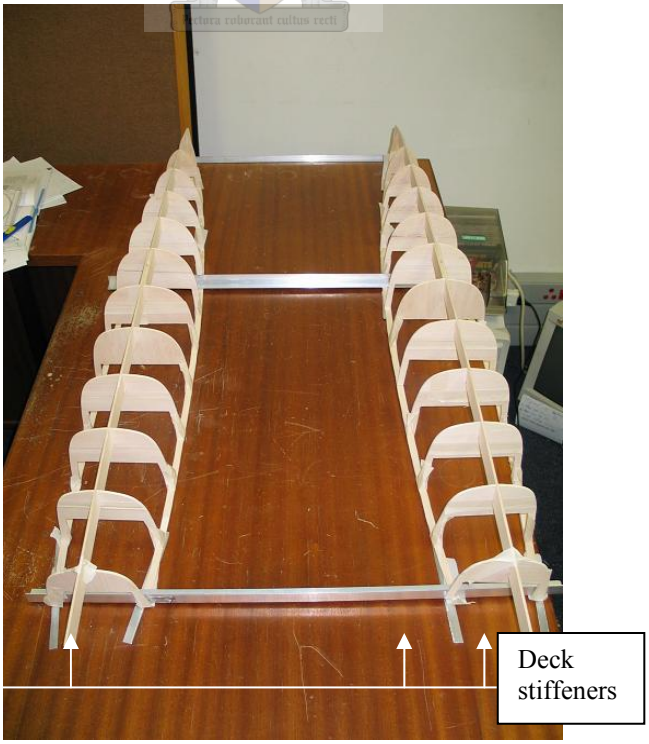

Figure E.1.b) Assembled frames of both demihulls

E.2 Assembly after demihulls are manufactured

Figure E.2 – Picture of upside-down model without rudders and daggerboards

E.3 Attachment of rudders and daggerboards

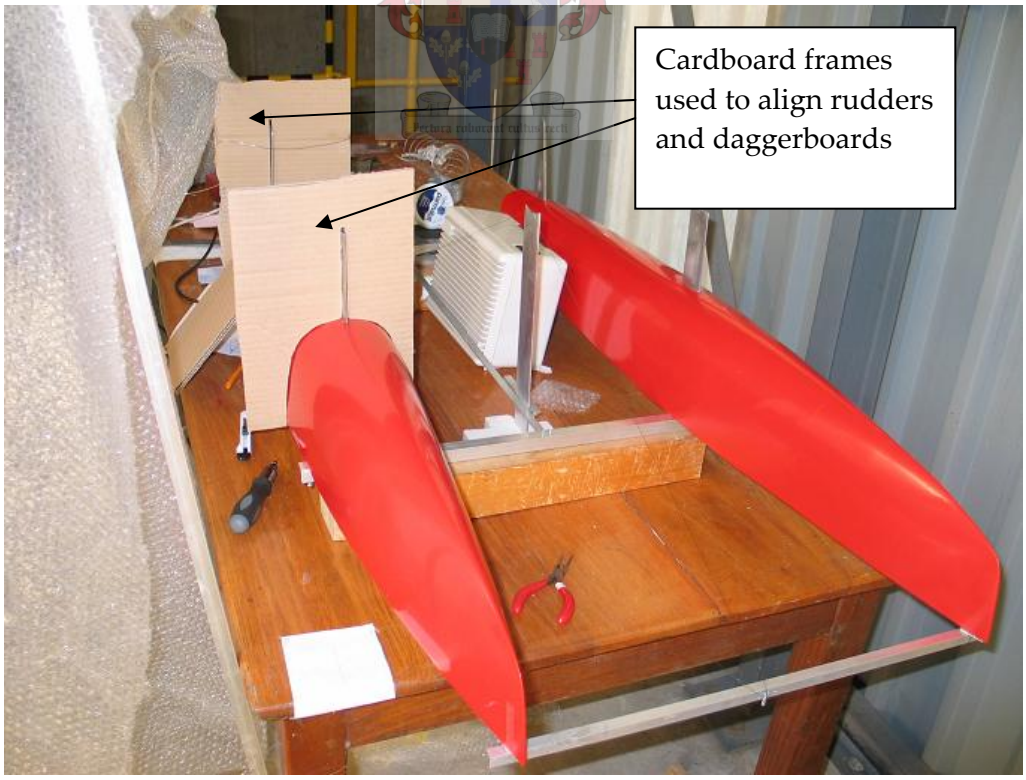

Figure E.3 – Picture of upside-down model – Gluing on of rudders and daggerboards

E.4 Initial Testing - Without Lifting Foils

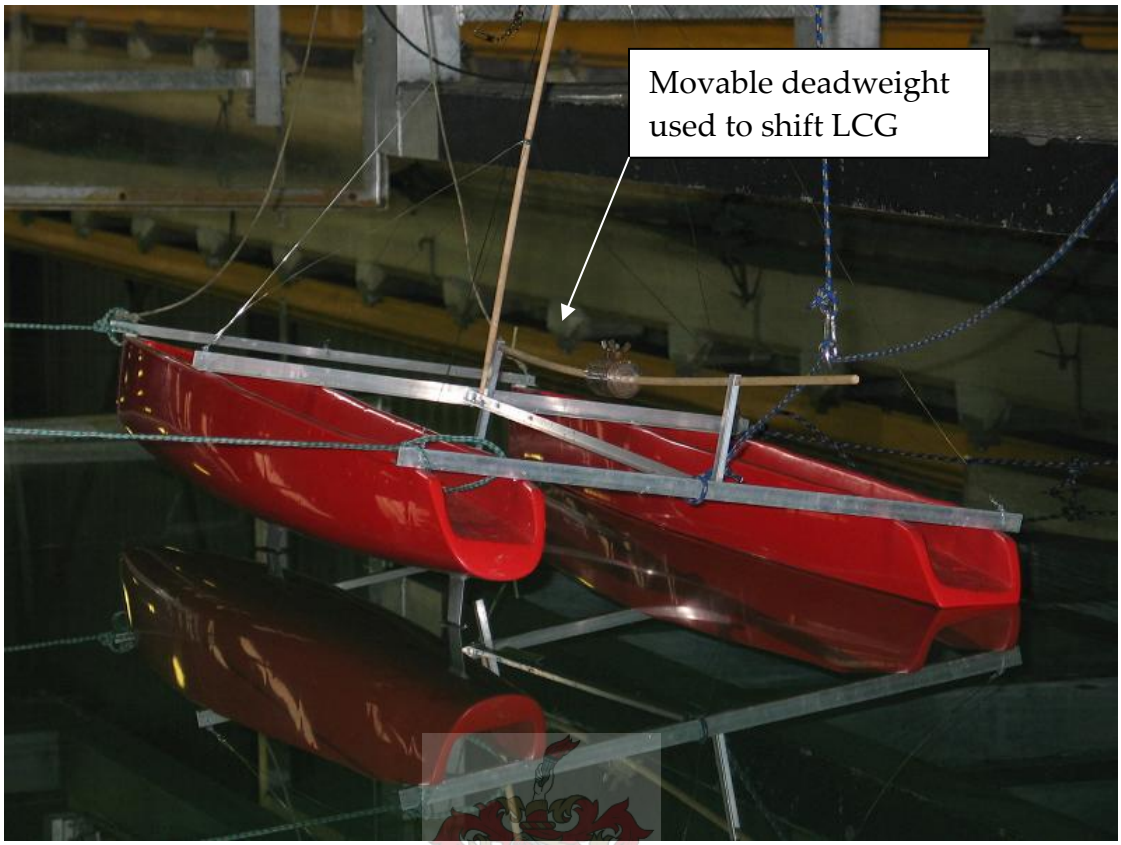

Figure E.4.a) Boat set at 10^0 heel angle

Initial model was tied in place before sidearms were manufactured. This methodology allowed too much play and was abandoned for the more rigid sidearms.

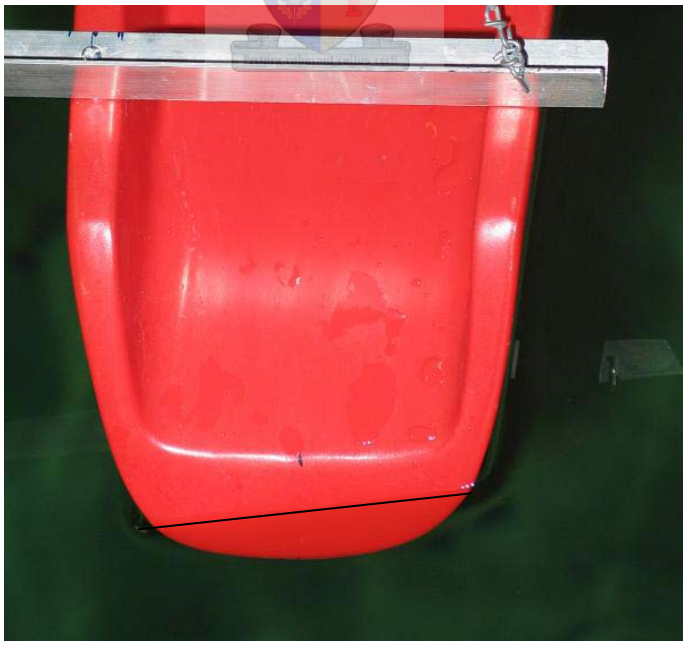

Figure E.4.b) The effect of heel on leeward demihull transom

10^0 heel angle

Figure E.4c) Wave pattern on leeward hull with 7^0 heel angle
Windward hull just emerged

E.5 Testing with Lifting Foils

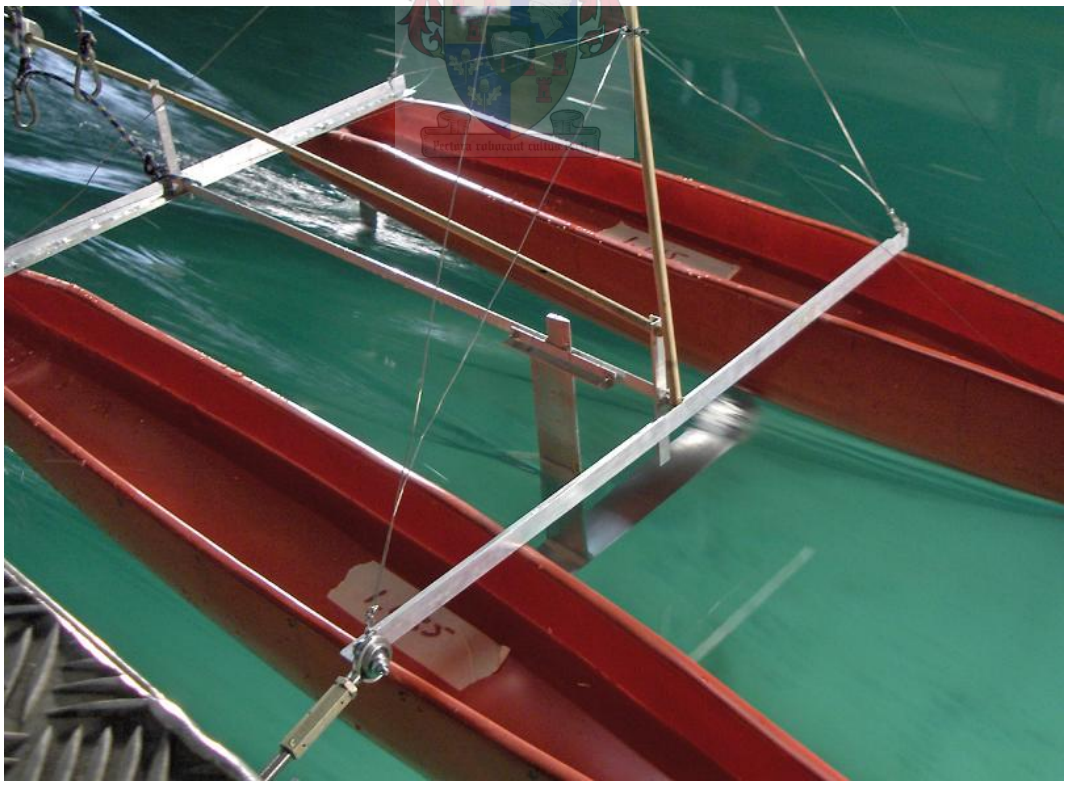

Figure E.5a) Model testing of HYSUCAT type configuration
Main foil at end of daggerboards - Model Speed 2.4 m/s
Showing wake and aft section high above water and rear foils at surface

E.6 Raising main foil to 1.5 chord lengths above the daggerboard ends.

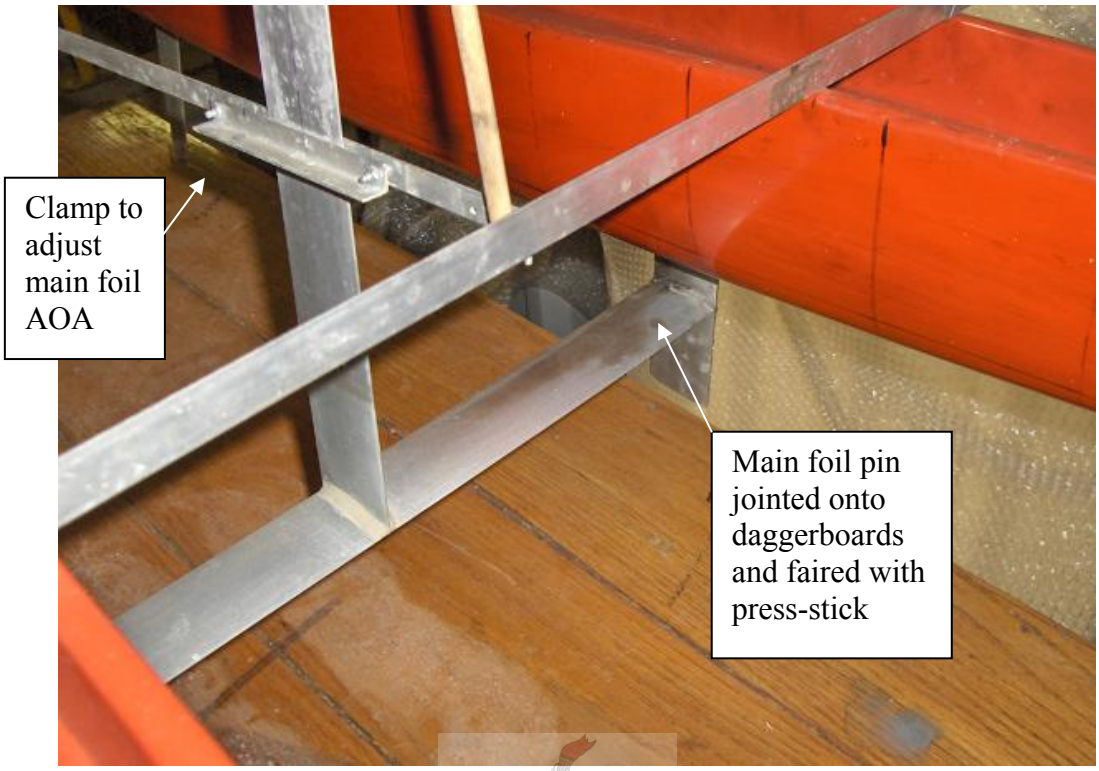

Figure E.6 a) Mounting of Main Foil

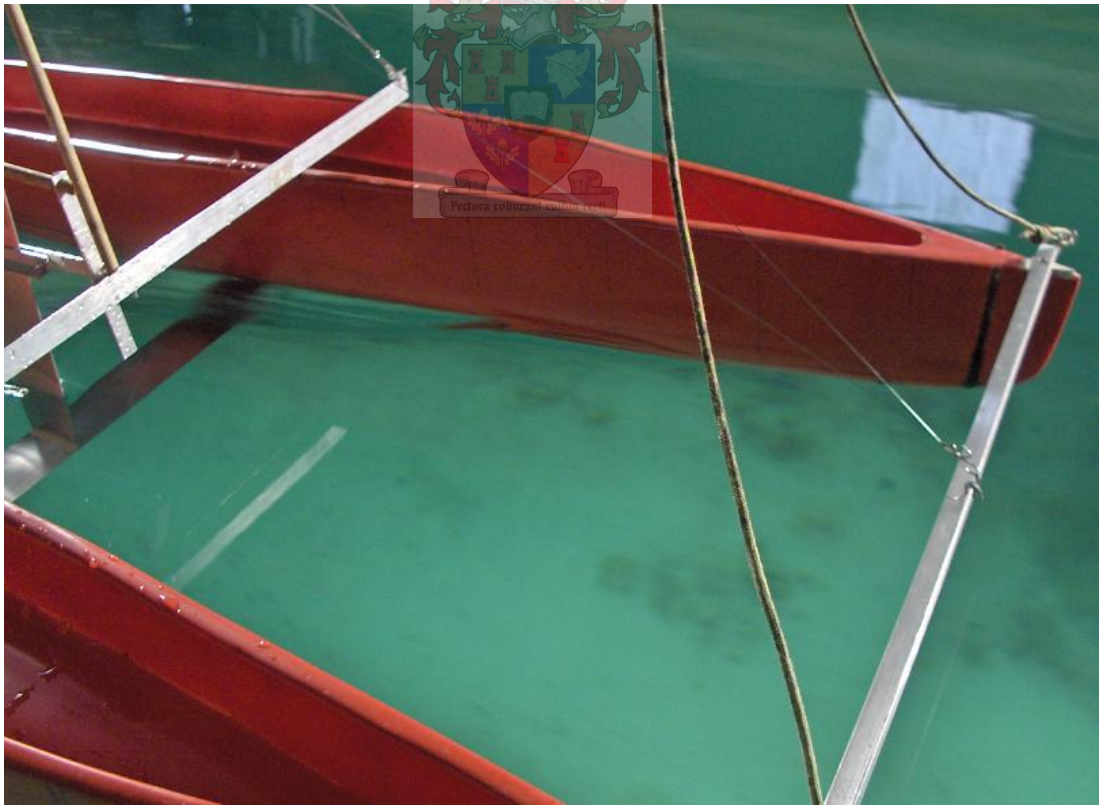

Figure E.6 b) Testing raised main foil position
Model speed 1.2 m/s (equivalent to ≈ 6 knots full scale)

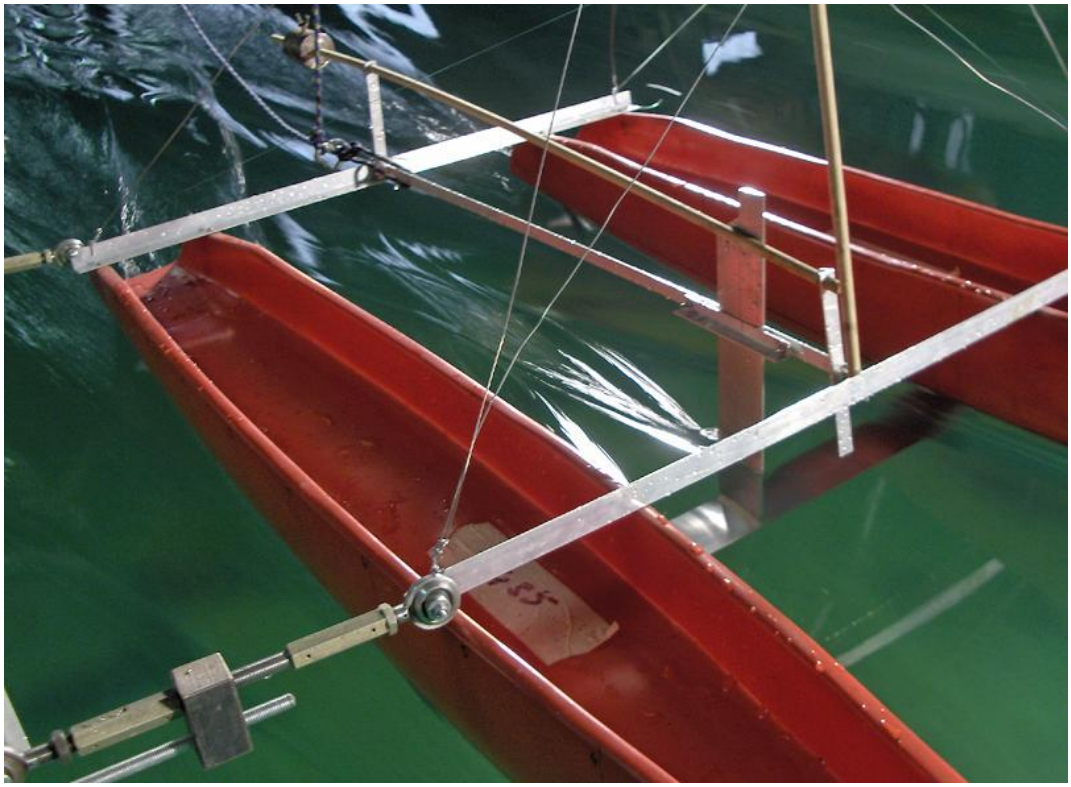

Figure E.6 c) Wake during testing of raised main foil HYSUCAT configuration
Model Speed 2 m/s
Aft sections are clear above the water

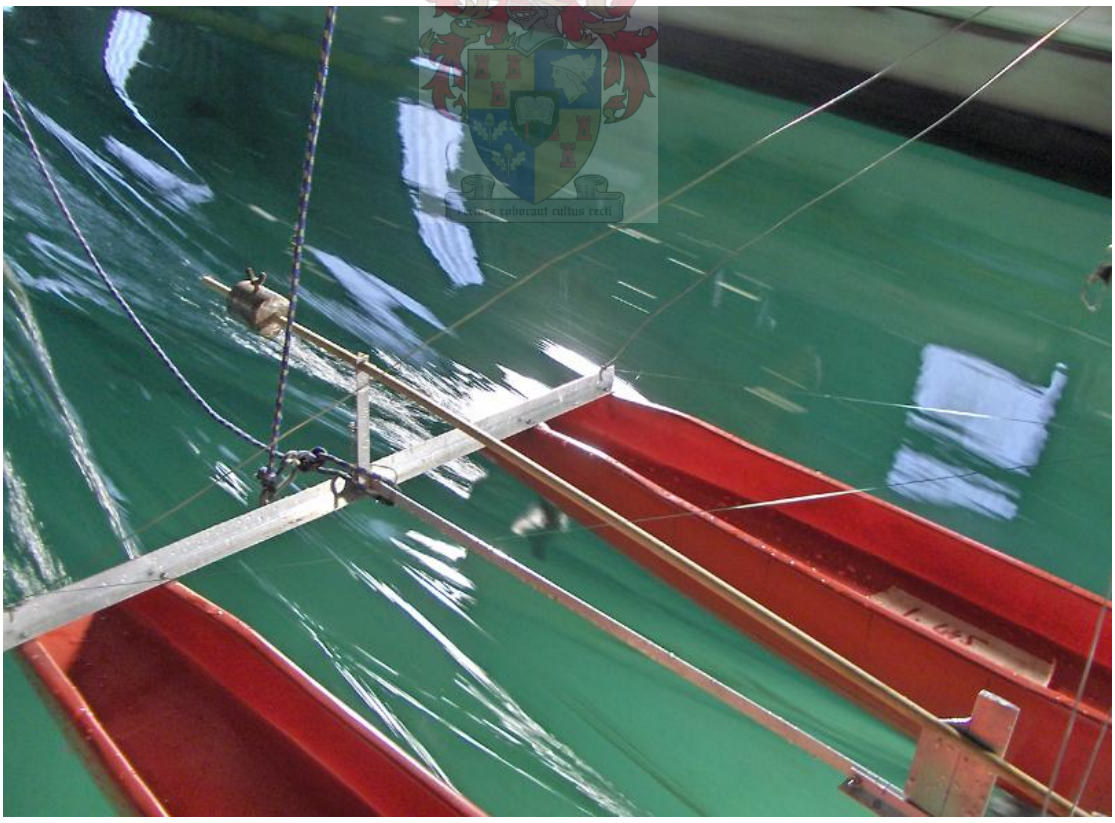

Figure E.6 d) Aft section as rear foils near the surface
Model Speed 2.4 m/s
Rear foils reach the surface at 2.6 m/s

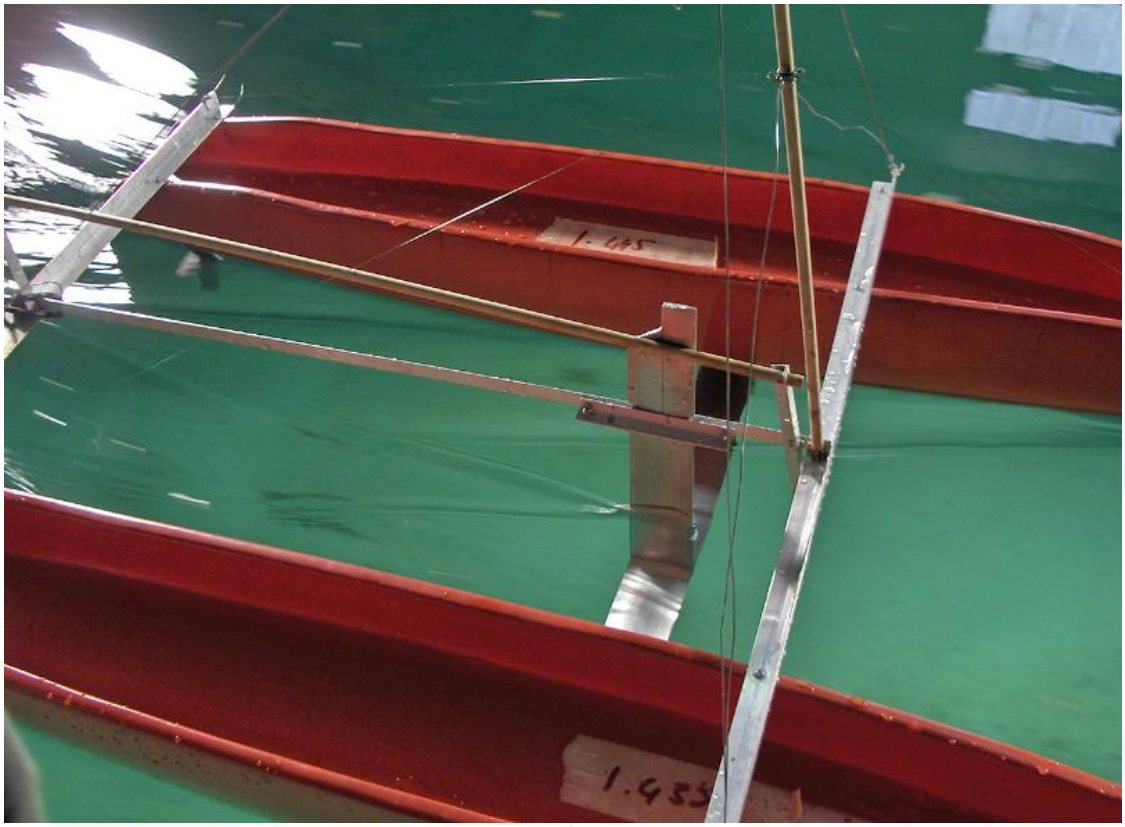

Figure E.6 e) Side view of model running below hump speed
Model Speed 2.2 m/s
Showing wake and aft section clear above water and strong wave patterns

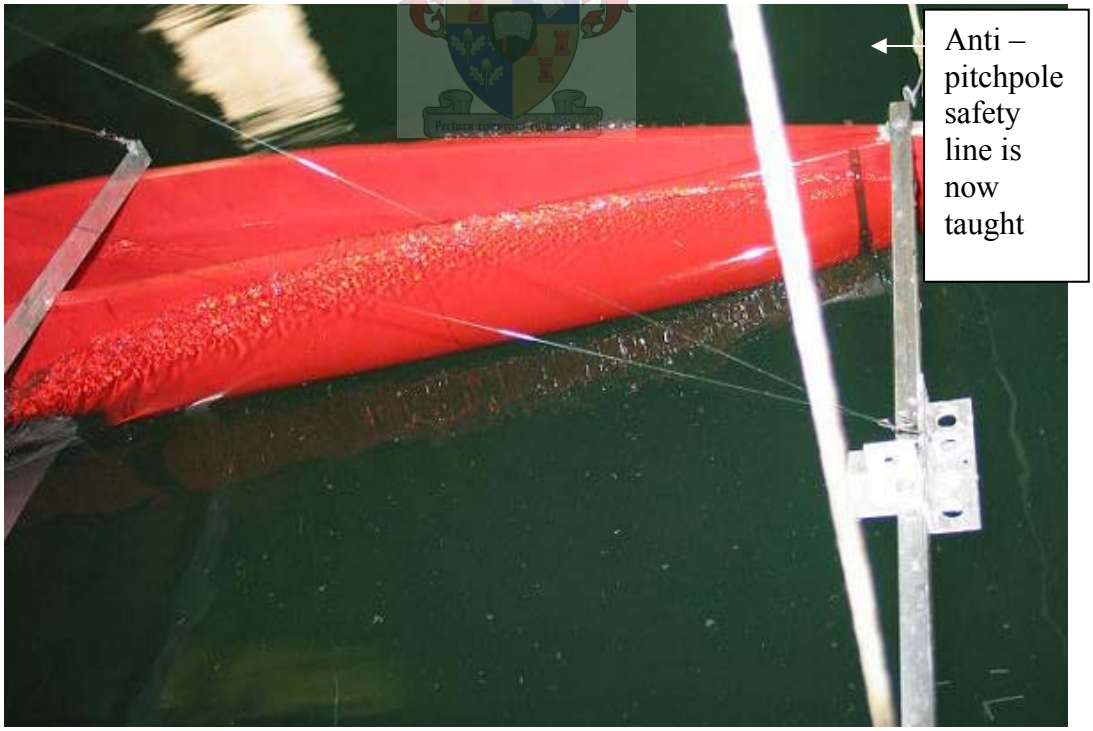

Figure E.6 f) The onset of nose dive with the HYSUCAT type configuration
Model speed 3.2 m/s
The spray begins the flood the boat and weigh down the bow.

E.7 Addition of Front (Canard) Foil

Figure E.7 a) Attachment of canard foil
Clamp system used to adjust AOA

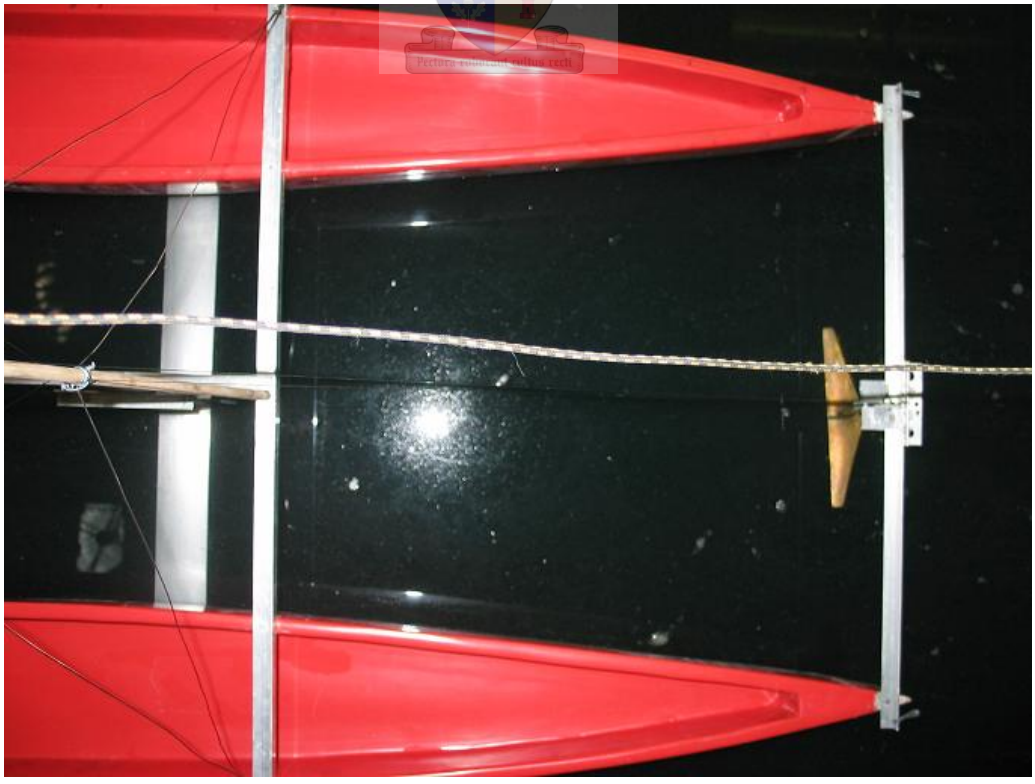

Figure E.7 b) Final foil configuration – no lifting foils on rudders

E.8 Testing the Final Foil Configuration

Figure E.8 a) Side of 'nose-up' running condition
Model Speed – 2.0 m/s (≈11 knots full scale)

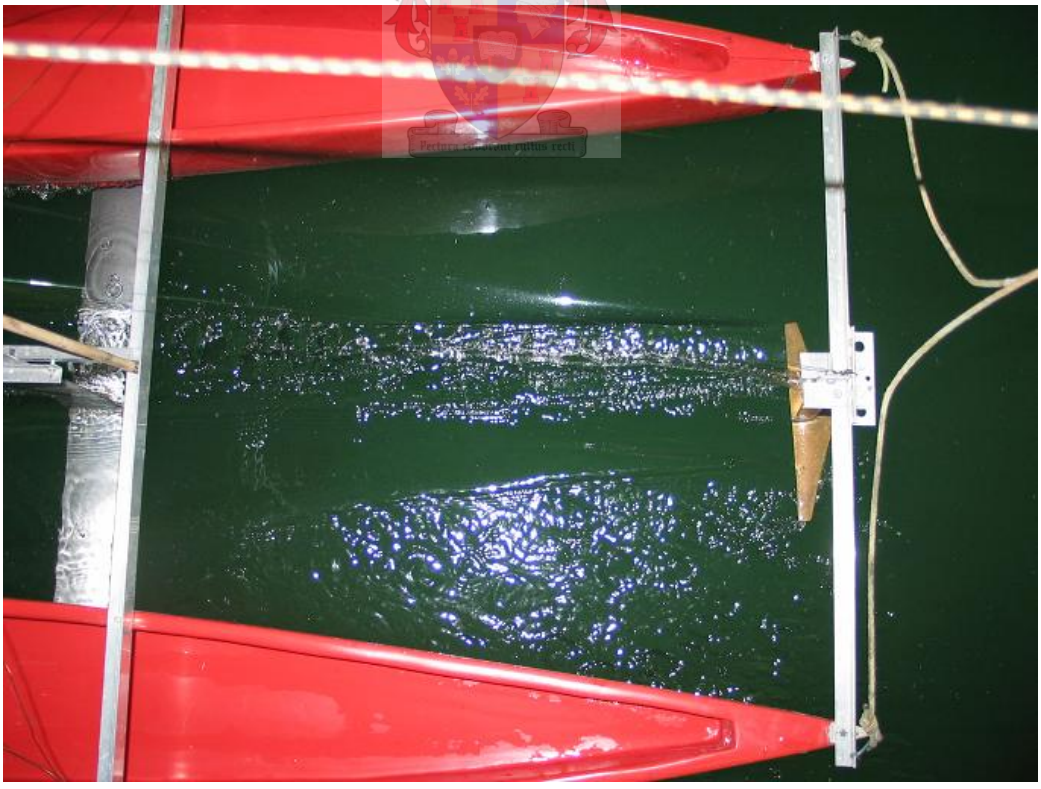

Figure E.8 b) Top view of 'nose-up' running condition
Model Speed – 2.6 m/s (≈14 knots full scale)
Strong ventilation and spray on Canard

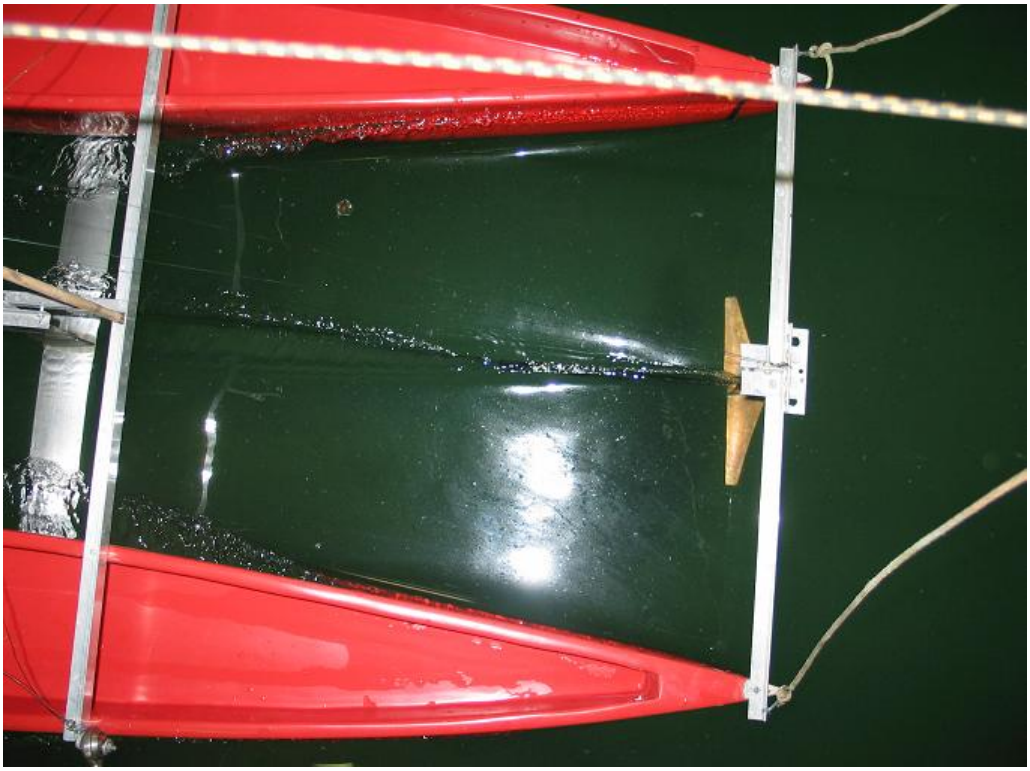

Figure E.8 c) Top view of 'nose-down' running condition.
Model Speed – 3.5 m/s (≈19 knots full scale)
Canard returns to surface after tweaking and drag is reduced

Figure E.8 d) Side view of nose down running condition
Model Speed – 3.5 m/s (≈19 knots full scale)
Close to pitchpole at similar speed to without lifting foils

F

Foil dimensions at model scale (not drawn to scale)

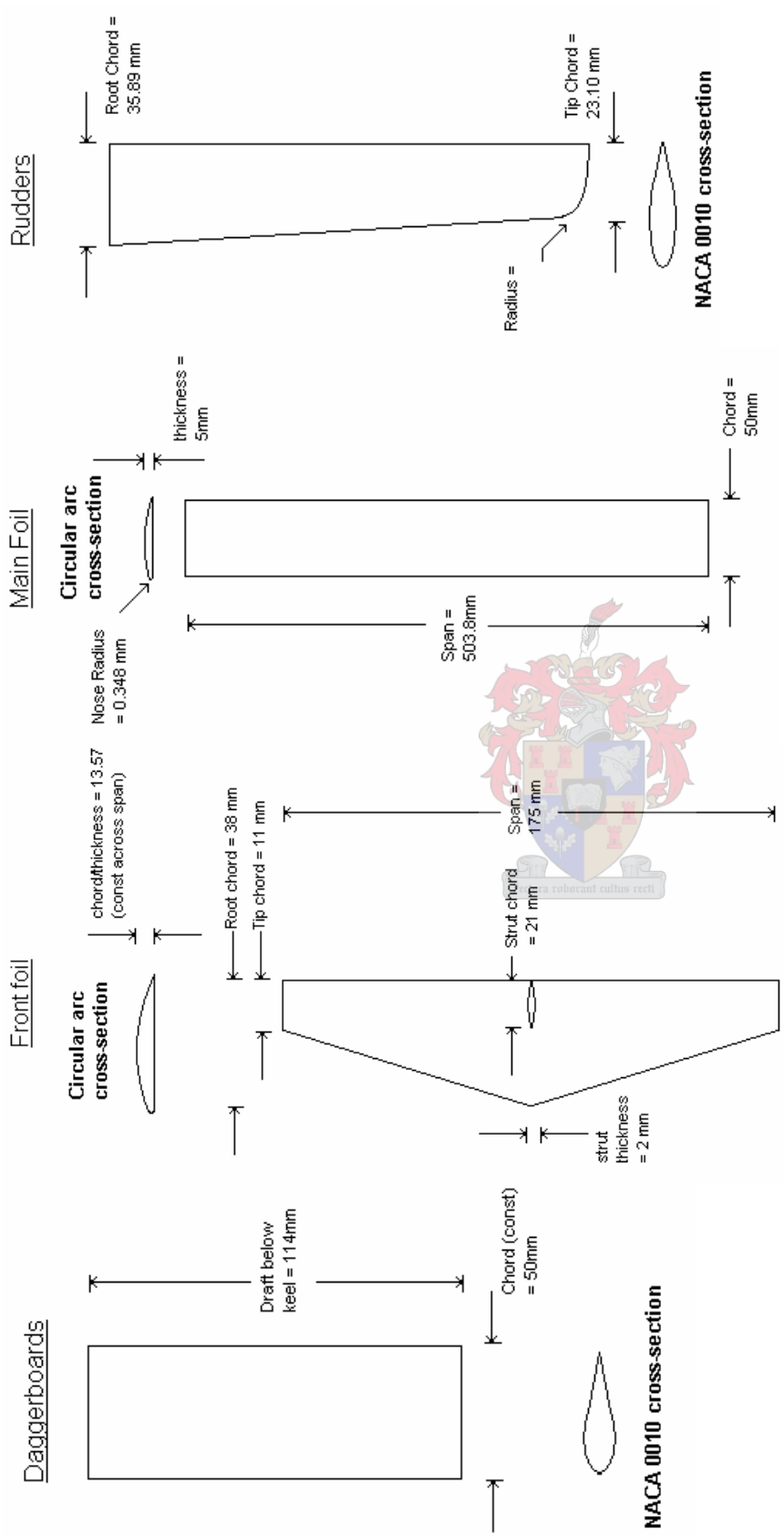

G

Summary of Hydrostatic Tests

In order to gain some initial insight into the behaviour of the model, hydrostatic tests were conducted in a program named MAXSURF. The hull shape of RH1 was generated in this program and then manipulated, varying Longitudinal Centre of Buoyancy (LCB) and Transverse Centre of Buoyancy (TCB) by adjusting the trim and heel respectively, and then correlating the trim and heel against their respective Centres of Buoyancy. The buoyancy created by the foils was ignored and for the final model, the rudders and daggerboards contributed an estimated 1.3% while the lifting foils contributed an estimated 2.2%, therefore their effect was deemed negligible.

Firstly the hull was trimmed to have zero degrees of heel. The waterline was then adjusted until the displacement was correct. The results for these were then extracted and plotted. It was observed that the boat runs flat (0 trim) when LCB is 48%L from stern. At 1 degree trim the LCB = 43%L and the transom is on the waterline. At 1.6 degrees trim the LCB is 40% and the transom is slightly below the waterline. See figure G.1 below.

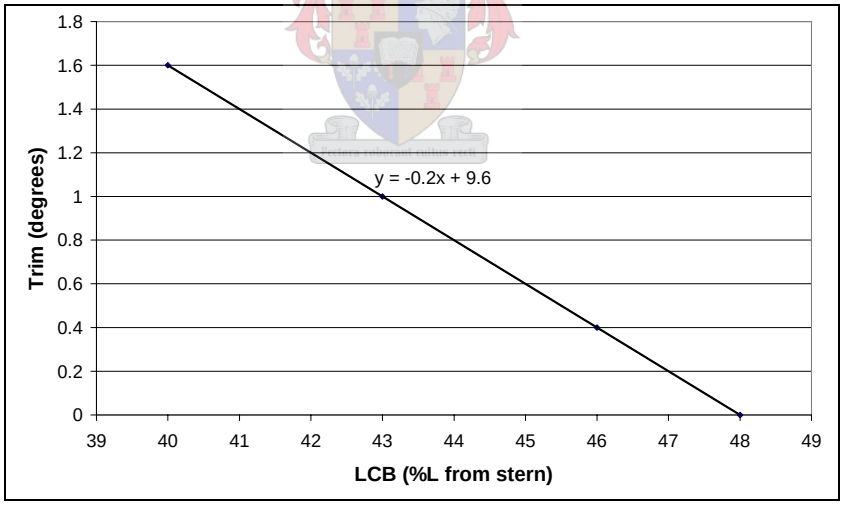

Figure G.1 - Graph of trim versus LCB with no heel

A sailing boat will inevitably have some heel (due to the sideward component to force on sails) and so the leeward hull would sit lower in the water. It is important for low speed applications that the transom is not too far below the surface as this would cause large amounts of recirculation flow with the associated turbulent wake and wave making drag. (As discussed in chapter 2.1.8)

It was therefore decided that a desirable range of LCB for RH1 is between 48% and 43% for low speed applications and the boat trim could be increased with increasing speed as a result of the lifting foil system. This however can't be too severe else it may cause an unstable imbalance of dynamic forces resulting in porpoising.

The effect of heel was then investigated and the shift in TCG (Transverse Centre of Gravity) was observed. A certain amount of trim is expected for most running conditions. For this reason, a moderate trim with LCB of 46%L was used for the assessment of the effect of heel. At about 6 degrees of heel, the windward hull is lifted from water and the TCG shifts almost onto the centreline of the leeward hull. The curve showing how the TCG changes with heel is included in the spread sheet of results. See figure G.2. Although not investigated, the heel is expected to affect trim with fixed COG. As the boat heels, the leeward hull will sink further into the water. Since the bow is finer than the stern, the nose is expected to trim down so as to maintain equilibrium.

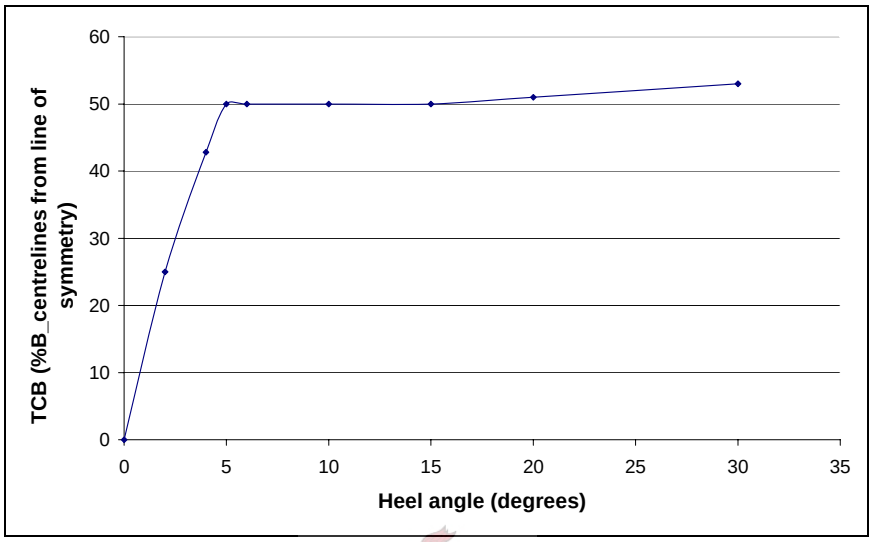

Figure G.2 - Graph of TCB versus heel with 1 degree trim.

Since the WSA affects the viscous drag, the change in WSA was graphed to show the effects of heel and trim. The graphs are shown below. The effect of trim on WSA was small, as to be expected, but it was interesting to note that the WSA reached a maximum around LCB = 43%. Remembering that the thrust force is elevated, creating a bow down pitching moment, the LCB would shift forward during running. Since the effect of the bow wave may offset the WSA result, the wave making resistance is also affected by trim and the difference in WSA with trim is so small, it was decided to set the LCG experimentally.

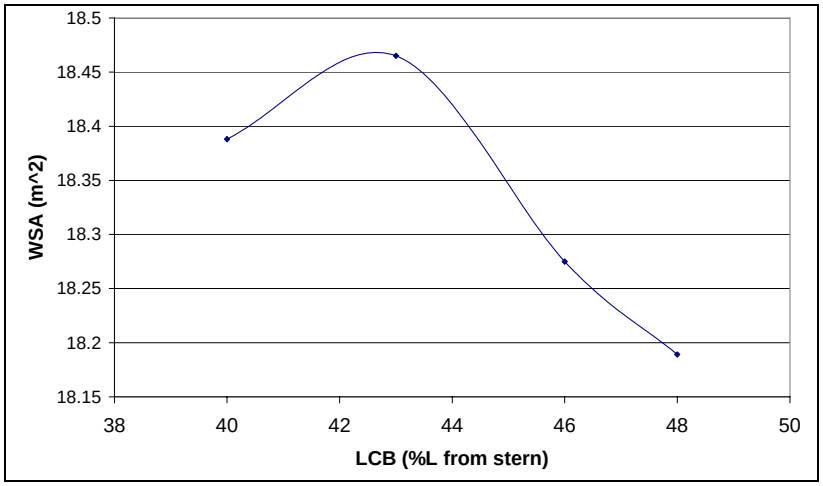

Figure G.3 - Graph of WSA versus LCB with no heel

The affect of heel on WSA was a lot more significant and the WSA drops by nearly 30%. This explains why the optimal heel angle for most sailing catamarans in moderate wind conditions is when the windward hull is just out of the water. Beyond that heel angle (in the case of RH1 – 6.5^0) the WSA remains nearly constant while the instability and unbalance arm increase. (See section 1.3)

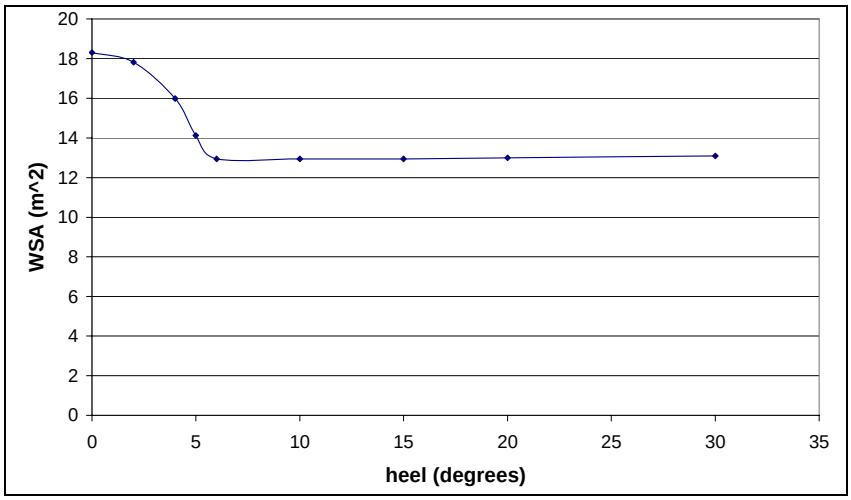

Figure G.4 - Graph of WSA versus heel angle with 1 degree trim

H

Total lifts and drags at various speeds for both rudders and daggerboards

From balancing moments, the maximum stable side force is around 15N – forces above this are highlighted.

	Lift force at various speeds				
Alpha	**Speeds**	1.2	2.4	3.6	4
0		0	0	0	0
0.5		0.53788886	2.151555	4.841	5.976543
1		1.07577772	4.303111	9.681999	11.95309
1.5		1.61366658	6.454666	14.523	17.92963
2		2.15155543	8.606222	19.364	23.90617
2.5		2.68944429	10.75778	24.205	29.88271
3		3.22733315	12.90933	29.046	35.85926
3.5		3.76522201	15.06089	33.887	41.8358
4		4.30311087	17.21244	38.728	47.81234
4.5		4.84099973	19.364	43.569	53.78889
5		5.37888859	21.51555	48.41	59.76543
5.5		5.91677745	23.66711	53.251	65.74197

	Induced Drag force at various speeds			
Speeds	1.2	2.4	3.6	4
0	0	0	0	0
0	0.00102719	0.004109	0.009245	0.011413
0	0.00410876	0.016435	0.036979	0.045653
0	0.00924472	0.036979	0.083202	0.102719
0	0.01643506	0.06574	0.147915	0.182612
0	0.02567977	0.102719	0.231118	0.285331
0	0.03697887	0.147915	0.33281	0.410876
0	0.05033236	0.201329	0.452991	0.559248
0	0.06574022	0.262961	0.591662	0.730447
0	0.08320247	0.33281	0.748822	0.924472
0	0.1027191	0.410876	0.924472	1.141323
0	0.12429011	0.49716	1.118611	1.381001

Summary of Viscous and Profile drag on foils (Full scale)

Speed	**3.33**	**6.803**	**10.323**
rudders and daggerboards	0.022642821	0.094502438	0.217597512
lifting foils	0.042924243	0.1791493	0.412501971
struts	0.007373147	0.030772683	0.070855943
lifting plus struts	0.05029739	0.209921983	0.483357914
Total (kN)	0.072940211	0.304424421	0.70095543

Summary of Viscous and Profile drag on foils (Model scale)

Speed	**1.134506265**	**2.317731567**	**3.5169694**
rudders and daggerboards	0.176978102	0.491844635	0.8482992
lifting foils	3.11E-01	0.492963882	0.7002794
struts	5.64E-02	0	0
Total (N)	0.54447048	0.984808517	1.54858

All of the above were calculated using equations 3.13 -> 3.16.

I

Note: The offset matrix of the two demi-hulls is displayed at the end of the input file as this provides a more compact and easily read document.

```
========================================================================
                          MICHLET version 6
                               INPUT FILE
========================================================================
Note 1: RH1 Hull
Note 2: Used: full scale dims LOA = 11.2 but WLL = 9.62 alt 8.83
Note 3: Without lifting foils
Note 4:
Note 5:
========================================================================
Course Particulars (0=None)
0
Number of Hulls (1, 2,..., 5)
2
Gravitational Acceleration (m/sec/sec) (min 9.6, max 9.9)
9.81
Water Density (kg/cubic metre) (min 995.0, max 1030.0)
1025.9
Water Kin. Viscosity (sq. m/sec * 10^-6) (min 0.8, max 1.31)
1.18831
Water Depth (metres) (max=10000.0)
10000.0
Sea State (0=Calm)
0
Ship Motion Method (0=None)
0
Minimum Speed (m/sec) (min 0.01, max 39.9)
3.33
Maximum Speed (m/sec) (max 40.0) excl top speed for now - not even step
11.10596
Number of Speeds (min 2, max 50) test last 2 speeds together
6
Leeway Parameters (0=None)
0
Wave Drag Method (0=None, 1,ntheta=Michell, 2,ntheta,Re=Michell+BL)
1,360
Skin Friction Method (0=None, 1=ITTC1957)
1
Form Factor Type (0=None, 1=Holtrop, 2=Scragg)
0
Transom Condition (0=Wet, 1=Dry, 2,Ftcrit=Simple Finite Hollow)
2,4.14
Added Resistance Method (0=None)
0
Pressure Signature Method (0=None)
0
Number of Offset Stations (rows) (odd integer: min 5, max 81)
21
Number of Offset Waterlines (columns) (odd integer: min 5, max 41)
21
Sectorial Wave Elevation Patch Parameters (R0,R1,Beta,Nr,Nbeta)
10.0,40.0,22.5,100,100
Rectangular Wave Elevation Patch Parameters (x0,x1,y0,y1,Nx,Ny)
```

```
10.0,40.0,-15.0,15.0,100,100
============================ FIRST HULL ==============================
Offsets
(Shown at end)
Displacement Volume (cubic metres) 2600/1025.9
1.267
Length (metres)
9.62
Draft (metres)
0.3
Longitudinal Separation (metres) (0.0 for a monohull)
0.0
Lateral Separation Distance (metres) (0.0 for a monohull)
0.0
Loading Particulars (0=None)
0
Trim (0=None, 2=Exp)
2,1.18,1.89,1.63,1.23,0.45,-0.69
Sink (0=None, 2=Exp)
2,-0.06,0.01,-0.05,-0.02,-0.06,0.14
Heel (0=None)
0
Appendages (0=None)
0
Other Particulars (0=None)
0
============================ SECOND HULL =============================
Offsets
(Shown at end)
Displacement Volume (cubic metres) 2600/1025
1.267
Length (metres)
9.62
Draft (metres)
0.3
Longitudinal Separation (metres) (0.0 for a monohull)
0.0
Lateral Separation Distance (metres) (0.0 for a monohull)
4.34
Loading Particulars (0=None)
0
Trim (0=None, 2=Exp)
2,1.18,1.89,1.63,1.23,0.45,-0.69
Sink (0=None, 2=Exp)
2,-0.06,0.01,-0.05,-0.02,-0.06,0.14
Heel (0=None)
0
Appendages (0=None)
0
Other Particulars (0=None)
0
```

Offsets

0.00000, 0.00000, 0.00000, 0.00000, 0.00000, 0.00000, 0.00000, 0.00000, 0.00000, 0.00000, 0.00000, 0.00000, 0.00000, 0.00000, 0.00000, 0.00000, 0.00000, 0.00000, 0.00000, 0.00000
0.00000, 0.00000, 0.00000, 0.00000, 0.00000, 0.00000, 0.00000, 0.00000, 0.00000, 0.00000, 0.00000, 0.00000, 0.00000, 0.00000, 0.00000, 0.01000, 0.02550, 0.04300, 0.06100, 0.07600, 0.08900
0.00000, 0.00000, 0.00000, 0.00000, 0.00000, 0.00000, 0.00000, 0.00000, 0.00000, 0.00000, 0.00000, 0.00028, 0.02440, 0.04900, 0.07300, 0.09380, 0.11300, 0.12900, 0.14200, 0.15400, 0.16500
0.00000, 0.00000, 0.00000, 0.00000, 0.00000, 0.00000, 0.00000, 0.00000, 0.00000, 0.00838, 0.02794, 0.06500, 0.10820, 0.13500, 0.15500, 0.17150, 0.18700, 0.20000, 0.21200, 0.22300, 0.23200
0.00000, 0.00000, 0.00000, 0.00000, 0.00000, 0.00000, 0.01541, 0.05160, 0.08480, 0.11450, 0.14300, 0.16700, 0.19000, 0.20800, 0.22500, 0.23800, 0.25200, 0.26400, 0.27500, 0.28500, 0.29300
0.00000, 0.00000, 0.00000, 0.00000, 0.02535, 0.06635, 0.10450, 0.13870, 0.16900, 0.19530, 0.22110, 0.24120, 0.25960, 0.27410, 0.28760, 0.29950, 0.31090, 0.32200, 0.33230, 0.34170, 0.34870
0.00000, 0.00000, 0.01589, 0.06290, 0.10941, 0.14929, 0.18534, 0.21593, 0.24279, 0.26601, 0.28633, 0.30449, 0.32011, 0.33098, 0.34274, 0.35469, 0.36411, 0.37389, 0.38460, 0.39224, 0.40059
0.00000, 0.02764, 0.08393, 0.13060, 0.17900, 0.21678, 0.24963, 0.27783, 0.30170, 0.32223, 0.33830, 0.35405, 0.36765, 0.37883, 0.39018, 0.40254, 0.41125, 0.42079, 0.43065, 0.43775, 0.44580
0.00029, 0.06902, 0.12979, 0.17929, 0.22525, 0.26308, 0.29399, 0.32074, 0.34294, 0.36186, 0.37690, 0.39116, 0.40365, 0.41651, 0.42806, 0.43966, 0.44924, 0.45934, 0.46735, 0.47553, 0.48351
0.00087, 0.07957, 0.14604, 0.20351, 0.24805, 0.28798, 0.31933, 0.34595, 0.36803, 0.38660, 0.40274, 0.41654, 0.42858, 0.44319, 0.45523, 0.46530, 0.47669, 0.48741, 0.49428, 0.50425, 0.51235
0.00000, 0.05079, 0.12965, 0.19783, 0.24861, 0.29156, 0.32662, 0.35523, 0.37884, 0.39848, 0.41647, 0.43092, 0.44332, 0.45868, 0.47106, 0.48047, 0.49338, 0.50335, 0.51147, 0.52257, 0.53093
0.00000, 0.00000, 0.07282, 0.15614, 0.22341, 0.27394, 0.31707, 0.35019, 0.37718, 0.39948, 0.41869, 0.43506, 0.44876, 0.46344, 0.47567, 0.48620, 0.49914, 0.50841, 0.51892, 0.52924, 0.53788
0.00000, 0.00000, 0.00000, 0.00000, 0.16595, 0.23546, 0.29044, 0.33159, 0.36418, 0.39058, 0.41101, 0.42974, 0.44578, 0.45804, 0.47106, 0.48352, 0.49461, 0.50498, 0.51720, 0.52511, 0.53401
0.00000, 0.00000, 0.00000, 0.00000, 0.06416, 0.17134, 0.24193, 0.29817, 0.33934, 0.37090, 0.39584, 0.41572, 0.43523, 0.44640, 0.45985, 0.47344, 0.48335, 0.49540, 0.50761, 0.51382, 0.52288
0.00000, 0.00000, 0.00000, 0.00000, 0.00000, 0.03971, 0.15479, 0.23346, 0.29130, 0.33354, 0.36770, 0.39309, 0.41474, 0.43131, 0.44480, 0.45689, 0.46915, 0.48077, 0.49149, 0.49917, 0.50821
0.00000, 0.00000, 0.00000, 0.00000, 0.00000, 0.00000, 0.00000, 0.10114, 0.19604, 0.26398, 0.31250, 0.34952, 0.37631, 0.40185, 0.42061, 0.43452, 0.44941, 0.46048, 0.47020, 0.48173, 0.49091
0.00000, 0.00000, 0.00000, 0.00000, 0.00000, 0.00000, 0.00000, 0.00000, 0.00000, 0.10276, 0.19267, 0.25931, 0.30638, 0.34190, 0.37225, 0.39629, 0.41401, 0.42910, 0.44243, 0.45431, 0.46501
0.00000, 0.00000, 0.00000, 0.00000, 0.00000, 0.00000, 0.00000, 0.00000, 0.00000, 0.00000, 0.00000, 0.05131, 0.15359, 0.22624, 0.27554, 0.31658, 0.34763, 0.37272, 0.39464, 0.40924, 0.42382
0.00000, 0.00000, 0.00000, 0.00000, 0.00000, 0.00000, 0.00000, 0.00000, 0.00000, 0.00000, 0.00000, 0.00000, 0.00000, 0.07328, 0.16066, 0.22369, 0.27266, 0.30835, 0.33791, 0.36073
0.00000, 0.00000, 0.00000, 0.00000, 0.00000, 0.00000, 0.00000, 0.00000, 0.00000, 0.00000, 0.00000, 0.00000, 0.00000, 0.00000, 0.00000, 0.00000, 0.05963, 0.14867, 0.21171, 0.25721
0.00000, 0.00000, 0.00000, 0.00000, 0.00000, 0.00000, 0.00000, 0.00000, 0.00000, 0.00000, 0.00000, 0.00000, 0.00000, 0.00000, 0.00000, 0.00000, 0.00000, 0.00000, 0.00000, 0.00000

Resistance Components Section of Michlet Output File

SHIP RESISTANCE COMPONENTS (kN)

U (m/sec),	Rh ,	Rlee
3.330000,	0.000000,	0.000000
4.885192,	0.000000,	0.000000
6.440384,	0.000000,	0.000000
7.995576,	0.000000,	0.000000
9.550768,	0.000000,	0.000000
11.105960,	0.000000,	0.000000

U (m/sec),	Rf ,	Rform ,	Rv
3.330000,	0.249524,	0.000000,	0.249524
4.885192,	0.518462,	0.000000,	0.518462
6.440384,	0.828361,	0.000000,	0.828361
7.995576,	1.292706,	0.000000,	1.292706
9.550768,	1.805376,	0.000000,	1.805376
11.105960,	2.791011,	0.000000,	2.791011

U (m/sec),	Rwtrans,	Rwdiv ,	Rw
3.330000,	0.091151,	0.115373,	0.206525
4.885192,	0.498359,	0.542928,	1.041286
6.440384,	0.143538,	0.885279,	1.028818
7.995576,	0.052920,	1.160866,	1.213787
9.550768,	0.016808,	1.234469,	1.251277
11.105960,	0.014063,	2.041501,	2.055564

U (m/sec),	Rwtinter,	Rwdinter,	Rwinter
3.330000,	0.029709,	0.003827,	0.033535
4.885192,	0.198965,	-0.169397,	0.029568
6.440384,	0.066841,	-0.076048,	-0.009207
7.995576,	0.025693,	-0.064933,	-0.039240
9.550768,	0.008284,	-0.005640,	0.002644
11.105960,	0.006977,	-0.018967,	-0.011991

U (m/sec),	Rr ,	Rt
3.330000,	0.206525,	0.456048
4.885192,	1.041286,	1.559749
6.440384,	1.028818,	1.857179
7.995576,	1.213787,	2.506493
9.550768,	1.251277,	3.056653
11.105960,	2.055564,	4.846575

J

Calculating Centre of Effort (C.E.) of sails

Sail Areas

Sail	Designation	Area
Main sail	Sm	41
Jib	Sj	20
Schreecher	Ss	57
Asymetric Spinnaker	Sas	89
Total (in use)	St	(function of heading)

x =	**x coordinate of CE**
y =	**y coordinate of CE**
z =	**z coordinate of CE**
subscript denotes which sail / total	

Converting to model dims

Beating Main plus jib

St = 61

Sail	x coord	y coord	z coord
Main	5.15	0.2	5.33
Jib	9.93	0.4	4.1

xt	yt	zt	xt	yt	zt
6.717213115	0.2655738	4.92672131	0.7810713	0.03088067	0.57287457
59.9751171	4.659189	43.9885831			
%L	%B	%L			

Tight Reaching main plus schreecher

St = 98

Sail	x coord	y coord	z coord
Main	5.44	0.9	5.33
Schreecher	9.64	1.67	4.1

xt	yt	zt	xt	yt	zt
7.882857143	1.3478571	4.61459184	0.9166113	0.15672757	0.53658045
70.38265306	23.646617	41.2017128			
%L	%B	%L			

Broad Reaching main plus spinnaker

St = 130

Sail	x coord	y coord	z coord
Main	6.72	1.57	5.33
Spinnaker	8.16	1	4.3

xt	yt	zt	xt	yt	zt
7.705846154	1.1797692	4.62484615	0.8960286	0.13718247	0.53777281
68.8021978	20.697706	41.2932692			
%L	%B	%L			

Mast Position 0.58*L from transom or 0.42*L from bow

As the boat heels, the y position of the force vector will change globally however remain the same relative to the mast.
More heel will result in more of a yawing moment, as the y (global) increases with heel.

K

Sources of error

- **Model design**

The exclusion of the wet deck was considered reasonable since for most running conditions it is clear of the water level. For the higher speeds the spray in the tunnel would've been high enough to reach the wet deck and been deflected down thus creating additional lift near the front of this structure. This would cause the bows to trim up and reduce the displacement slightly while also providing additional drag due to an increase in WSA. From the experience of the student, this was considered to have minimal effect over the speed range and the 2 effects would cancel one another out to an extent. During testing it was found that significant spray was developed at the bow. This flow over the bow could have been improved in the design by including spray rails to deflect the flow down, thus providing additional lift and also reducing the WSA.

- **Model Manufacture**

While manufacturing the demi-hulls, inaccuracies may have developed as the frames lacked stiffness and may have become misaligned. To avoid this they were held in a framework). The fairing of the foam may also have resulted in slight inaccuracies. The fairness and surface roughness were considered excellent when compared to other model manufacturing techniques. The symmetry of the hulls was not perfect (although visually not apparent) and the two hulls were not identical as they were faired by hand. (Although also not visually apparent) It was in hindsight decided that a mould for both demihulls should be used in future as this would provide greater symmetry but errors in this regard are considered small as the WSA and area curves of the two demi-hulls are similar.

- **Foil Manufacture**

The accuracy of the NC cutter path, which cut the foils, is very good (within 3μm) but the deflection of the foils during machining due to vibration and the force applied by the cutter is hard to quantify. Since the foils were then sanded, errors in the shape would primarily have come from this process. The sanding was done by hand so there are undoubtedly some small inaccuracies in the shape but when comparing to a template of the cross-section, these could not be detected visually and therefore are considered negligible since scaling errors will dominate over these errors.

- **Misalignment of the demihulls**

The longitudinal positions of the crossbeams were measured from both bow and stern and the hulls were aligned by measuring the distances between the centrelines on the bows and sterns. The alignment was finally checked by measuring diagonals across the boat from bow to stern and front to rear crossbeam in both directions. Since all related measurements fell within 2 millimetres it was decided that the hulls were aligned well.

- **Misalignment of the rudders and daggerboards.**

As mentioned in Chapter 5, the rudder and daggerboards were located via pins and held in place by cardboard templates during gluing. The alignment was calculated to be within 2^0 in the vertical direction and have an angle of

attack relative to the hull of less than 0.6^0. Referring to appendix H, it was determined that this misalignment would have little effect on the drag but may influence the side forces on the hull substantially. Since this was not being modelled, this would not affect the testing.

- **Turbulent stimulators**

Due to geometry it was fairly difficult to glue the turbulent stimulators to the hull and took several attempts. This resulted in the glue layer being relatively thick (0.5 mm in places). This would result in additional form and separation drag. This could not be avoided but is considered a common factor in model testing.

- **Spray resulting from the turbulence stimulators.**

This factor was observed visually to be significant in the upper limits of the speed range being tested, and even then, was not very large. When using sand strips as turbulent stimulators, this error is unavoidable.

- **Precision of Heel and Leeway angles.**

The heel and leeway angles were set when the trolley was stationary to within a calculated 0.21 and 0.18 degrees respectively. During running however, the trim and rise of the boat would create additional errors. The maximum rise at the mast base was calculated at 64.2mm resulting in a max error in heel angle of 1.2^0 (increase) when the heel angle was set to 10^0. This was compensated for when setting the heel angle by under setting the heel angle and accounting for flex in the system. This was determined experimentally. The change in leeway angle due to variation in running conditions was measured during experimentation and adjustments were made for each speed.

- **Slight imbalance in weight distribution.**

During the static waterline tests, it was noticed that initially the weight distribution was not even as the one hull 'sat' deeper than the other. This was then adjusted and the misalignment of the COG was measured as less than 0.5% of the B_{WL}. In reality the COG will shift laterally depending on the loading condition. (Crew and fuel and water tank positioning)

- **Misalignment of side arms and tow rope.**

The tow rope and side-arms were required to have no lateral or vertical components as this would affect the drag reading. The maximum combined lateral and vertical displacements of the tow rope were measured at 30mm. This equates to a misalignment of 1.04^0 and an error of less than 0.02%. The vertical component of the side arms would affect the volumetric displacement of the hulls while the lateral component would affect the drag reading. The max lateral displacement was measured as 8mm which for that sidearm length equates to 2.0^0 while the max vertical displacement was measured at 11mm which equated to 2.7^0. The side forces were calculated theoretically in appendix H and so the maximum change in displacement was calculated as 1.7% and the maximum change in drag was calculated as 5.7%, due to the misalignment of the side-arms. This would only be of major influence during the leeway tests when the side forces on the model become significant.

- **Water on deck**

Large droplets formed on the deck of the model during testing as a result of spray when ventilation or near nose-dive occurred. This would add significantly to weight of the model and although the deck of the prototype may in reality become wet, the surface tension would not scale correctly so this would not be proportional to the prototype. In order to minimise this, all large droplets of water were removed from the deck, and fortunately the process of taking on water took place in conditions of instability, so the foil configuration was then changed until the boat

remained stable across the speed range. This stable configuration would therefore not have inaccuracies due to water on the deck.

- **Torsion of front cross-beam**

Drag on the front foil may lead to slight changes in angle of attack (AOA) of the front foil. This was measured to be within 0.3^0. During experimentation it was found that above a certain speed, the front foil rises to the surface for most sensible angles of attack (AOA) and therefore its AOA above this speed is not critical. Since it is near this speed that the drag becomes significant, causing the torsion of the front cross-beam, this will result in little change in the running conditions. Since optimisation of the foil system is not part of the scope of this research project, it was considered not essential that the front foil AOA is exact. For an optimisation project however, a more rigid cross-beam is recommended.

- **Consistency of foil roughness**

The foils were made of aluminium and were not anodised. The water in the towing tank was found to be highly corrosive due to all the chlorine based chemicals used to keep the water free of algae. As a result, both uniform and pitting corrosion were observed on the foils, in between testing. As a result, the foils were sanded lightly and polished with fine rubbing compound before each day of testing. Despite attempts to achieve the same roughness each time, this was clearly not achieved as resistance readings varied by up to 5% (all other factors made same). This made comparing results taken on different days unreliable so tests for 1 aspect (e.g. effects of leeway) were completed on in the same session)

- **Consistency in model weight**

The total weight of the model was checked throughout testing to ensure no leaks in the model resulted in inaccuracies. Table K.1 below gives a summary of all measurements taken and shows a maximum of 4.3% error in total model weight.

Date	Weight (kgs)	Comment	% over-weight
21-Jun	4.062	Done prelim tests, heel and some yaw tests without lifting foils	1.55
27-Jun	4.079	After no leeway, no heel, no lifting foils. Both dags have been re-glued. x-beam on mast included	1.975
03-Jul	4.075	After leeway, no lifting foils tests- boat left over night to dry completely	1.875
07-Jul	4.077	After second round of leeway tests.	1.925
28-Jul	4.143	Addition of front foil	3.575
02-Aug	4.156	Addition of more support to front x-beam.	3.9
07-Aug	4.162	Before leeway with foils and WSA tests.	4.05
08-Aug	4.171	After leeway and WSA tests. Boat still wet	4.275

Table K.1 – Weight of model during testing

- **Calibration and accuracy of measuring devices**

The calibration and accuracy of all devices used, except the trolley speed measurement (as explained in Chapter 5) was checked. Below is a table summarising all the errors. As can be seen from the summary, all devices used will provide suitable accuracy.

Device	Upper limit	Lower limit	Error	Calibration
Scale for weighing model	50kg	20g	1g = 0.025%	Bought on 15 April same year as testing – reading was tested against marked weights and another lab scale – corresponded to both to within less than 1%.
Load cell (measuring drag)	50kg	3N (determined from experimentation – below this, errors become significant)	20g	A mass was weighed by the above scale and used to calibrate the voltage output from the load cell. This was last conducted approximately 1 month before testing commenced.
Front and rear trim displacement sensors	532mm	0mm	0.1%	These were calibrated at the same time as the load cell.

Table K.2 – Error characteristics of measuring instruments.

L

Velocity Prediction Program

In order to model a sailing yacht completely and predict its full scale performance, a Velocity Prediction Program or VPP is required. This uses data from the hull and then predicts the boats speed for a given sailing condition.

The first input of a VPP would be the wind speed and the point of sail or angle of the wind relative to the boat. Of course, since the boat speed itself determines the angle and magnitude of the resulting flow over the sails, this will need to be iterated until convergence.

Next, fluid properties would need to be entered (although air and water are fairly constant and could be fixed for a simple code). These will help determine the aerodynamic and hydrodynamic forces and moments.

Also important would be the sail and foil geometry as this would influence the Centre of Effort (CE) on the sails and Centre of Lateral Resistance (CLR) respectively, which in turn is required for the balance of the boat.

Finally, some means of describing the hydrostatic and dynamic characteristics of the hull is needed. There are many hydrostatic programs available and codes for these can either be linked to the VPP or outputs from these programs can be entered manually into VPP. This can then help predict the balance of the boat. Alternatively more accurate results could be determined experimentally.

The hydrodynamic drag of the hull would then need to be described in terms of towing tank tests or empirical equations, the later being more convenient but less accurate and sensitive to subtle changes in the hull shape.

A suggested flow diagram for a VPP is given on the following page and a number of notes regarding its assumptions and general points follow.

VPP flow diagram

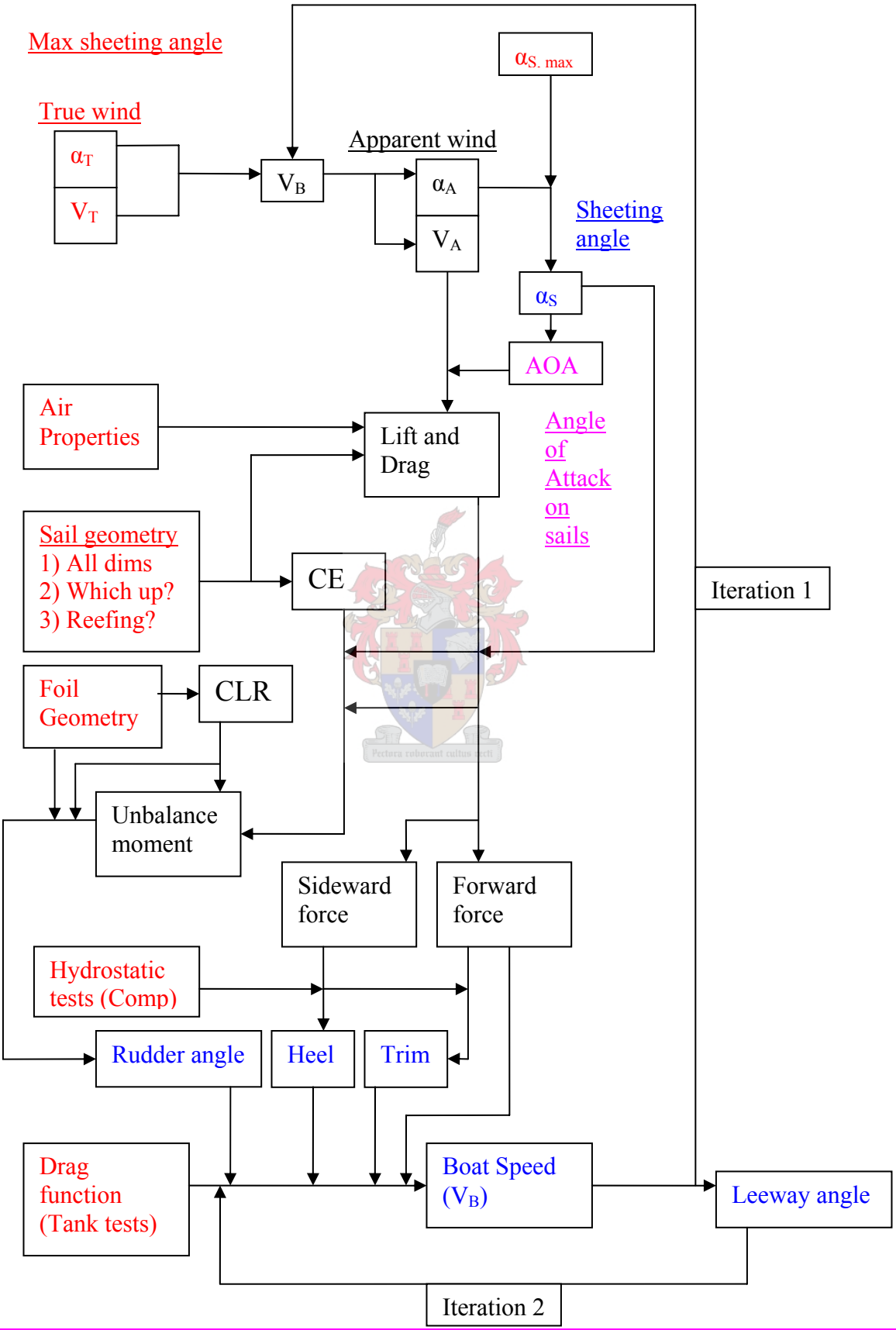

Notes

1) All inputs on left had side (in Red) and Outputs (in blue)
2) Only applicable for small rudder angles, the combination of leeway and rudder angle become non-linear near stall and so the separation of leeway angle in determining the effect of rudder angle from CLR becomes inaccurate. Since lift is linear with angle of attack the lift caused by Leeway is ignored in calculating rudder angle (balance) and the moment countering the unbalance moment is the lift caused by rudder angle multiplied by distance rudder aft of CLR.
3) The dynamic effects on heel and trim are ignored. Heel and trim are calculated from hydrostatic tests to determine the shift in COB to compensate for moments set up by forward and sideward forces. (functions required)
4) The lift and drag on the sails, in combination with apparent wind angle are used to determine the unbalance moment but the forward and sideward could be used just as easily – it was simply easier to do this diagrammatically.
5) Since the apparent wind is normally not drastically different for the true wind, after the first iteration loop has been run, a reasonable (though not accurate) leeway angle is expected. The resistance curve may be severely affected by the leeway angle so it is recommended that iteration loops are run alternatively, until convergence on leeway and velocity. There should also be convergence on heel trim and rudder angle. All of these are outputs to the system. If towing tank tests are being used, the results could be checked experimentally.
6) The sheeting angle is equal to the apparent wind angle for upwind sailing while anything broader than a broad reach result in a the sail reaching it's maximum sheeting angle and a relative Angle of Attack is formed between apparent wind and sheeting angle. This changes the lift and drag characteristics of the sail. The following if/else type loop is suggested…

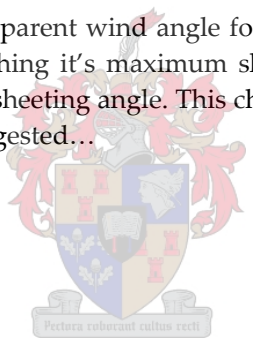

If $\alpha_A < \alpha_{S,max}$

$\alpha_S = \alpha_A$

else

$\alpha_S = \alpha_{S,max}$

end

This ensures the sheeting angle is correct. For more accuracy, the average angle of entry on the sails could be included. A fully accurate model would require analysing the sails in CFD.

7) Rudder stall angle could also be inputted and a warning on stall outputted. This is for straight line motion, if the boat is turning, the flow angle over the rudder changes, reducing AOA if heading up and increasing AOA if bearing off.

M

Initial Model Testing

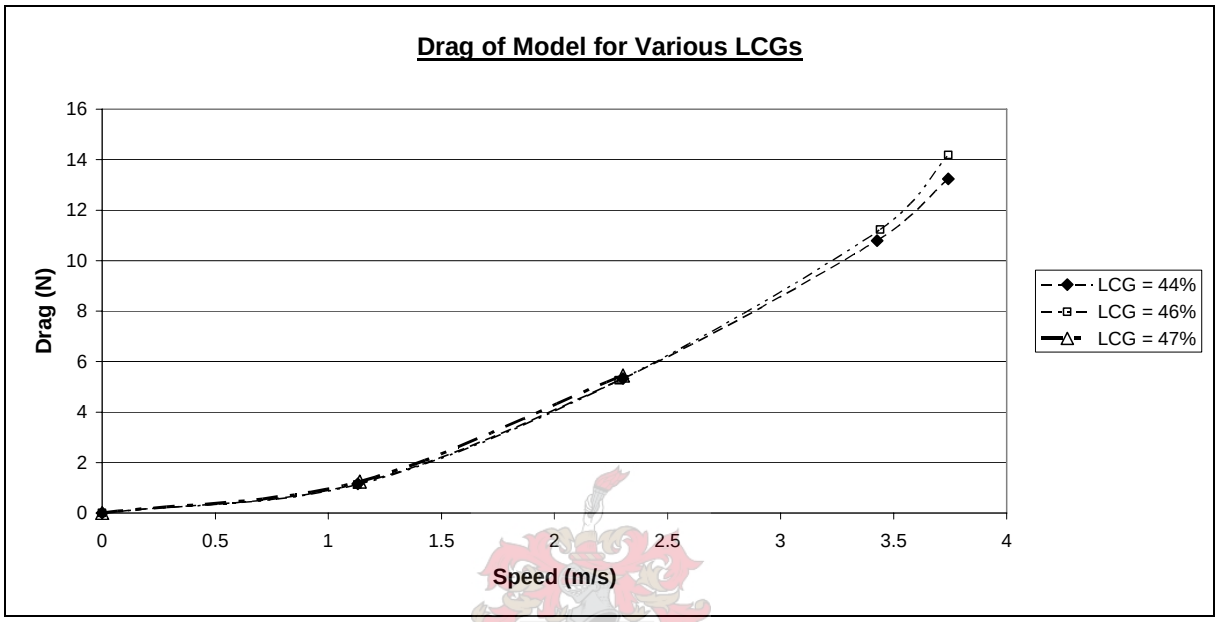

Figure M.1 – Assessing the resistance curve for various LCG's.

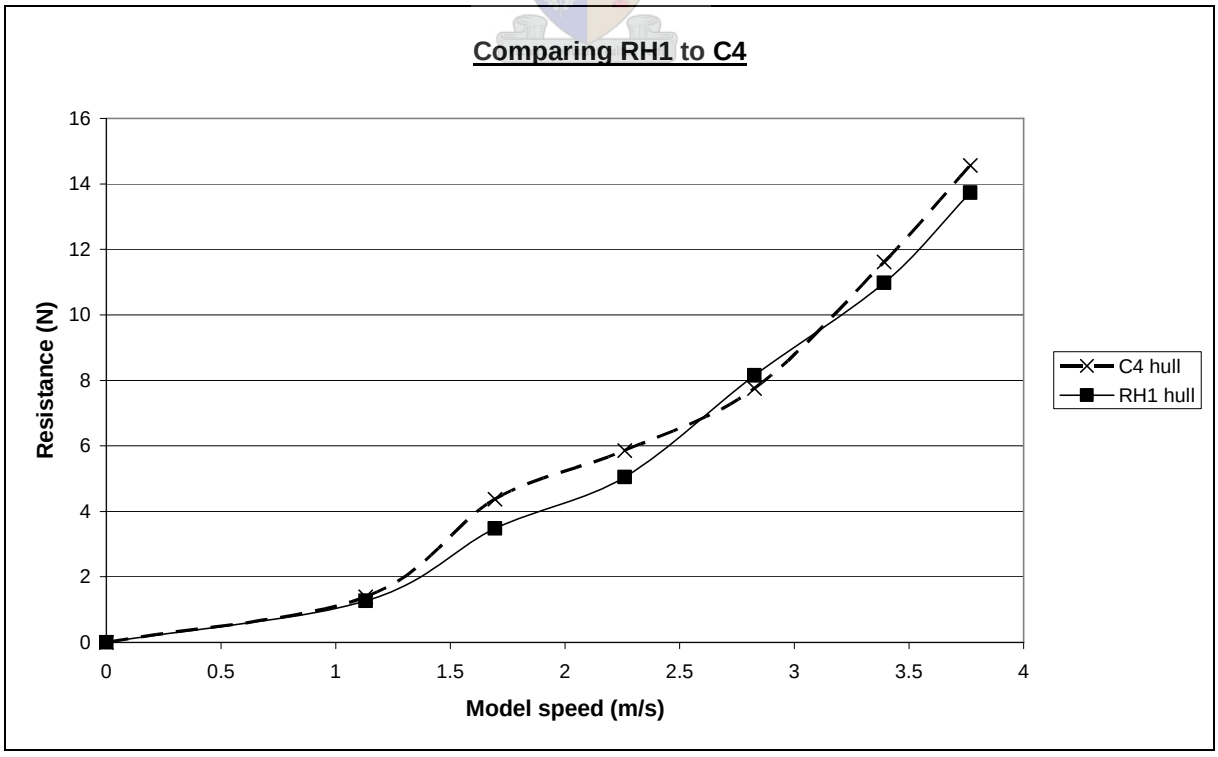

Figure M.2 – Comparing Resistance Characteristics
of C4 [IM91] to that of RH1 without lifting foils

Experimental Testing With the Addition of Hydrofoils

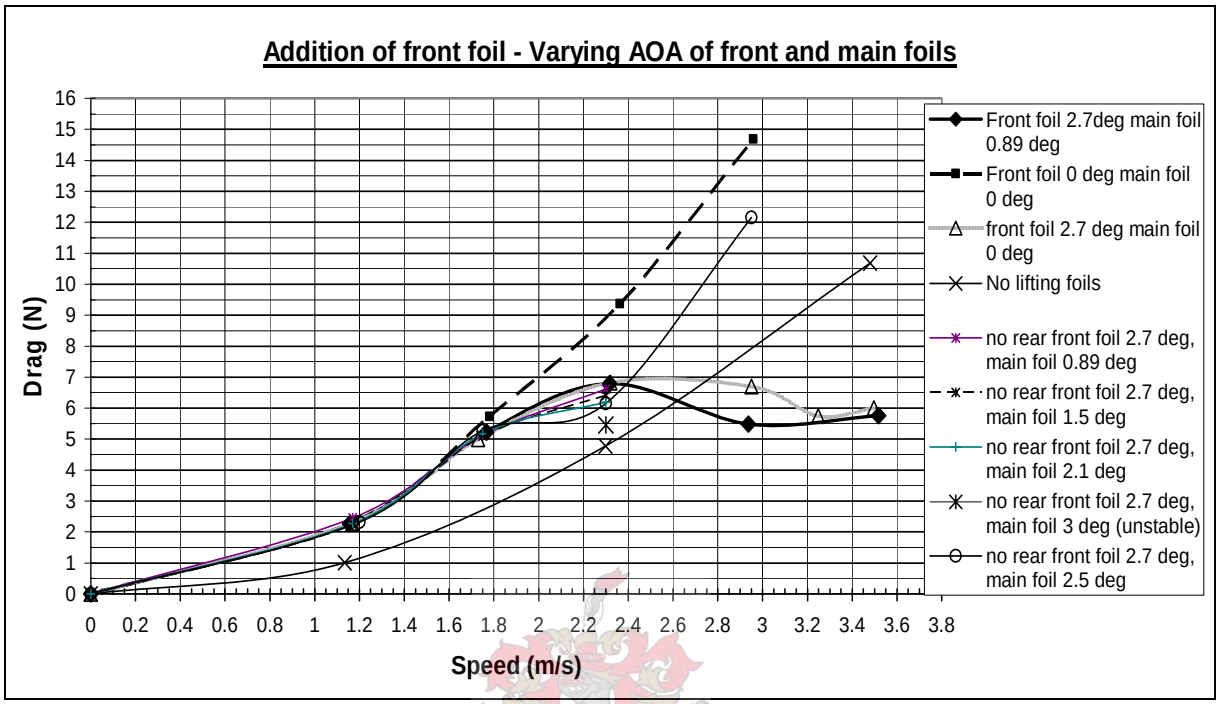

Figure M.3 – Resistance vs Model Speed for Various Lifting Foil Configurations

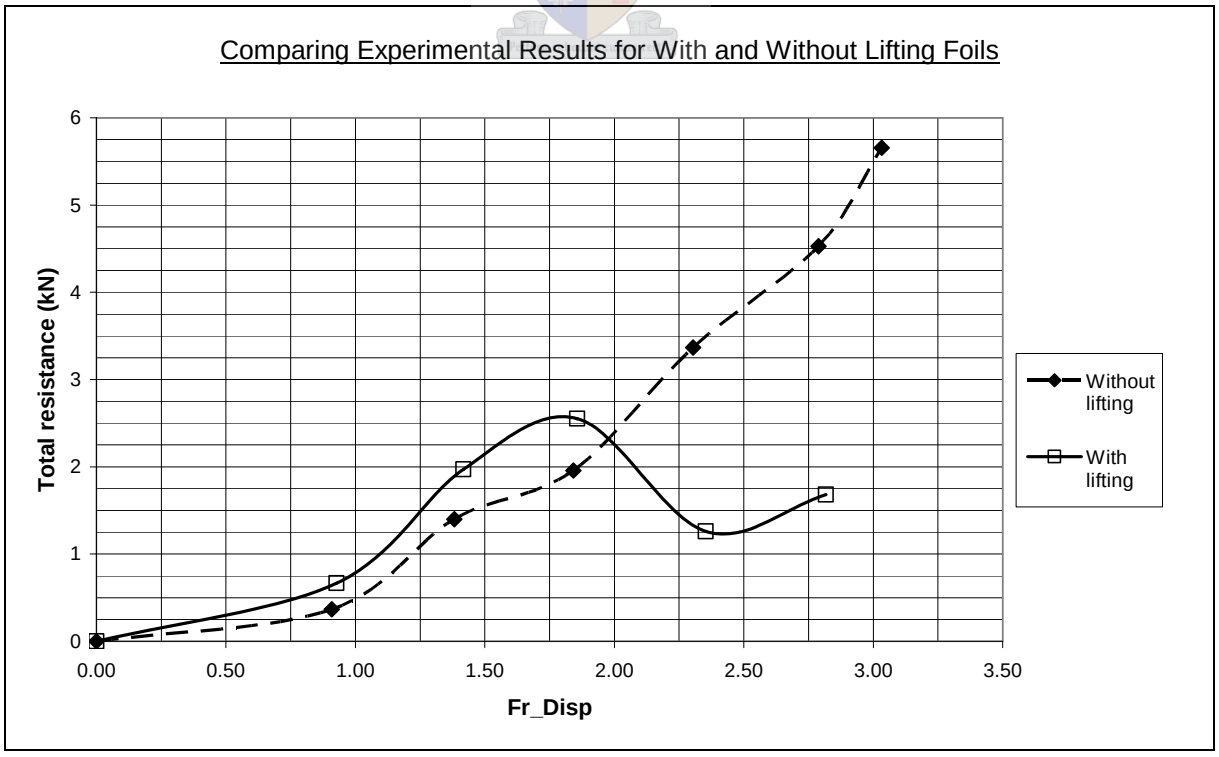

Figure M.4 - Comparing Full Scale Resistance of RH1 with and without lifting foils

Testing the Effects of Leeway

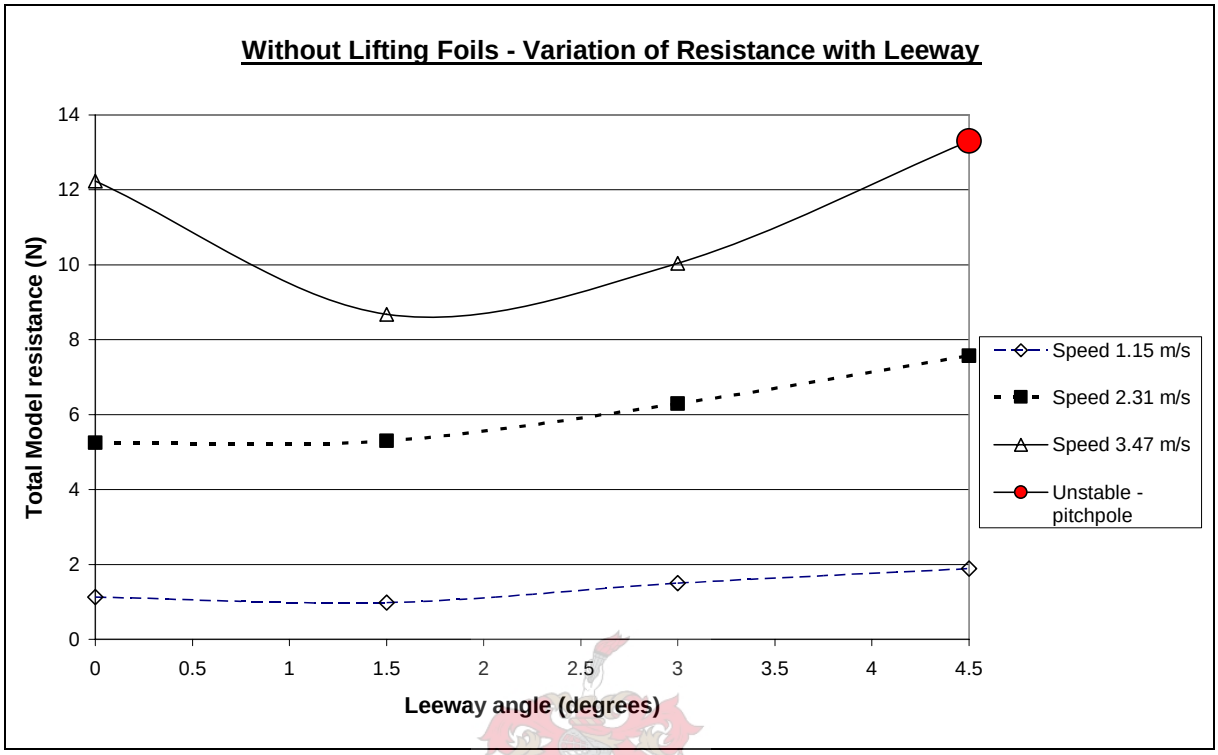

M.5 – Testing the effects of leeway without lifting foils

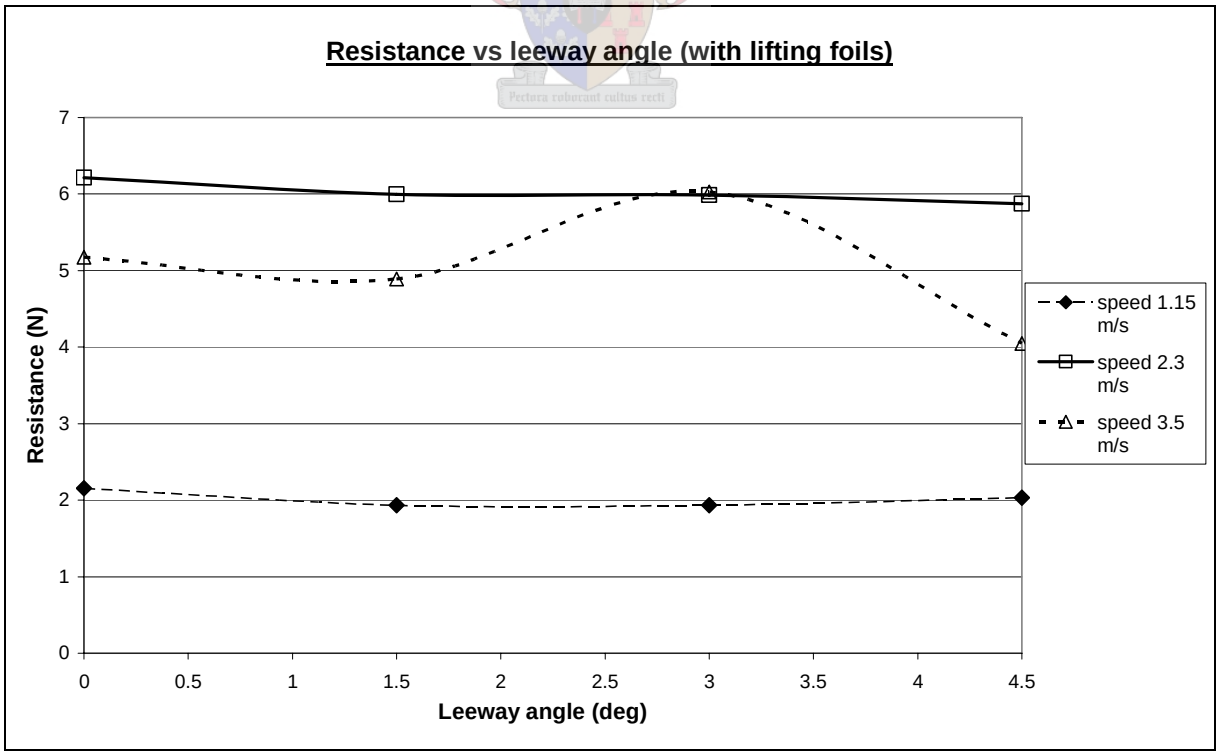

M.6 – Testing the effects of leeway with lifting foils

Testing the Effects of Heel

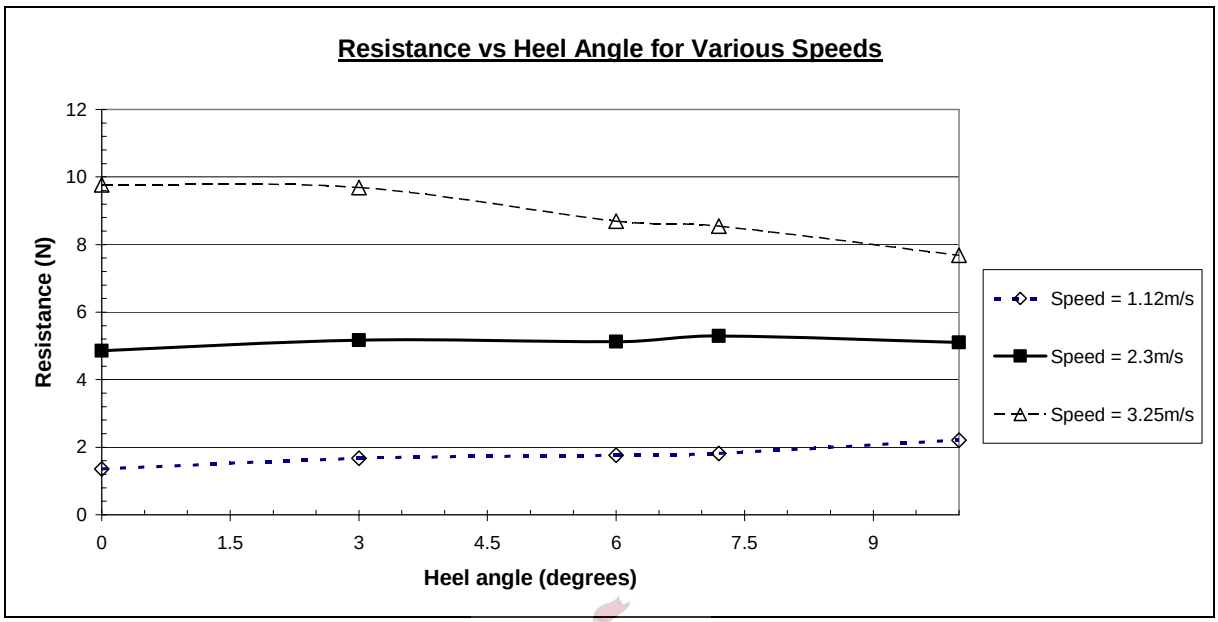

M.7 – Testing the effects of heel without lifting foils

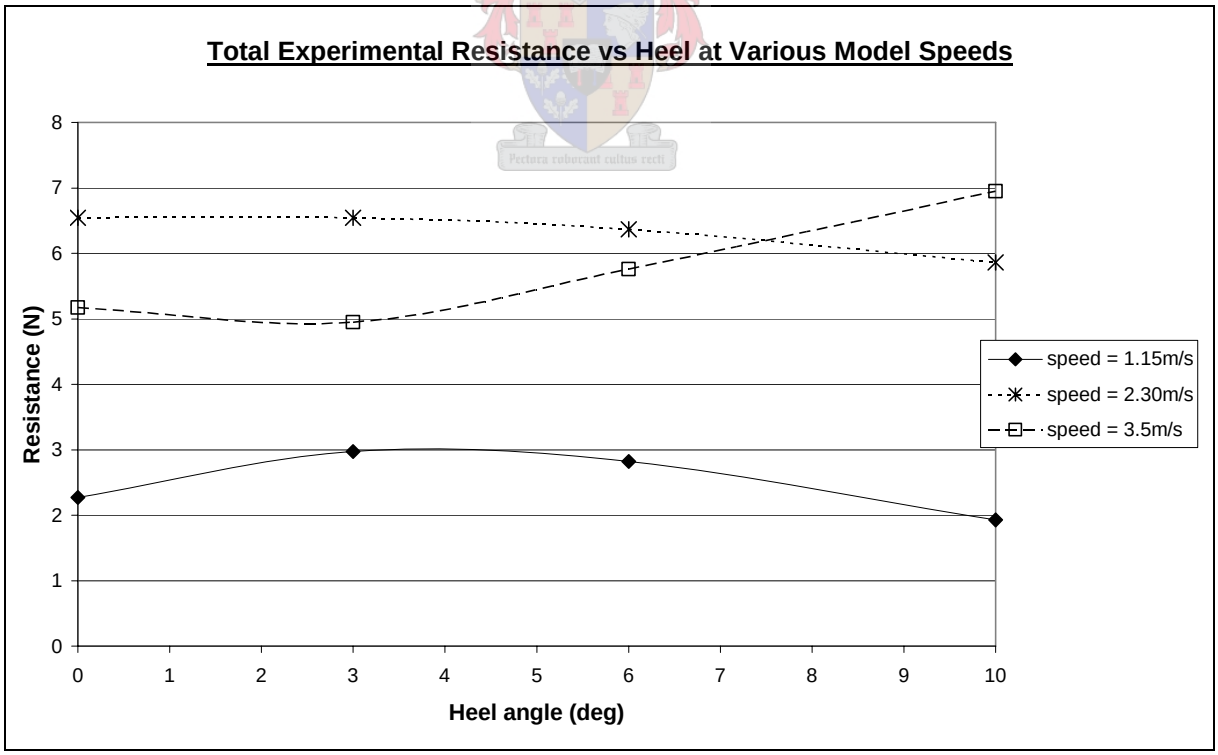

M.8 – Testing the effects of heel with lifting foils

Testing the change in WSA with speed

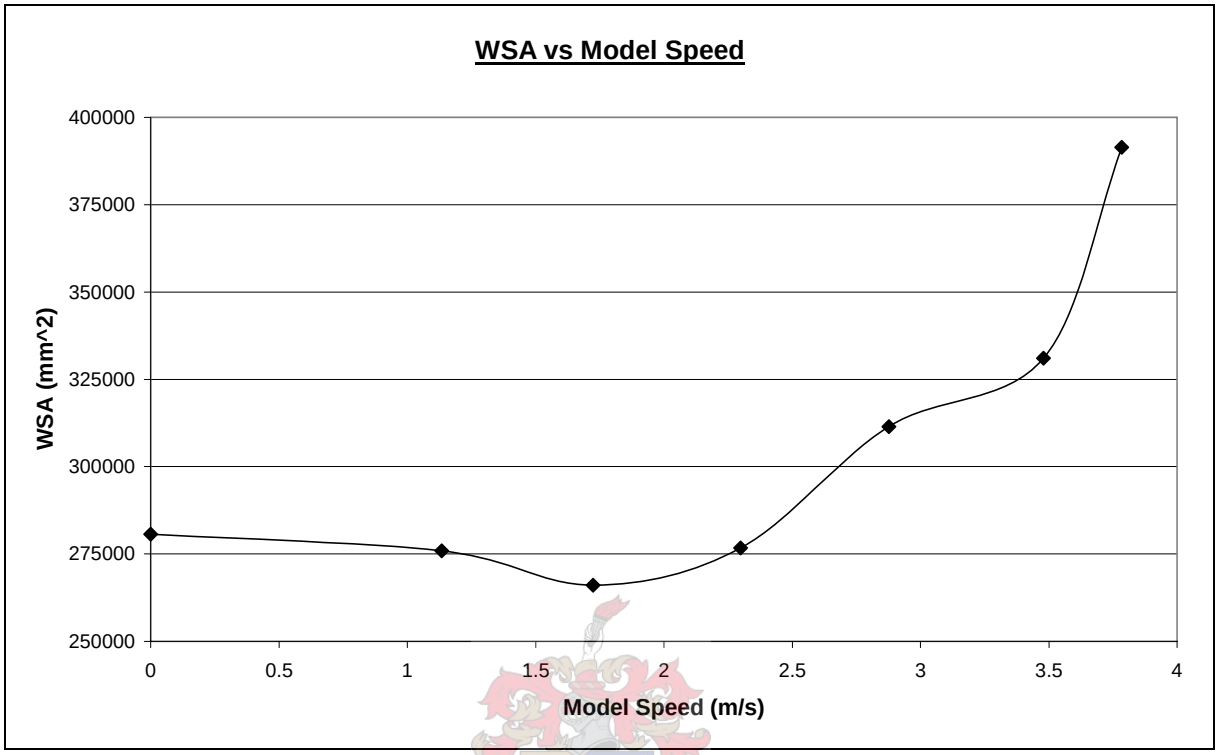

M.9 – The measured WSA at various model speeds without lifting foils

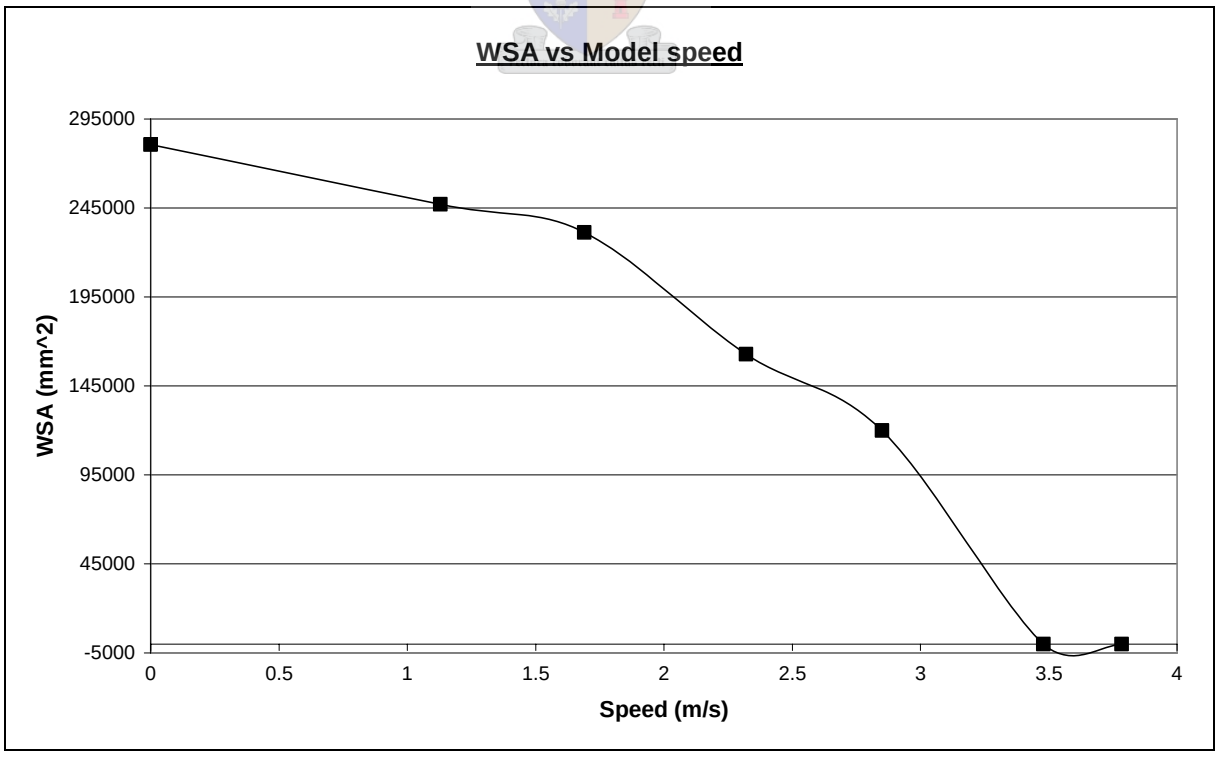

M.10 – The measured WSA at various model speeds with lifting foils

Graphs Showing Convergence of AUTOWING Results

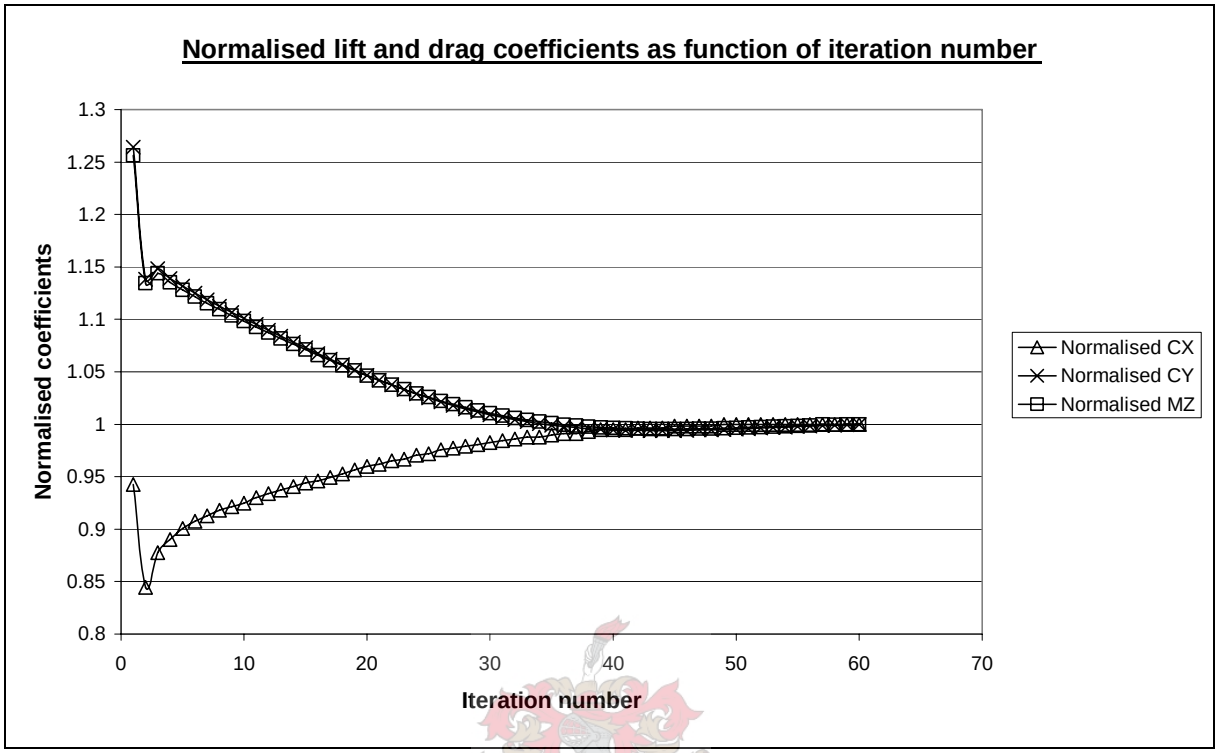

M.11 – The normalised coefficients of lift and drag and trim moment vs iteration number

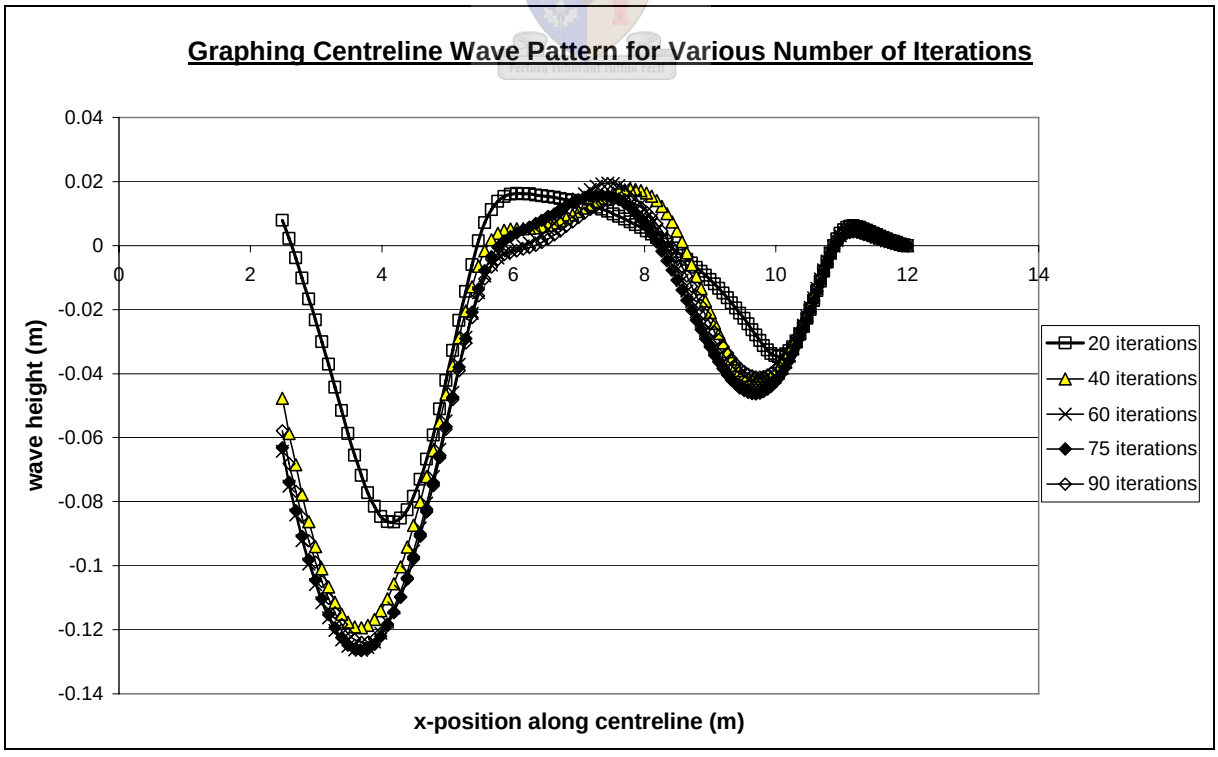

Figure M.12 – The wave surface for constant input values, after various iterations

Wave Patterns and Lift at various speeds
AUTOWING Results

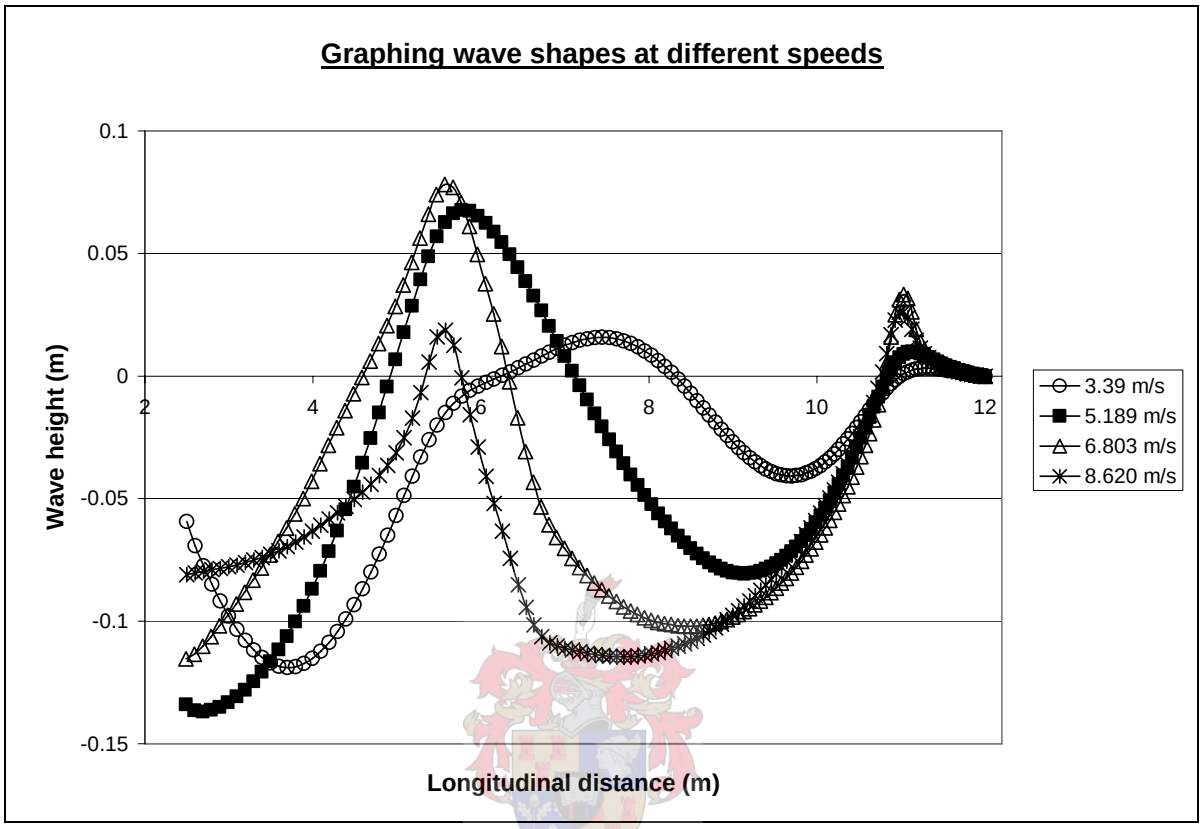

Figure M.13 – The wave surface at various speeds

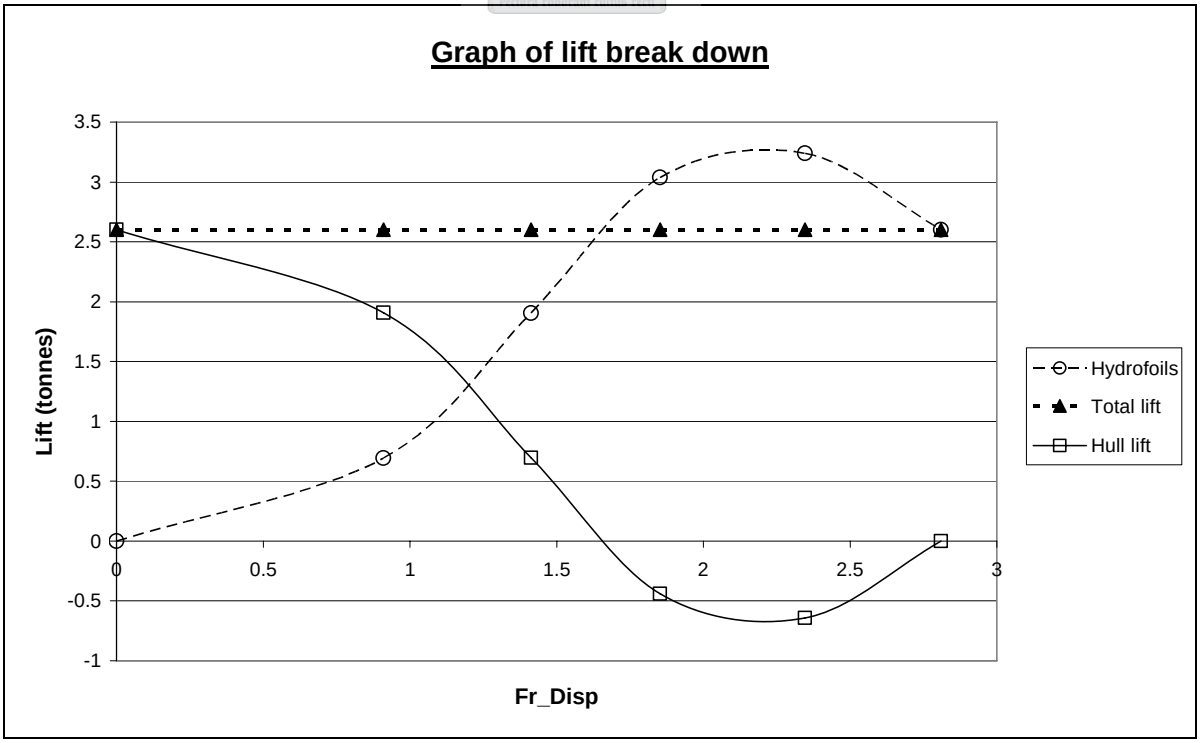

Figure M.14 – The calculated lift generated by the hydrofoils and hull

Graphs Comparing Computational and Experimental Results

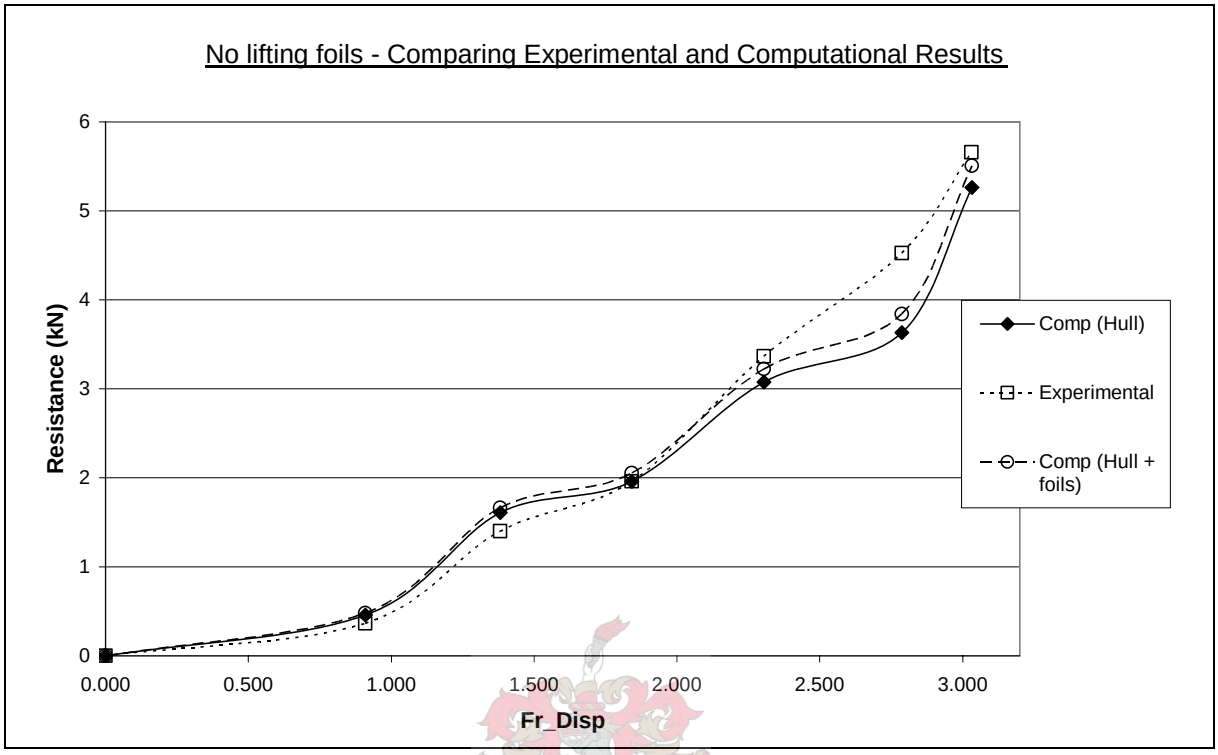

Figure M.15 – Comparing experimental and computational resistance vs displacement Froude number (without lifting foils)

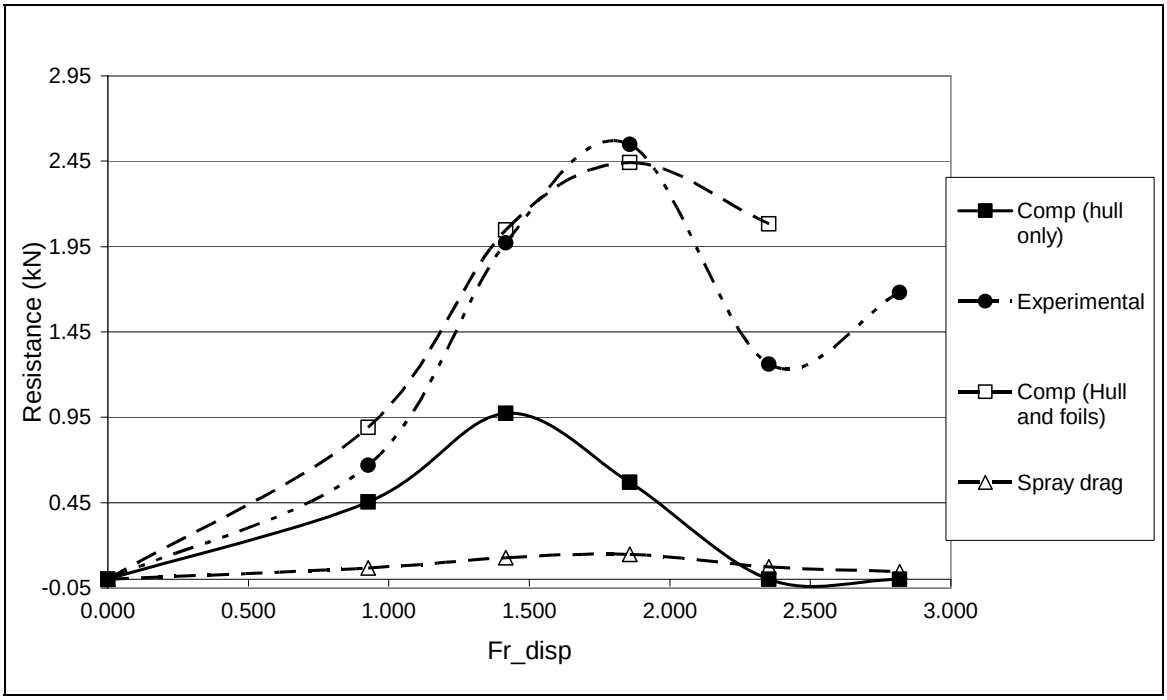

Figure M.16 – Comparing experimental and computational resistance vs displacement Froude number (with lifting foils)

N

Determining Wetted Surface Area (WSA) of a Hull

When working out the wetted surface area of a hull, it is common practice in naval architecture to divide the hull up into several stations and then determine the wetted girth at each station. This can then be used to estimate the area between each station. Using the trapezoidal rule (assuming straight lines between stations) is a poor approximation and so Simpson's rule assumes that the actual curve can be represented by a function of the form…

$y_0 = a_0 + a_1 x + a_2 x^2$

Derivation of Simpson's Rule [Muc87]

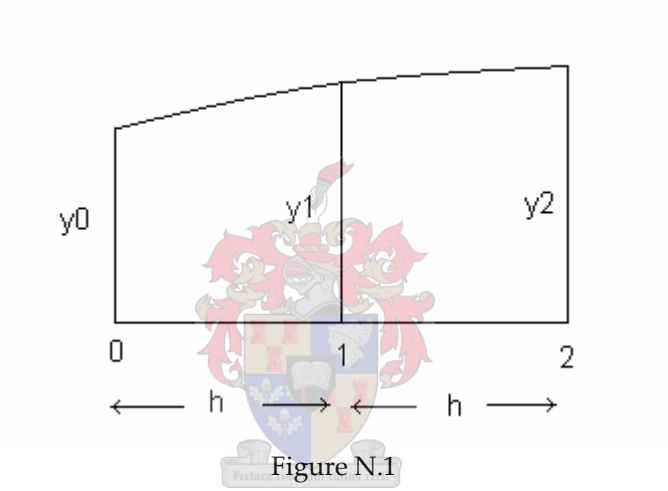

Figure N.1

x	y
0	a_0
1	$a_0 + a_1 + a_2$
2	$a_0 + 2a_1 + 4a_2$

Table N.1

Therefore if we assume h = 1, the area between station 0 and 2 is …

$$\int_0^2 (a_0 + a_1 x + a_2 x^2) = 2a_0 + 2a_1 + \frac{8}{3}a_2 \qquad \text{(N.1)}$$

Now from tableN.1, $a_0 = y_0$, $y_1 = y_0 + a_1 + a_2$ and $y_2 = y_0 + 2a_1 + 4a_2$

From substitution, we get $a_2 = (y_2 - 2y_1 + y_0)/2$ and $a_1 = -(3/2)y_0 - y_2/2 + 2y_1$

Finally the area is computed by substituting the values for a_2 and a_1 into equation N.1 and again multiplied by h to allow for $h \neq 1$, we get

$$Area = \frac{h}{3}(y_0 + 4y_1 + y_2) \qquad \text{(N.2)}$$

The area of each pair of intervals are then calculated and added up. This gives a coefficient pattern of 1, 4, 2, 4, 2… 4, 1 and will only work for an even number of intervals.

Adaptation for odd number of intervals.

If there are now an odd number of intervals, the area of the last interval can be calculated in a similar way. Basically all that changes is that the integral is over the interval 1 => 2 instead of 0 => 2. This yields…

$$\int_1^2 (a_0 + a_1 x + a_2 x^2) = a_0 + \frac{3}{2}a_1 + \frac{7}{3}a_2 \qquad \text{(N.3)}$$

After substituting as before, the following equation results for the area of the second interval- only (1 to 2).

$$Area = h \cdot (\frac{-1}{12} y_0 + \frac{2}{3} y_1 + \frac{10}{24} y_2) \qquad \text{(N.4)}$$

O

Stability Index Analysis

The seaworthiness of a yacht is usually assessed in terms of a Stability Index. As described by Larsson et al. [LE02], ISO/TC 188 Working Group 22 outlines the seaworthiness of a sailing monohull craft between 6m and 24m. The stability index or STIX is given by the formula below so that the yacht can be placed in a suitable category also indicated in table O.1.

Category	Range of STIX	Description
A	32 and higher	Very seaworthy
B	23-32	Good seaworthiness
C	14-23	Poor seaworthiness
D	5-14	Sheltered waters only

Table O.1 – Categories of seaworthiness for sailing monohulls

$$\mathrm{STIX} = (8 + 2.2 \cdot L_{BS}) \cdot (\mathrm{FDL} \cdot \mathrm{FBD} \cdot \mathrm{FKR} \cdot \mathrm{FIR} \cdot \mathrm{FDS} \cdot \mathrm{FWM} \cdot \mathrm{FDF})^{0.5} + \delta \qquad \text{for } L_{BS} \geq 10$$

Clearly it is desirable to keep all factors as large as possible. Each factor is described below and the effect that the addition of hydrofoils will have on them.

1. **Base length factor** - L_{BS} is a weighted average of the LOA and LWL and is an indication of the size of the vessel. Since the waterline length will decrease with speed, this factor will be reduced.
2. **Displacement length factor** - **FDL** – Small displacement compared to the size of the vessel is seen as a disadvantage with regard to control of the vessel. Since the displacement of the vessel is increased due to added weight of the foils, so is this factor.
3. **Beam displacement factor – FBD** – large beams are problematic as they are susceptible to wave-induced capsize and tend to remain capsized. Narrow beams have poor form stability and are also problematic, therefore a compromise is desired. Catamarans tend to have large beams and the addition of foils will not affect this.
4. **Knock down recovery factor- FKR** – The ability of the vessel to spill water out of its sails. In the situation of capsize, the lifting foils will not affect this.
5. **Inversion recovery factor – FIR** – The ability of a yacht to recover unaided after an inversion. The additional weight of the lifting foils will lower the COG thus improving this but this effect is likely to be small. (Φ_V is increased slightly)
6. **Dynamic stability factor – FDS** – this is the amount of work required from external forces to capsize the boat. Since the boat is lifted by the foils, the heeling moment arm is increased and a smaller side force is required to capsize the boat.
7. **Wind moment factor – FWM** – The wind speed required to cause downflooding. As above, the wind speed required would be less due to the increase in lever arm. The apparent wind would also be higher for a given true wind speed as the boat speed is increased.
8. **Downflooding factor- FDF** – This is the risk of downflooding (where water reaches below deck level) in a knockdown and is unaffected by the lifting foils since the lift tends to zero as the heel angle tends to 90^0, where downflooding is a factor.
9. **Reserve buoyancy factor – δ** – this is an additional factor increasing STIX if there is reserve buoyancy when the boat is completely flooded. This is unaffected by the addition of lifting foils.